JAERI-Data/Code
94-012

BENCHMARK PROBLEMS FOR INTERMEDIATE AND HIGH ENERGY ACCELERATOR SHIELDING

September 1994

Hiroshi NAKASHIMA, Yukio SAKAMOTO, Shun-ichi TANAKA
Akira HASEGAWA[*1], Tokio FUKAHORI, Takahiko NISHIDA
Nobuo SASAMOTO, Susumu TANAKA, Takashi NAKAMURA[*2]
Kazuo SHIN[*3], Hideo HIRAYAMA[*4], Syuichi BAN[*4]
Yoshitomo UWAMINO[*5], Kenji ISHIBASHI[*6], Kiyomitsu KAWACHI[*7]
Katsumi HAYASHI[*8], Satoshi IWAI[*9], Osamu SATO[*10]
and Naoki YAMANO[*11]

日本原子力研究所
Japan Atomic Energy Research Institute

本レポートは，日本原子力研究所が不定期に公刊している研究報告書です。
入手の問合わせは，日本原子力研究所技術情報部情報資料課（〒319-11 茨城県那珂郡東海村）あて，お申し越しください。なお，このほかに財団法人原子力弘済会資料センター（〒319-11 茨城県那珂郡東海村日本原子力研究所内）で複写による実費頒布をおこなっております。

This report is issued irregularly.
Inquiries about availability of the reports should be addressed to Information Division, Department of Technical Information, Japan Atomic Energy Research Institute, Tokai-mura, Naka-gun, Ibaraki-ken 319-11, Japan.

編集兼発行　日本原子力研究所
印　　刷　㈱原子力資料サービス

JAERI－Data/Code 94－012

Benchmark Problems for Intermediate and High Energy Accelerator Shielding

Hiroshi NAKASHIMA, Yukio SAKAMOTO, Shun-ichi TANAKA
Akira HASEGAWA[*1], Tokio FUKAHORI, Takahiko NISHIDA
Nobuo SASAMOTO[+], Susumu TANAKA[++], Takashi NAKAMURA[*2]
Kazuo SHIN[*3], Hideo HIRAYAMA[*4], Syuichi BAN[*4]
Yoshitomo UWAMINO[*5], Kenji ISHIBASHI[*6], Kiyomitsu KAWACHI[*7]
Katsumi HAYASHI[*8], Satoshi IWAI[*9], Osamu SATO[*10]
and Naoki YAMANO[*11]

Department of Reactor Engineering
Tokai Research Establishment
Japan Atomic Energy Research Institute
Tokai-mura, Naka-gun, Ibaraki-ken

(Received August 24, 1994)

Six kinds of benchmark problems were selected for evaluating the model codes and the nuclear data for the intermediate and high energy accelerator shielding by the Shielding Subcommittee in the Research Committee on Reactor Physics. The benchmark problems contain three kinds of neutron production data from thick targets due to proton, alpha and electron, and three kinds of shielding data for secondary neutron and photon generated by proton. Neutron and photoneutron reaction cross section data are also provided for neutrons up to 500 MeV and photons up to 300 MeV, respectively.

+ Department of Synchrotron Radiation Facility Project
++ Advanced Radiation Technology Center, Takasaki Radiation Chemistry Research Establishment
*1 Nuclear Power Engineering Corporation
*2 Tohoku University
*3 Kyoto University
*4 National Laboratory for High Energy Physics
*5 The Institute of Physical and Chemical Research
*6 Kyushu University
*7 National Institute of Radiological Science
*8 Hitachi Engineering Co. Ltd.
*9 Mitubishi Atomic Power Industry, INC
*10 Mitubishi Research Institute, INC
*11 Sumitomo Atomic Energy Industries, Ltd.

Keywords: Accelerator, Shielding Benchmark Problems, Electron, Photon, Neutron, Proton, Alpha, Codes, Nuclear Data

中高エネルギー加速器遮蔽のためのベンチマーク問題

日本原子力研究所東海研究所原子炉工学部

中島　宏・坂本　幸夫・田中　俊一・長谷川　明[*1]
深堀　智生・西田　雄彦・笹本　宣雄[+]・田中　進[++]
中村　尚司[*2]・秦　和夫[*3]・平山　英夫[*4]・伴　秀一[*4]
上蓑　義朋[*5]・石橋　健二[*6]・河内　清光[*7]・林　克己[*8]
岩井　敏[*9]・佐藤　理[*10]・山野　直樹[*11]

（1994年8月24日受理）

中高エネルギー領域の加速器遮蔽のための計算モデル及び核データの評価を目的として，炉物理研究専門委員会・遮蔽専門部会において，6種類のベンチマーク問題が選択された。このベンチマーク問題には，陽子，α粒子及び電子による厚いターゲットからの中性子収量に関する3種類のデータと，陽子による2次中性子及び光子に関する3種類の遮蔽実験データが収録されている。また，500 MeVまでの中性子と300 MeVまでの光子に対して，中性子反応断面積及び光核反応中性子生成断面積も収録されている。

東海研究所：〒319－11　茨城県那珂郡東海村白方字白根2－4
＋　大型放射光施設開発室
＋＋　高崎研究所放射線高度利用センター
＊1　財団法人・原子力発電技術機構
＊2　東北大学
＊3　京都大学
＊4　高エネルギー物理学研究所
＊5　理化学研究所
＊6　九州大学
＊7　放射線医学総合研究所
＊8　日立エンジニアリング㈱
＊9　三菱原子力工業㈱
＊10　㈱三菱総合研究所
＊11　住友原子力工業㈱

Contents

目　　次

Preface

Experimental benchmark data are very important to develop the model codes and nuclear data for shielding calculations of intermediate and high energy neutrons and photons in accelerators. So far, annotated references have been collected concerning neutron and photon production from thick targets, and shielding experiment and calculation of high energy particles.[1,2] Besides, twenty-five benchmark problems for accelerator shielding calculations from the references have been compiled by the Working Group of Accelerator Shielding in the Research Committee on Radiation Behavior in the Atomic Energy Society of Japan.[3]

In this work, six kinds of benchmark problems have been selected with respect to thick target neutron yield and shielding data of secondary neutron and photon generated by proton by the Shielding Subcommittee in the Research Committee on Reactor Physics of JAERI, where the qualities as the benchmark: well defined source and geometry conditions, well defined physical meaning of measured data, and material composition, were specially considered for comparing with the evaluated data by the model codes and nuclear data. Finally, all information necessary for the analysis were presented in a form of digital data in this report. In addition, the reaction cross sections of neutrons up to 500 MeV and photoneutron production cross sections of photons up to 300 MeV have also been provided, which are essential to the analysis of the present benchmark problems.

References

1. Nakamura T. et al.:"Annotated References on Neutron and Photon Production from Thick Targets Bombarded by Charged Particles," Atomic Data and Nuclear Data Tables, 32, 471-501 (1985).
2. Hirayama H. et al.:"Annotated References of Shielding Experiment and Calculation of High Energy Particles," KEK report 90-18 (1990).
3. Hirayama H. et al.:"Accelerator Shielding Benchmark Problems," KEK report 92-17 (1993).

1. Thick Target Neutron Yield Problems

1.1 Neutron Yields from Stopping-Length Carbon, Aluminum, Iron and Depleted Uranium Targets for 256-MeV Protons

(Summary)

1) Accelerator(Organization)	:	LAMPF (Los Alamos National Laboratory)
2) Projectile(Energy)	:	Proton (256MeV)
3) Target Material	:	Carbon, Aluminum, Iron and Depleted Uranium
4) Shielding Material	:	No Shield
5) Geometry	:	Cylindrical Geometry
6) Instruments	:	BC-418 Plastic Scintillator (Time-of-Flight Method)
7) Measured Quantities	:	Absolute Neutron Yields

1. Experimental Arrangement

Figure 1.1.1 shows a plan view of the target 2 area of the Weapon Neutron Research Facility (WNR) and the detector stations available for TOF measurements. The proton beam with energies between 113 and 800 MeV from the Los Alamos Clinton P.Anderson Meson Physics Facility (LAMPF) bombards the target at the center of the room. The experimental area is a circular of 12 m in diameter at beam elevation, which is surrounded by a compacted tuff of 10 m and a concrete wall of 0.4 m on the inside the room. Several radial penetrations view the center of the room at beam elevation, forming neutron flight paths with line of sight to the target. Four flight paths with detector stations were used as given in Table 1.1.1.

2. Method of Measurement and Instrument

The time-of-flight method was applied for measuring the neutron spectra. The neutron detectors for 60 and 120 degree were BC-418 plastic scintillators of 5.08 cm in diameter and 5.08 cm long. For the shorter flight paths, scintillators of 5.08 cm in diameter and 2.54 cm long were used. The detector efficiencies were calculted by the Stanton code at three kinds of bias: the mimimum below the full-energy peak of the 60-keV peak from ^{241}Am, the half-height of the Compton edge by ^{137}Cs and twice the half-

height of the Compton edge by ^{22}Na.

The absolute intensity of proton beam was determined by monitoring the secondary electron produced by the proton beam through a gold-plated aluminum foil with linearlity to proton current within 1 % and absolute uncetainty of 5 %.

3. Target Geometry and Beam Condition

The target materials were carbon, aluminum, and iron, all in their natural isotopic abundance, and ^{238}U. Targets for each element are longer than the stopping length for 256-MeV-proton. The diameters of the targets were comparable to the lengths to minimize the escape probability of secondary proton with energy near that of the primary beam. The physical characteristics of the targets are listed in Table 1.1.2.

The WNR can receive macropulses less than 800 μs at rates up to 12 Hz. which is made up by micropulses of about $1.6x10^5$ (5 ns spacing), each containing protons of about 3×10^8 in a burst < 200 ps. The macropulses are tailored at a chopper, leaving 70 individual micropulses/macropulse with 12-μs spacing.

4. Measured Results

The absolute neutron yields for each target are shown in Figs 1.1.2 through 1.1.5, and tabulated in Tables 1.1.3 through 1.1.6. These data are corrected for background, dead time and attenuation of air. Uncertainties for the measurements up to 20 MeV are assigned as 20 %, and those above 20 MeV are 33 %.

5. Model for Calculation

a. Source Condition

Mono-directional 256 MeV proton.

b. Calculation Geometry

The model configuration is shown in Fig. 1.1.6, in which proton beam is injected at the center of the cylindrical target along the axis. The dimensions and densities of the targets and the detector solid angles from the targets are given in Tables 1.1.1 and 1.1.2.

6. Normalization Between Calculation and Measurement

All absolute experimental data are given in unit of n/MeV/steradian/proton.

References

1. Meier M. M., Goulding C. A., Morgan G. L. and Ullmann J. L.: "Neutron Yields from Stopping- and Near-Stopping-Length Targets for 256-MeV Protons," Nucl. Sci. Eng., 104, 339-363 (1990).
2. Meier M. M., Amian W. E., Goulding C. A., Morgan G. L. and Moss C. E.: "Differential Neutron Production Cross Sections and Neutron Yields from Stopping-Length Targets for 256-MeV Protons," LA-11518-MS, Los Alamos National Laboratory (1989).

Table 1.1.1 Detector solid angles for each flight path angles.

Flight Angle (θ) (degree)	30	60	120	150
Flight Length (m)	28.7	58.5	66.8	30.2
Detector Solid Angle (Δθ) (degree)	0.0507	0.0249	0.0218	0.0482

θ and Δθ is shown in Fig. 1.1.6.

Table 1.1.2 Physical characteristics of the targets.

Element	Radius(d) (cm)	Length(L) (cm)	Density (g/cm^3)
Carbon	8.00	30.00	1.646
Alminum	8.00	20.00	2.715
Iron	8.00	8.00	7.86
^{238}U	4.00	5.00	18.98

d and L are shown in Fig. 1.1.6.

Table 1.1.3 Absolute neutron yields for the stopping-length carbon at 256 MeV.

Energy (MeV)	Neutron Yield (n/MeV/sr/proton)			
	30 degree	60 degree	120 degree	150 degree
4.900E-01*	1.042E-03	3.093E-03	1.809E-03	1.814E-03
5.250E-01	1.206E-03	2.868E-03	2.022E-03	1.953E-03
5.750E-01	1.294E-03	2.767E-03	2.193E-03	2.010E-03
6.250E-01	1.408E-03	2.687E-03	2.303E-03	1.983E-03
6.750E-01	1.364E-03	2.296E-03	2.060E-03	1.889E-03
7.250E-01	1.454E-03	2.382E-03	2.139E-03	1.868E-03
7.750E-01	1.499E-03	2.447E-03	2.255E-03	1.886E-03
8.250E-01	1.562E-03	2.416E-03	2.284E-03	1.893E-03
8.750E-01	1.619E-03	2.499E-03	2.379E-03	1.939E-03
9.250E-01	1.754E-03	2.941E-03	2.925E-03	2.118E-03
9.750E-01	1.630E-03	2.513E-03	2.408E-03	1.933E-03
1.075E+00	1.540E-03	2.172E-03	2.115E-03	1.767E-03
1.150E+00	1.589E-03	2.171E-03	2.106E-03	1.760E-03
1.250E+00	1.614E-03	2.224E-03	2.109E-03	1.811E-03
1.350E+00	1.520E-03	1.886E-03	1.787E-03	1.641E-03
1.450E+00	1.593E-03	2.003E-03	1.896E-03	1.669E-03
1.550E+00	1.580E-03	1.987E-03	1.831E-03	1.651E-03
1.650E+00	1.564E-03	1.919E-03	1.790E-03	1.618E-03
1.750E+00	1.508E-03	1.815E-03	1.638E-03	1.536E-03
1.850E+00	1.569E-03	1.928E-03	1.774E-03	1.587E-03
1.950E+00	1.705E-03	2.057E-03	1.948E-03	1.684E-03
2.100E+00	1.419E-03	1.719E-03	1.589E-03	1.444E-03
2.300E+00	1.526E-03	1.994E-03	1.927E-03	1.524E-03
2.500E+00	1.541E-03	2.175E-03	2.141E-03	1.572E-03
2.700E+00	1.219E-03	1.664E-03	1.577E-03	1.241E-03
2.900E+00	8.998E-04	1.224E-03	1.198E-03	9.018E-04
3.100E+00	1.131E-03	1.493E-03	1.262E-03	9.800E-04
3.300E+00	7.515E-04	9.419E-04	7.957E-04	6.511E-04
3.500E+00	6.066E-04	7.554E-04	6.389E-04	5.463E-04
3.700E+00	6.490E-04	7.867E-04	6.886E-04	5.608E-04
3.900E+00	7.356E-04	8.380E-04	6.912E-04	5.915E-04
4.100E+00	8.262E-04	9.616E-04	7.707E-04	6.510E-04
4.300E+00	7.273E-04	8.460E-04	7.157E-04	5.667E-04
4.500E+00	8.189E-04	9.167E-04	7.288E-04	5.934E-04
4.700E+00	8.867E-04	1.009E-03	7.936E-04	6.245E-04
4.900E+00	8.906E-04	1.001E-03	7.467E-04	5.951E-04
5.250E+00	7.956E-04	8.031E-04	5.958E-04	5.067E-04
5.750E+00	7.924E-04	8.400E-04	6.158E-04	5.136E-04
6.250E+00	5.951E-04	5.912E-04	4.006E-04	3.426E-04
6.750E+00	7.827E-04	6.816E-04	4.486E-04	3.968E-04
7.250E+00	5.784E-04	5.734E-04	3.700E-04	3.108E-04
7.750E+00	3.712E-04	4.326E-04	2.699E-04	2.178E-04
8.250E+00	4.537E-04	4.631E-04	2.918E-04	2.412E-04
8.750E+00	4.672E-04	4.665E-04	2.794E-04	2.280E-04
9.250E+00	4.271E-04	4.319E-04	2.604E-04	2.199E-04
9.750E+00	4.387E-04	4.464E-04	2.740E-04	2.172E-04
1.075E+01	4.135E-04	4.115E-04	2.375E-04	1.931E-04

*Read as 4.900×10^{-1}.

Table 1.1.3 (Continued.)

Energy (MeV)	Neutron Yield (n/MeV/sr/proton)			
	30 degree	60 degree	120 degree	150 degree
1.150E+01*	3.695E-04	3.716E-04	2.092E-04	1.606E-04
1.250E+01	3.665E-04	3.543E-04	1.885E-04	1.486E-04
1.350E+01	3.577E-04	3.490E-04	1.667E-04	1.293E-04
1.450E+01	3.648E-04	3.297E-04	1.560E-04	1.153E-04
1.550E+01	3.469E-04	3.081E-04	1.421E-04	1.009E-04
1.650E+01	3.416E-04	3.023E-04	1.316E-04	9.256E-05
1.750E+01	3.508E-04	3.051E-04	1.263E-04	8.701E-00
1.850E+01	3.464E-04	3.037E-04	1.201E-04	7.792E-05
1.950E+01	3.411E-04	2.939E-04	1.097E-04	7.031E-05
2.100E+01	3.337E-04	2.662E-04	9.269E-05	5.855E-05
2.300E+01	3.270E-04	2.550E-04	7.783E-05	4.684E-05
2.500E+01	3.224E-04	2.461E-04	6.713E-05	3.834E-00
2.700E+01	3.199E-04	2.368E-04	5.626E-05	3.175E-05
2.900E+01	3.210E-04	2.295E-04	4.978E-05	2.640E-05
3.100E+01	3.209E-06	2.249E-04	4.408E-05	2.159E-05
3.300E+01	3.180E-04	2.191E-04	3.810E-05	1.778E-05
3.500E+01	3.268E-04	2.073E-04	3.118E-05	1.668E-05
3.700E+01	3.200E-04	2.077E-04	2.650E-05	1.450E-05
3.900E+01	3.198E-04	1.948E-04	2.248E-05	1.089E-05
4.100E+01	3.210E-04	1.866E-04	2.059E-05	9.590E-06
4.300E+01	3.218E-04	1.863E-04	1.680E-05	8.026E-06
4.500E+01	3.215E-04	1.813E-04	1.583E-05	6.636E-06
4.700E+01	3.195E-04	1.764E-04	1.350E-05	5.964E-06
4.900E+01	3.161E-04	1.718E-04	1.083E-05	5.126E-06
5.250E+01	3.195E-04	1.624E-04	9.470E-06	3.983E-06
5.750E+01	3.160E-04	1.482E-04	6.906E-06	2.446E-06
6.250E+01	3.157E-04	1.384E-04	5.079E-06	1.885E-06
6.750E+01	3.111E-04	1.246E-04	3.597E-06	1.255E-06
7.250E+01	3.106E-04	1.124E-04	2.722E-06	7.529E-07
7.750E+01	3.064E-04	1.005E-04	1.705E-06	5.410E-07
8.250E+01	3.029E-04	9.066E-05	1.238E-06	3.117E-07
8.750E+01	2.961E-04	8.117E-05	8.636E-07	2.420E-07
9.250E+01	2.985E-04	7.042E-05	6.106E-07	1.459E-07
9.750E+01	2.820E-04	6.087E-05	4.527E-07	
1.075E+02	2.743E-04	4.844E-05	1.857E-07	
1.150E+02	2.603E-04	3.536E-05	6.074E-08	
1.250E+02	2.418E-04	2.428E-05		
1.350E+02	2.250E-04	1.604E-05		
1.450E+02	2.029E-04	1.035E-05		
1.550E+02	1.803E-04	6.540E-06		
1.650E+02	1.524E-04	3.699E-06		
1.750E+02	1.263E-04	1.865E-06		
1.850E+02	9.921E-05	9.293E-07		
1.950E+02	7.286E-05	4.435E-07		
2.100E+02	3.962E-05	7.753E-08		
2.300E+02	1.032E-05			
2.500E+02	1.098E-06			

*Read as 1.150×10^{1}.

Table 1.1.4 Absolute neutron yields for the stopping-length alminum at 256 MeV.

Energy (MeV)	Neutron Yield (n/MeV/sr/proton)			
	30 degree	60 degree	120 degree	150 degree
4.900E-01*	3.616E-03	9.457E-03	5.900E-03	5.280E-03
5.250E-01	4.278E-03	9.063E-03	6.782E-03	5.895E-03
5.750E-01	4.907E-03	9.057E-03	7.310E-03	6.456E-03
6.250E-01	5.010E-03	9.137E-03	7.922E-03	6.831E-03
6.750E-01	5.566E-03	8.307E-03	7.604E-03	7.102E-03
7.250E-01	5.450E-03	8.040E-03	7.593E-03	6.898E-03
7.750E-01	4.360E-03	6.317E-03	6.225E-03	5.577E-03
8.250E-01	4.921E-03	6.948E-03	6.922E-03	6.107E-03
8.750E-01	5.558E-03	7.820E-03	7.950E-03	6.691E-03
9.250E-01	6.932E-03	1.059E-02	1.067E-02	8.355E-03
9.750E-01	6.308E-03	8.922E-03	8.538E-03	7.447E-03
1.075E+00	5.626E-03	7.154E-03	6.964E-03	6.439E-03
1.150E+00	4.596E-03	5.842E-03	5.957E-03	5.463E-03
1.250E+00	5.128E-03	6.485E-03	6.449E-03	5.879E-03
1.350E+00	5.107E-03	5.704E-03	5.620E-03	5.697E-03
1.450E+00	4.541E-03	5.271E-03	5.275E-03	5.128E-03
1.550E+00	4.484E-03	5.126E-03	5.129E-03	4.942E-03
1.650E+00	4.787E-03	5.324E-03	5.239E-03	5.115E-03
1.750E+00	4.357E-03	4.630E-03	4.691E-03	4.719E-03
1.850E+00	4.856E-03	5.504E-03	5.359E-03	5.180E-03
1.950E+00	4.390E-03	5.096E-03	5.121E-03	4.655E-03
2.100E+00	3.794E-03	4.158E-03	4.153E-03	4.018E-03
2.300E+00	4.026E-03	4.959E-03	5.033E-03	4.164E-03
2.500E+00	3.991E-03	5.270E-03	5.358E-03	4.085E-03
2.700E+00	3.402E-03	4.163E-03	4.128E-03	3.371E-03
2.900E+00	3.321E-03	4.279E-03	4.134E-03	3.154E-03
3.100E+00	3.086E-03	3.691E-03	3.526E-03	2.896E-03
3.300E+00	2.662E-03	2.964E-03	2.760E-03	2.458E-03
3.500E+00	2.347E-03	2.602E-03	2.316E-03	2.171E-03
3.700E+00	2.183E-03	2.372E-03	2.141E-03	1.945E-03
3.900E+00	2.053E-03	2.151E-03	1.841E-03	1.797E-03
4.100E+00	1.940E-03	2.033E-03	1.775E-03	1.686E-03
4.300E+00	1.910E-03	2.024E-03	1.783E-03	1.614E-03
4.500E+00	1.826E-03	1.365E-03	1.688E-03	1.522E-03
4.700E+00	1.760E-03	1.962E-03	1.692E-03	1.470E-03
4.900E+00	1.684E-03	1.900E-03	1.819E-03	1.363E-03
5.250E+00	1.408E-03	1.464E-03	1.208E-03	1.118E-03
5.750E+00	1.320E-03	1.435E-03	1.162E-03	1.002E-03
6.250E+00	1.074E-03	1.103E-03	8.618E-04	7.850E-04
6.750E+00	9.407E-04	9.954E-04	7.364E-04	6.670E-04
7.250E+00	8.670E-04	8.690E-04	6.471E-04	5.849E-04
7.750E+00	8.024E-04	8.638E-04	5.941E-04	5.324E-04
8.250E+00	7.308E-04	7.471E-04	5.331E-04	4.704E-04
8.750E+00	6.579E-04	6.826E-04	4.682E-04	4.038E-04
9.250E+00	6.446E-04	6.490E-04	4.369E-04	3.896E-04
9.750E+00	5.878E-04	6.035E-04	4.170E-04	3.576E-04
1.075E+01	5.305E-04	5.204E-04	3.415E-04	3.022E-04

*Read as 4.900×10^{-1}.

Table 1.1.4 (Continued.)

Energy (MeV)	Neutron Yield (n/MeV/sr/proton)			
	30 degree	60 degree	120 degree	150 degree
1.150E+01*	4.849E-04	4.687E-04	3.003E-04	2.581E-04
1.250E+01	4.505E-04	4.200E-04	2.596E-04	2.239E-04
1.350E+01	4.258E-04	3.848E-04	2.298E-04	1.939E-04
1.450E+01	4.141E-04	3.572E-04	2.058E-04	1.729E-04
1.550E+01	4.025E-04	3.480E-04	1.894E-04	1.541E-04
1.650E+01	3.972E-04	3.372E-04	1.765E-04	1.436E-04
1.750E+01	3.837E-04	3.187E-04	1.641E-04	1.278E-04
1.850E+01	3.821E-04	3.173E-04	1.542E-04	1.173E-04
1.950E+01	3.725E-04	3.033E-04	1.425E-04	1.042E-04
2.100E+01	3.492E-04	2.672E-04	1.142E-04	8.660E-05
2.300E+01	3.340E-04	2.523E-04	9.982E-05	7.054E-05
2.500E+01	3.229E-04	2.367E-04	8.532E-05	5.748E-05
2.700E+01	3.229E-04	2.365E-04	7.234E-05	4.804E-05
2.900E+01	3.174E-04	2.222E-04	6.292E-05	3.944E-05
3.100E+01	3.128E-04	2.160E-04	5.647E-05	3.433E-05
3.300E+01	3.106E-04	2.067E-04	4.981E-05	2.834E-05
3.500E+01	3.088E-04	1.945E-04	4.074E-05	2.619E-05
3.700E+01	3.057E-04	1.922E-04	3.589E-05	2.185E-05
3.900E+01	2.987E-04	1.788E-04	3.193E-05	1.816E-05
4.100E+01	2.950E-04	1.675E-04	2.707E-05	1.631E-05
4.300E+01	2.909E-04	1.632E-04	2.408E-05	1.349E-05
4.500E+01	2.904E-04	1.663E-04	2.187E-05	1.163E-05
4.700E+01	2.904E-04	1.606E-04	1.893E-05	9.695E-06
4.900E+01	2.832E-04	1.534E-04	1.613E-05	8.446E-06
5.250E+01	2.815E-04	1.471E-04	1.421E-05	6.947E-06
5.750E+01	2.758E-04	1.342E-04	1.041E-05	4.599E-06
6.250E+01	2.710E-04	1.236E-04	7.524E-06	3.221E-06
6.750E+01	2.667E-04	1.120E-04	5.799E-06	2.407E-06
7.250E+01	2.587E-04	1.015E-04	4.384E-06	1.547E-06
7.750E+01	2.540E-04	9.133E-05	3.343E-06	1.151E-06
8.250E+01	2.485E-04	8.198E-05	2.322E-06	8.866E-07
8.750E+01	2.409E-04	7.301E-05	1.533E-06	5.300E-07
9.250E+01	2.328E-04	6.336E-05	1.200E-06	3.819E-07
9.750E+01	2.240E-04	5.589E-05	8.428E-07	2.738E-07
1.075E+02	2.134E-04	4.482E-05	5.516E-07	1.651E-07
1.150E+02	1.972E-04	3.273E-05	2.063E-07	
1.250E+02	1.804E-04	2.391E-05		
1.350E+02	1.678E-04	1.613E-05		
1.450E+02	1.509E-04	1.053E-05		
1.550E+02	1.323E-04	6.548E-06		
1.650E+02	1.144E-04	3.933E-06		
1.750E+02	9.464E-05	2.289E-06		
1.850E+02	7.527E-05	1.143E-06		
1.950E+02	5.699E-05	5.499E-07		
2.100E+02	3.248E-05	1.191E-07		
2.300E+02	1.028E-05			
2.500E+02	1.279E-06			

*Read as 1.150×10^{1}.

Table 1.1.5 Absolute neutron yields for the stopping-length iron at 256 MeV.

Energy (MeV)	Neutron Yield (n/MeV/sr/proton)			
	30 degree	60 degree	120 degree	150 degree
4.700E-01*		4.791E-02	1.628E-02	2.603E-02
4.900E-01	1.382E-02	3.965E-02	1.567E-02	2.391E-02
5.250E-01	1.437E-02	3.324E-02	1.549E-02	2.243E-02
5.750E-01	1.764E-02	3.701E-02	1.954E-02	2.482E-02
6.250E-01	2.605E-02	5.537E-02	2.874E-02	3.410E-02
6.750E-01	2.183E-02	3.535E-02	2.061E-02	2.704E-02
7.250E-01	2.116E-02	3.604E-02	2.060E-02	2.694E-02
7.750E-01	1.767E-02	2.669E-02	1.671E-02	2.207E-02
8.250E-01	1.966E-02	3.101E-02	1.943E-02	2.384E-02
8.750E-01	1.948E-02	3.132E-02	1.935E-02	2.333E-02
9.250E-01	2.307E-02	4.042E-02	2.566E-02	2.709E-02
9.750E-01	1.965E-02	3.356E-02	1.997E-02	2.344E-02
1.075E+00	1.806E-02	2.531E-02	1.633E-02	2.088E-02
1.150E+00	1.993E-02	2.948E-02	1.825E-02	2.266E-02
1.250E+00	1.708E-02	2.400E-02	1.504E-02	1.951E-02
1.350E+00	1.571E-02	1.977E-02	1.246E-02	1.756E-02
1.450E+00	1.466E-02	1.833E-02	1.190E-02	1.630E-02
1.550E+00	1.393E-02	1.747E-02	1.115E-02	1.556E-02
1.650E+00	1.375E-02	1.686E-02	1.101E-02	1.511E-02
1.750E+00	1.327E-02	1.615E-02	1.017E-02	1.449E-02
1.850E+00	1.202E-02	1.494E-02	9.737E-03	1.321E-02
1.950E+00	1.095E-02	1.340E-02	8.958E-03	1.193E-02
2.100E+00	1.017E-02	1.181E-02	7.788E-03	1.089E-02
2.300E+00	1.034E-02	1.351E-02	9.090E-03	1.101E-02
2.500E+00	9.346E-03	1.273E-02	8.893E-03	9.995E-03
2.700E+00	8.267E-03	1.075E-02	7.234E-03	8.617E-03
2.900E+00	7.441E-03	1.002E-02	6.822E-03	7.746E-03
3.100E+00	6.398E-03	7.916E-03	5.380E-03	6.577E-03
3.300E+00	5.462E-03	6.451E-03	4.243E-03	5.584E-03
3.500E+00	4.793E-03	5.349E-03	3.488E-03	4.795E-03
3.700E+00	4.250E-03	4.626E-03	3.081E-03	4.274E-03
3.900E+00	3.787E-03	3.964E-03	2.608E-03	3.725E-03
4.100E+00	3.581E-03	3.851E-03	2.477E-03	3.496E-03
4.300E+00	3.443E-03	3.691E-03	2.484E-03	3.300E-03
4.500E+00	3.135E-03	3.313E-03	2.203E-03	2.955E-03
4.700E+00	3.027E-03	3.341E-03	2.250E-03	2.868E-03
4.900E+00	2.814E-03	3.091E-03	2.026E-03	2.606E-03
5.250E+00	2.355E-03	2.424E-03	1.564E-03	2.141E-03
5.750E+00	2.129E-03	2.310E-03	1.509E-03	1.896E-03
6.250E+00	1.710E-03	1.772E-03	1.100E-03	1.479E-03
6.750E+00	1.464E-03	1.492E-03	9.433E-04	1.237E-03
7.250E+00	1.279E-03	1.323E-03	8.024E-04	1.036E-03
7.750E+00	1.159E-03	1.268E-03	7.132E-04	9.554E-04
8.250E+00	1.039E-03	1.100E-03	6.330E-04	8.122E-04
8.750E+00	9.314E-04	9.821E-04	5.507E-04	6.998E-04
9.250E+00	8.918E-04	9.383E-04	5.036E-04	6.469E-04
9.750E+00	8.126E-04	8.637E-04	4.785E-04	5.808E-04
1.075E+01	7.180E-04	7.325E-04	3.831E-04	4.811E-04

*Read as 4.700×10^{-1}.

Table 1.1.5 (Continued.)

Energy (MeV)	Neutron Yield (n/MeV/sr/proton)			
	30 degree	60 degree	120 degree	150 degree
1.150E+01*	6.476E-04	6.650E-04	3.297E-04	4.033E-04
1.250E+01	5.874E-04	5.721E-04	2.788E-04	3.367E-04
1.350E+01	5.452E-04	5.284E-04	2.472E-04	2.868E-04
1.450E+01	5.153E-04	4.862E-04	2.174E-04	2.515E-04
1.550E+01	4.930E-04	4.672E-04	1.965E-04	2.203E-04
1.650E+01	4.903E-04	4.468E-04	1.843E-04	2.020E-04
1.750E+01	4.667E-04	4.256E-04	1.694E-04	1.795E-04
1.850E+01	4.508E-04	4.102E-04	1.554E-04	1.588E-04
1.950E+01	4.383E-04	3.973E-04	1.425E-04	1.412E-04
2.100E+01	4.012E-04	3.469E-04	1.198E-04	1.169E-04
2.300E+01	3.849E-04	3.213E-04	1.018E-04	9.270E-05
2.500E+01	3.664E-04	3.060E-04	8.740E-05	7.685E-05
2.700E+01	3.493E-04	2.897E-04	7.491E-05	6.383E-05
2.900E+01	3.474E-04	2.769E-04	6.644E-05	5.467E-05
3.100E+01	3.383E-04	2.675E-04	5.983E-05	4.591E-05
3.300E+01	3.320E-04	2.551E-04	5.422E-05	3.889E-05
3.500E+01	3.336E-04	2.431E-04	4.368E-05	3.477E-05
3.700E+01	3.224E-04	2.356E-04	3.824E-05	2.936E-05
3.900E+01	3.174E-04	2.188E-04	3.482E-05	2.462E-05
4.100E+01	3.146E-04	2.131E-04	3.047E-05	2.201E-00
4.300E+01	3.050E-04	2.129E-04	2.810E-05	1.793E-05
4.500E+01	2.991E-04	2.045E-04	2.536E-05	1.605E-05
4.700E+01	2.932E-04	1.934E-04	2.131E-05	1.373E-05
4.900E+01	2.924E-04	1.915E-04	2.013E-05	1.103E-05
5.250E+01	2.871E-04	1.770E-04	1.620E-05	8.414E-06
5.750E+01	2.780E-04	1.583E-04	1.226E-05	5.818E-06
6.250E+01	2.696E-04	1.459E-04	9.899E-06	4.266E-06
6.750E+01	2.584E-04	1.312E-04	6.568E-06	2.978E-06
7.250E+01	2.505E-04	1.232E-04	5.222E-06	2.235E-06
7.750E+01	2.454E-04	1.071E-04	3.584E-06	1.403E-06
8.250E+01	2.321E-04	9.646E-05	2.822E-06	1.050E-06
8.750E+01	2.243E-04	8.578E-05	2.373E-06	7.858E-07
9.250E+01	2.154E-04	7.410E-05	1.663E-06	4.850E-07
9.750E+01	2.021E-04	6.825E-05	9.489E-07	3.470E-07
1.075E+02	1.921E-04	5.390E-05	5.619E-07	2.307E-07
1.150E+02	1.765E-04	4.011E-05		
1.250E+02	1.593E-04	2.979E-05		
1.350E+02	1.437E-04	1.990E-05		
1.450E+02	1.267E-04	1.264E-05		
1.550E+02	1.100E-04	8.290E-06		
1.650E+02	9.139E-05	4.996E-06		
1.750E+02	7.389E-05	2.755E-06		
1.850E+02	5.700E-05	1.682E-06		
1.950E+02	4.148E-05	7.216E-07		
2.100E+02	2.328E-05	2.600E-07		
2.300E+02	7.316E-06			
2.500E+02	1.147E-06			

*Read as 1.150×10^{1}.

Table 1.1.6 Absolute neutron yields for the stopping-length uranium at 256 MeV.

Energy (MeV)	Neutron Yield (n/MeV/sr/proton)			
	30 degree	60 degree	120 degree	150 degree
4.900E-01*	7.837E-02	4.271E-02	1.217E-01	1.272E-01
5.250E-01	8.745E-02	5.608E-02	1.309E-01	1.267E-01
5.750E-01	9.592E-02	7.240E-02	1.409E-01	1.290E-01
6.250E-01	9.917E-02	8.351E-02	1.406E-01	1.256E-01
6.750E-01	9.413E-02	7.919E-02	1.243E-01	1.165E-01
7.250E-01	9.458E-02	8.512E-02	1.262E-01	1.137E-01
7.750E-01	9.507E-02	8.893E-02	1.266E-01	1.120E-01
8.250E-01	9.171E-02	8.969E-02	1.239E-01	1.085E-01
8.750E-01	8.999E-02	9.029E-02	1.224E-01	1.068E-01
9.250E-01	9.357E-02	1.029E-01	1.404E-01	1.109E-01
9.750E-01	8.449E-02	8.795E-02	1.146E-01	9.878E-02
1.075E+00	7.192E-02	6.859E-02	9.005E-02	8.413E-02
1.150E+00	6.588E-02	6.328E-02	8.248E-02	7.632E-02
1.250E+00	5.310E-02	6.203E-02	7.861E-02	7.330E-02
1.350E+00	5.496E-02	4.912E-02	6.183E-02	6.410E-02
1.450E+00	5.278E-02	4.788E-02	6.092E-02	6.131E-02
1.550E+00	5.024E-02	4.638E-02	5.806E-02	5.907E-02
1.650E+00	4.755E-02	4.296E-02	5.504E-02	5.520E-02
1.750E+00	4.426E-02	3.934E-02	4.903E-02	5.126E-02
1.850E+00	4.387E-02	4.009E-02	5.102E-02	5.052E-02
1.950E+00	4.354E-02	4.096E-02	5.243E-02	5.023E-02
2.100E+00	3.876E-02	3.497E-02	4.395E-02	4.430E-02
2.300E+00	4.011E-02	4.047E-02	5.224E-02	4.572E-02
2.500E+00	3.999E-02	4.336E-02	5.654E-02	4.507E-02
2.700E+00	3.468E-02	3.538E-02	4.517E-02	3.917E-02
2.900E+00	3.270E-02	3.466E-02	4.434E-02	3.671E-02
3.100E+00	2.953E-02	2.988E-02	3.734E-02	3.310E-02
3.300E+00	2.485E-02	2.348E-02	2.901E-02	2.780E-02
3.500E+00	2.193E-02	1.982E-02	2.414E-02	2.449E-02
3.700E+00	2.056E-02	1.858E-02	2.219E-02	2.264E-02
3.900E+00	1.810E-02	1.549E-02	1.861E-02	2.012E-02
4.100E+00	1.702E-02	1.502E-02	1.801E-02	1.878E-02
4.300E+00	1.600E-02	1.443E-02	1.756E-02	1.775E-02
4.500E+00	1.464E-02	1.305E-02	1.570E-02	1.618E-02
4.700E+00	1.391E-02	1.293E-02	1.561E-02	1.537E-02
4.900E+00	1.277E-02	1.194E-02	1.419E-02	1.413E-02
5.250E+00	1.029E-02	8.983E-03	1.056E-02	1.133E-02
5.750E+00	8.755E-03	8.051E-03	9.558E-03	9.655E-03
6.250E+00	6.568E-03	5.633E-03	6.449E-03	7.097E-03
6.750E+00	5.227E-03	4.492E-03	5.074E-03	5.608E-03
7.250E+00	4.146E-03	3.517E-03	3.964E-03	4.371E-03
7.750E+00	3.499E-03	2.883E-03	3.254E-03	3.710E-03
8.250E+00	2.864E-03	2.435E-03	2.664E-03	2.917E-03
8.750E+00	2.326E-03	1.916E-03	2.091E-03	2.279E-03
9.250E+00	2.071E-03	1.697E-03	1.774E-03	1.979E-03
9.750E+00	1.784E-03	1.495E-03	1.565E-03	1.630E-03
1.075E+01	1.424E-03	1.139E-03	1.126E-03	1.230E-03

*Read as 4.900×10^{-1}.

Table 1.1.6 (Continued.)

Energy (MeV)	Neutron Yield (n/MeV/sr/proton)			
	30 degree	60 degree	120 degree	150 degree
1.150E+01*	1.170E-03	8.998E-04	8.648E-04	9.120E-04
1.250E+01	9.959E-04	7.433E-04	6.653E-04	6.976E-04
1.350E+01	8.693E-04	6.417E-04	5.424E-04	5.482E-04
1.450E+01	8.015E-04	5.738E-04	4.568E-04	4.513E-04
1.550E+01	7.502E-04	5.237E-04	3.967E-04	3.785E-04
1.650E+01	7.155E-04	5.117E-04	3.593E-04	3.339E-04
1.750E+01	6.744E-04	4.734E-04	3.226E-04	2.868E-04
1.850E+01	6.497E-04	4.478E-04	2.970E-04	2.644E-04
1.950E+01	6.229E-04	4.310E-04	2.727E-04	2.259E-04
2.100E+01	5.618E-04	3.712E-04	2.230E-04	1.871E-04
2.300E+01	5.141E-04	3.325E-04	1.809E-04	1.512E-04
2.500E+01	4.758E-04	3.070E-04	1.538E-04	1.227E-04
2.700E+01	4.424E-04	2.845E-04	1.326E-04	9.692E-05
2.900E+01	4.285E-04	2.702E-04	1.142E-04	8.285E-05
3.100E+01	4.042E-04	2.539E-04	1.017E-04	6.940E-05
3.300E+01	3.893E-04	2.379E-04	8.642E-05	5.939E-05
3.500E+01	3.683E-04	2.431E-04	7.054E-05	5.056E-05
3.700E+01	3.587E-04	2.245E-04	6.070E-05	4.272E-05
3.900E+01	3.394E-04	2.174E-04	5.679E-05	3.604E-05
4.100E+01	3.316E-04	1.898E-04	4.881E-05	2.978E-05
4.300E+01	3.173E-04	1.848E-04	4.268E-05	2.677E-05
4.500E+01	3.094E-04	1.847E-04	3.932E-05	2.286E-05
4.700E+01	2.979E-04	1.743E-04	3.487E-05	2.003E-05
4.900E+01	2.894E-04	1.647E-04	2.977E-05	1.630E-05
5.250E+01	2.765E-04	1.517E-04	2.467E-05	1.297E-05
5.750E+01	2.576E-04	1.311E-04	1.912E-05	8.934E-06
6.250E+01	2.505E-04	1.151E-04	1.510E-05	6.072E-06
6.750E+01	2.292E-04	1.024E-04	1.080E-05	4.469E-06
7.250E+01	2.204E-04	9.198E-05	8.506E-06	3.146E-06
7.750E+01	2.080E-04	7.881E-05	6.390E-06	1.922E-06
8.250E+01	1.998E-04	6.798E-05	5.005E-06	1.562E-06
8.750E+01	1.891E-04	6.082E-05	3.995E-06	1.122E-06
9.250E+01	1.770E-04	5.218E-05	2.958E-06	7.023E-07
9.750E+01	1.671E-04	4.379E-05	2.143E-06	5.024E-07
1.075E+02	1.532E-04	3.599E-05	1.300E-06	3.352E-07
1.150E+02	1.413E-04	2.660E-05	1.215E-06	
1.250E+02	1.246E-04	1.944E-05		
1.350E+02	1.114E-04	1.311E-05		
1.450E+02	9.804E-05	8.689E-06		
1.550E+02	8.426E-05	5.635E-06		
1.650E+02	7.005E-05	3.289E-06		
1.750E+02	5.653E-05	2.043E-06		
1.850E+02	4.365E-05	1.128E-06		
1.950E+02	3.198E-05	5.262E-07		
2.100E+02	1.846E-05			
2.300E+02	6.205E-06			
2.500E+02	1.197E-06			

*Read as 1.150×10^{1}.

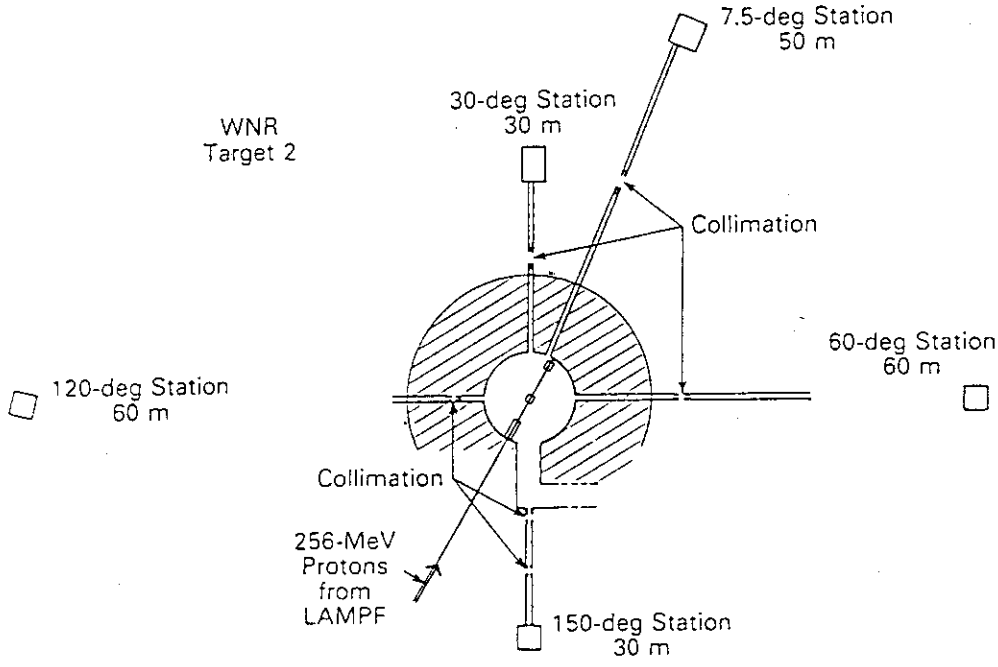

Fig. 1.1.1 Plan view of the target 2 area of WNR and detector stations available for TOF measurements.

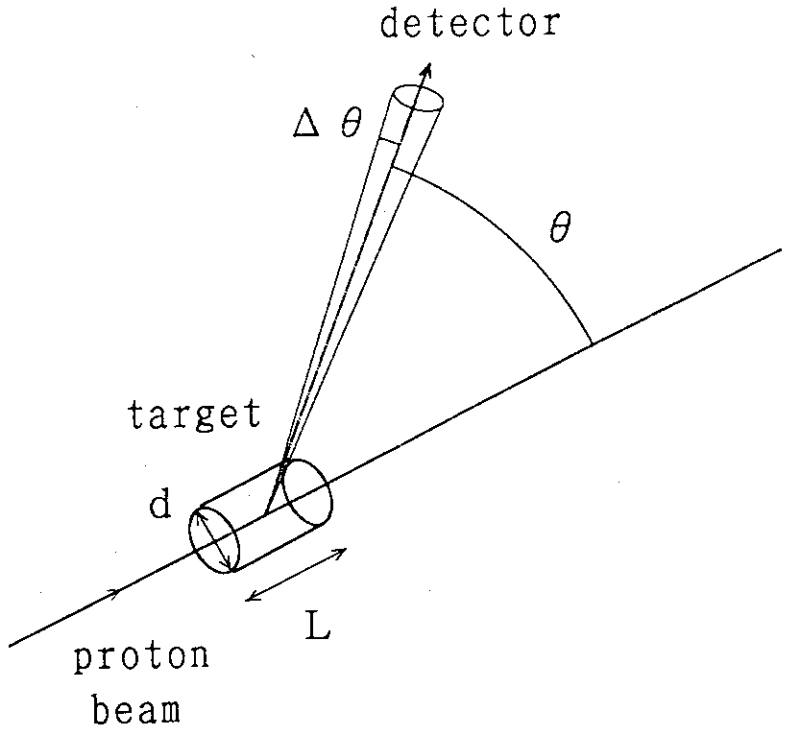

Fig. 1.1.6 Modeled configuration.

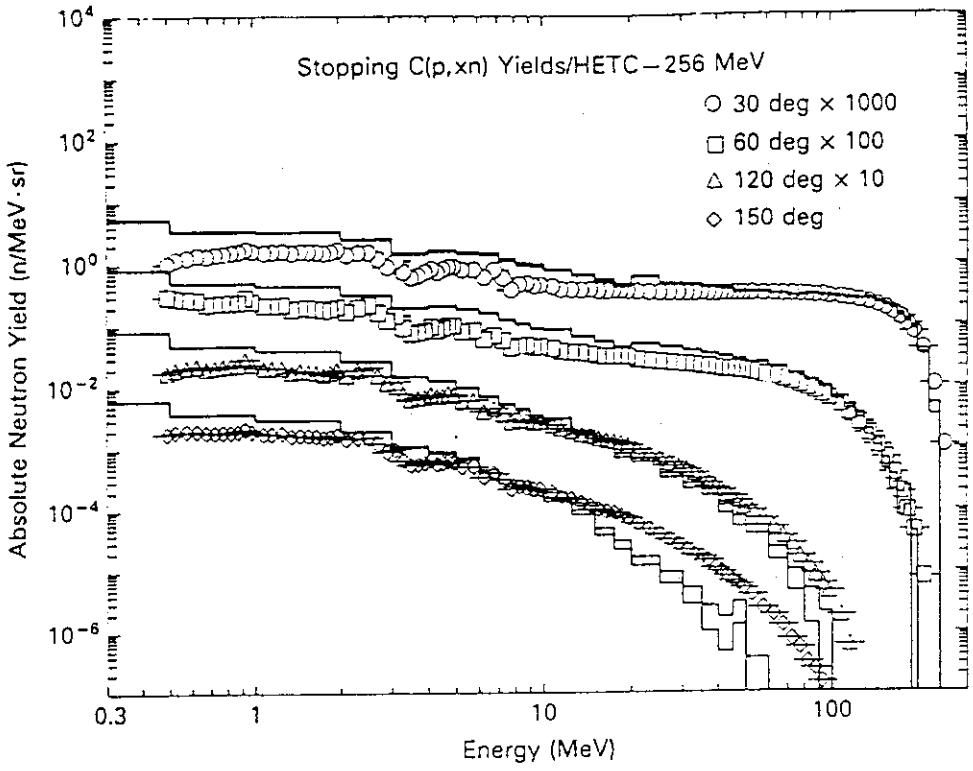

Fig. 1.1.2 Experimental absolute neutron yields for the stopping-length carbon target compared with HETC calculations.

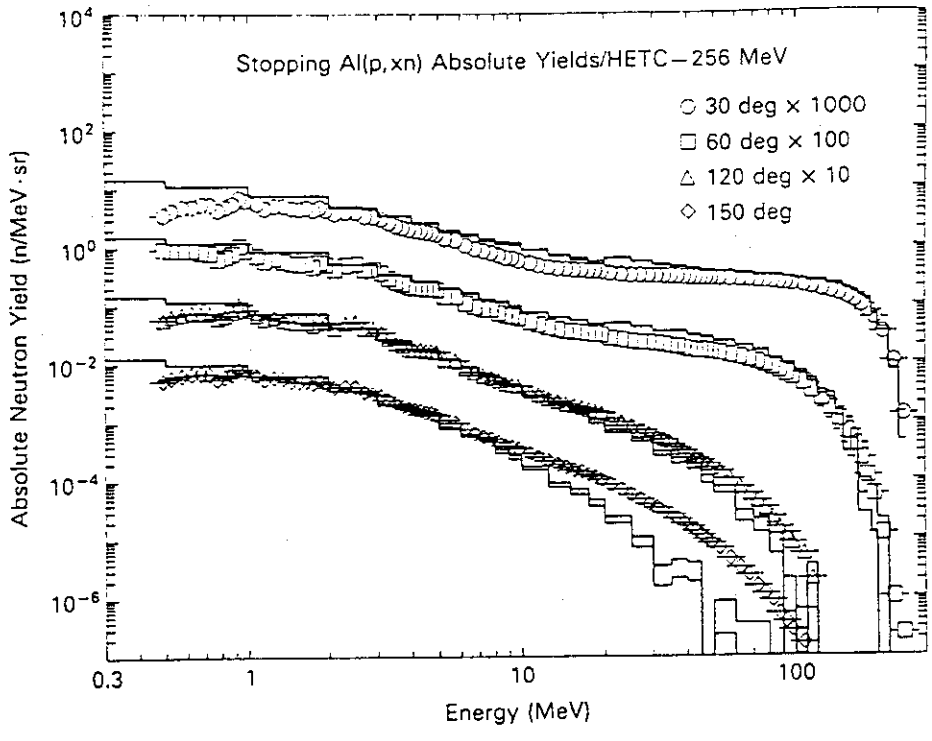

Fig. 1.1.3 Experimental absolute neutron yields for the stopping-length aluminum target compared with HETC calculations.

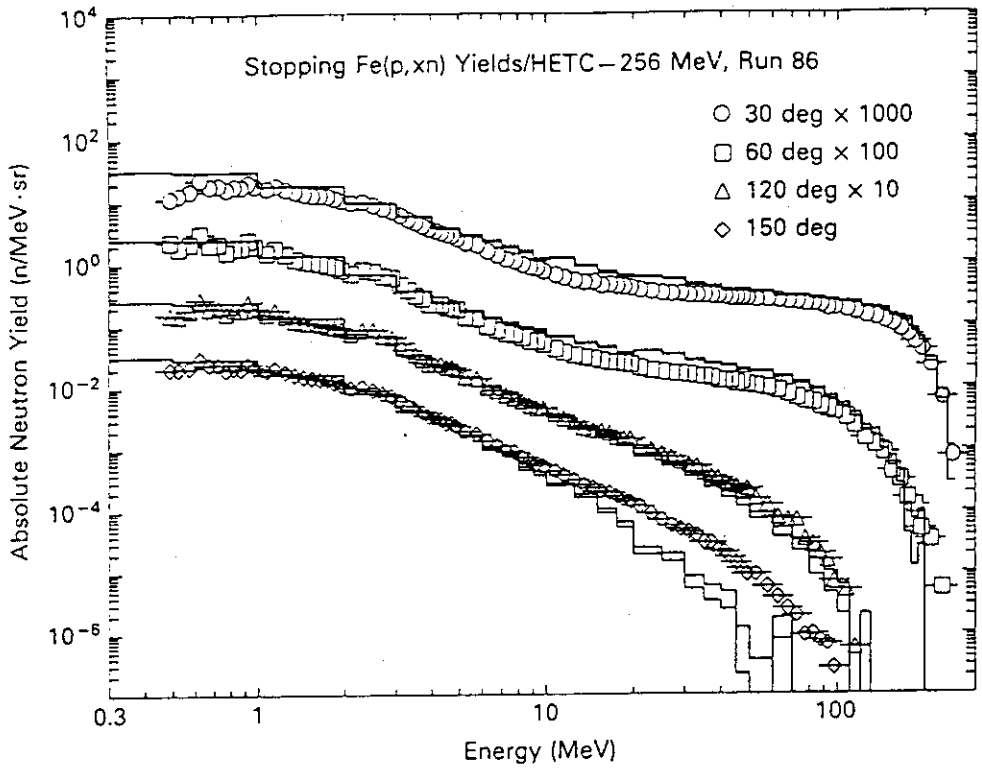

Fig. 1.1.4 Experimental absolute neutron yields for the stopping-length iron target compared with HETC calculations.

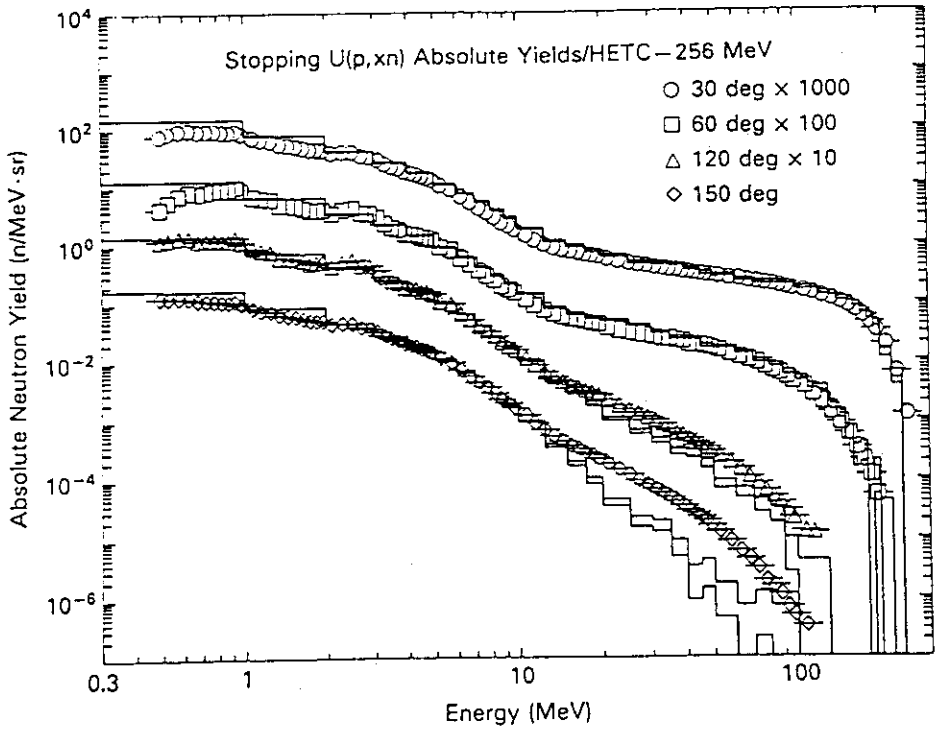

Fig. 1.1.5 Experimental absolute neutron yields for the stopping-length uranium target compared with HETC calculations.

1.2 Neutron Angular and Energy Distributions from 710-MeV Alphas Stopping in Water, Carbon, Steel and Lead

(Summary)

1) Accelerator(Organization)	:	Cyclotron (Space Radiation Effects Laboratory)
2) Projectile(Energy)	:	Alpha (710MeV)
3) Target Material	:	Water, Carbon, Steel and Lead
4) Shielding Material	:	No Shield
5) Geometry	:	Rectangular Block of Carbon, Steel and Lead Cylinder Contained with Water
6) Instruments	:	NE102 and NE213 Scintillation Counter (Time-of-Flight Method)
7) Measured Quantities	:	Absolute Neutron Yields

1. Experimental Arrangement

Figure 1.2.1 shows the experimental arrangement and indicates a typical placement of neutron counters. A 710-MeV alpha beam was extracted from the cyclotron and transports to the experimental area in an evacuated beam line. The external alpha beam passed through a beam telescope consisting of two thin NE102 plastic scintillators shown as S1 and S2 in Fig. 1.2.1. After traversing the beam telescope, an alpha particle stopped in the target T. The beam height is 1.5 m above the concrete floor of the experimental area. The detector angles are referenced to a sphere coordinate system with its origin at the center of the target and the positive z axis along the direction of the beam. No local shielding was used near the counters in order to minimize neutron in-scattering.

2. Method of Measurement and Instrument

Time-of-flight technique was applied for measuring the neutron angular spectra at 0, 6, 15, 30, 45, 60, 90, 120 and 150 degree, in which various sizes of NE102 scintillators were located at each angle as indicated in Table 1.2.1. A 5.1-cm diam by 5.1-cm thick NE213 counter was also placed at a flight path of 1 m from the target at 0, 45, 90 and 135 degree to measure the low energy portion of the neutron spectrum.

3. Target Geometry and Beam Conditions

The carbon, steel and lead targets were rectangular blocks as summarized in Table 1.2.2. The targets were oriented by the angle θ_T of the spherical coordinate system in Fig. 1.2.1. The water target was contained in a 22.9 cm long by 15.2 cm diam aluminum cylinder with a wall thickness of 1.4 mm. The beam entrance end of the cylinder was a 0.05 mm aluminum foil, and the exit end was a 3.2 mm thick aluminum plate. In this case, the alpha beam was induced along the axis of the cylindrical target.

The beam spot size incident on the target was about 2 cm high by 3 cm wide.

4. Measured Results

The absolute neutron yield for each targets are shown in Figs 1.2.2 through 1.2.6, and tabulated in Table 1.2.3. Low energy neutron yields are plotted in these figures and tabulated in Tables 1.2.4 and 1.2.5. Percent uncertainties from statistical error are listed in these tables and scale uncertainties are summarized in Table 1.2.6.

5. Model for Calculation

a. Source Condition

Mono-directional 710 MeV alpha.

b. Calculation Geometry

Figure 1.2.7 shows the modeled configuration. The dimensions and orientations are showed in Table 1.2.1. For the solid targets, alpha beam is injected to a side of rectangular blocks with orientation described by angle θ_T of spherical coordinate system in Fig. 1.2.7, while beam bombarded at the center of the target along the axis for the water target.

6. Normalization Between Calculation and Measurement

All absolute experimental data are given in unit of n/MeV/steradian/10^6alphas.

Reference

1. Cecil R. A., Anderson B. D., Baldwin A. R., Madey R., Galonsky A., Miller P., Young L. and Waterman F. M.: "Neutron Angular and Energy Distributions from 710-MeV Alphas Stopping in Water, Carbon, Steel, and Lead, and 640-MeV Alphas Stopping in Leads," Phys. Rev. C21, 2471-2484 (1980).

Table 1.2.1 NE102 scintillator dimensions and locations.

Angle (degree)	Thickness (cm)	Diameter (cm)	Flight Path (m)
Arrangement 1			
0	10.2	12.7	4.9
6	10.2	12.7	4.9
−15	21.6	12.7	5.0
−30	21.6	12.7	5.0
−45	20.3	23.9	5.0
Arrangement 2			
−60	10.2	12.7	3.0
−90	21.6	12.7	3.0
120	21.6	12.7	2.0
150	20.3	20.3	2.0

Table 1.2.2 Target dimensions and orientations.

Material	Carbon	Steel	Lead	Water
Geometry	Rectangular Block			Cylinder
Width(cm)	15.2	15.4	10.2	
Height(cm)	12.7	10.2	10.2	22.9
Diameter(cm)				15.2
Thickness (g/cm^2) (cm)	25.13 14.73	34.43 4.445	44.65 3.937	22.86 22.86
Orientaion θ_T (degree)	23.5	23.5	22.5	0.0

Table 1.2.3 Neutron yields from 710 MeV alpha stopping in carbon, water, steel, and lead targets.

Energy (MeV)	Neutron yield (Neutrons/10^6/alphas/MeV/sr)			
	Carbon	Water	Steel	Lead
		0 deg		
10.0	2250 (8.5)	2430 (10.0)	2470 (16.0)	3850 (5.4)
12.3	2380 (6.5)	2150 (8.6)	2430 (13.0)	3340 (4.9)
15.0	2480 (5.5)	1960 (7.9)	2570 (11.0)	2940 (4.6)
18.5	2210 (5.3)	1860 (7.2)	2250 (10.0)	2640 (4.4)
22.8	2780 (4.1)	2280 (5.6)	1840 (10.0)	2590 (4.0)
28.2	2740 (3.4)	2360 (4.4)	1760 (8.2)	2030 (3.7)
35.2	2850 (2.8)	2560 (3.6)	2050 (6.3)	2030 (3.2)
44.3	3180 (2.3)	2930 (2.8)	2070 (5.3)	1920 (2.8)
56.5	3920 (1.8)	3730 (2.2)	2380 (4.3)	1900 (2.5)
68.6	4720 (2.0)	4780 (2.4)	2740 (5.0)	2070 (2.9)
79.8	5740 (1.7)	5640 (2.1)	3150 (4.3)	2290 (2.6)
93.7	6340 (1.5)	6500 (1.8)	3600 (3.7)	2430 (2.3)
111.0	7190 (1.3)	7110 (1.6)	4130 (3.2)	2590 (2.0)
134.0	6900 (1.2)	6640 (1.4)	3850 (2.9)	2370 (1.9)
165.0	5260 (1.2)	4470 (1.5)	3000 (2.9)	1890 (1.8)
207.0	2370 (1.5)	1930 (2.0)	1350 (3.6)	865 (2.3)
268.0	488 (2.7)	369 (3.8)	242 (7.2)	170 (4.4)
363.0	40.2 (7.9)	29.5(12.0)	15.3(27.0)	14.7(13.0)
525.0	2.4(32.0)			
		6 deg		
10.0	2610 (7.9)		3390 (11.0)	4850 (5.0)
12.3	2450 (6.6)		2770 (11.0)	3450 (5.0)
15.0	2470 (5.6)		2220 (11.0)	3210 (4.5)
18.5	2510 (5.0)		2480 (8.9)	3030 (4.1)
22.8	2890 (4.1)		2700 (7.6)	2660 (4.0)
28.2	2620 (3.5)		1930 (7.4)	2250 (3.5)
35.2	2790 (2.9)		1870 (6.4)	2040 (3.2)
44.3	2940 (2.4)		2100 (5.1)	1930 (2.7)
56.5	3300 (2.0)		2280 (4.3)	1910 (2.4)
68.6	3820 (2.3)		2270 (5.4)	2020 (2.9)
79.8	4300 (2.0)		2630 (4.7)	2020 (2.7)
93.7	4450 (1.8)		2480 (4.5)	2110 (2.5)
111.0	4470 (1.7)		2470 (3.9)	2080 (2.3)
134.0	4190 (1.5)		2540 (3.6)	1780 (2.2)
165.0	3080 (1.6)		1820 (3.7)	1350 (3.2)
207.0	1550 (1.9)		902 (4.5)	637 (2.7)
268.0	406 (3.0)		244 (7.1)	165 (4.4)
363.0	50.0 (7.0)		30.7(17.0)	18 (12.0)
525.0	2.5(29.0)			

Table 1.2.3 (Continued.)

Energy (MeV)	Neutron yield (Neutrons/10^6/alphas/MeV/sr)							
	Carbon		Water		Steel		Lead	
				15 deg				
11.4	2540	(4.9)	1720	(7.4)	2640	(8.7)	4240	(3.5)
14.6	2550	(3.9)	1890	(5.6)	2610	(7.4)	3250	(3.4)
18.6	2510	(3.5)	2140	(4.5)	2210	(7.0)	2520	(3.5)
23.6	2690	(3.0)	2070	(4.1)	2100	(6.4)	2460	(3.1)
29.9	2480	(2.5)	1980	(3.3)	1980	(5.2)	2010	(2.8)
37.8	2450	(2.2)	1980	(2.8)	1870	(4.6)	1820	(2.5)
47.6	2430	(1.9)	1990	(2.5)	1790	(4.1)	1690	(2.2)
56.7	2590	(2.3)	2050	(3.1)	1780	(5.2)	1640	(2.8)
64.3	2650	(2.2)	2190	(2.8)	1940	(4.7)	1560	(2.7)
72.9	2660	(2.1)	2170	(2.8)	1770	(4.8)	1500	(2.7)
83.0	2480	(2.1)	2030	(2.7)	1660	(4.7)	1360	(2.7)
94.9	2300	(2.0)	1870	(2.6)	1530	(4.5)	1290	(2.6)
109.0	1960	(2.0)	1650	(2.6)	1330	(4.5)	1010	(2.7)
126.0	1580	(2.1)	1340	(2.6)	988	(4.8)	851	(2.7)
147.0	1050	(2.3)	925	(2.9)	732	(5.1)	558	(3.0)
172.0	578	(2.9)	518	(3.5)	378	(6.5)	317	(3.7)
205.0	271	(3.7)	236	(4.6)	146	(9.3)	133	(5.2)
249.0	91.9	(5.6)	78.3	(7.2)	50.6	(14.0)	46.4	(8.1)
309.0	16.3	(12.0)	14.3	(16.0)			5.1	(30.0)
				30 deg				
11.4	2180	(5.5)	1850	(7.5)	3020	(8.2)	4330	(3.6)
14.6	2260	(4.3)	1560	(6.7)	2410	(7.7)	2840	(3.9)
18.6	2100	(4.0)	1550	(5.8)	2260	(7.1)	2320	(3.9)
23.6	2130	(3.5)	1690	(4.8)	1670	(7.5)	2150	(3.5)
29.9	1790	(3.0)	1370	(4.2)	1510	(6.2)	1790	(3.0)
37.8	1590	(2.7)	1380	(3.5)	1230	(5.9)	1360	(3.0)
47.6	1520	(2.4)	1230	(3.3)	1290	(4.9)	1220	(2.7)
56.7	1440	(3.2)	1250	(4.0)	1050	(6.9)	1040	(3.7)
64.3	1480	(3.0)	1210	(3.9)	985	(6.8)	1000	(3.5)
72.9	1340	(3.0)	1270	(3.7)	891	(6.9)	938	(3.5)
83.0	1180	(3.0)	1120	(3.7)	710	(7.3)	767	(3.6)
94.9	911	(3.3)	832	(4.0)	615	(7.3)	635	(3.7)
109.0	620	(3.7)	589	(4.5)	421	(8.3)	413	(4.4)
126.0	425	(4.1)	386	(5.1)	279	(9.5)	272	(5.0)
147.0	272	(4.7)	236	(6.0)	184	(11.0)	143	(6.6)
172.0	133	(6.2)	126	(7.6)	104	(13.0)	87.1	(7.8)
205.0	55.3	(8.8)	50.1	(11.0)	38.2	(21.0)	33.8	(12.0)
249.0	19.2	(14.0)	14.8	(21.0)				

Table 1.2.3 (Continued.)

Energy (MeV)	Neutron yield (Neutrons/10^6/alphas/MeV/sr)			
	Carbon	Water	Steel	Lead
		45 deg		
11.1	1650 (3.3)	1370 (4.7)	2260 (5.1)	3270 (2.3)
14.1	1410 (3.0)	1290 (3.9)	1590 (5.2)	2320 (2.4)
17.9	1380 (2.7)	1250 (3.5)	1410 (5.0)	1720 (2.6)
22.7	1270 (2.5)	1200 (3.1)	1280 (4.7)	1530 (2.4)
28.6	1080 (2.2)	1020 (2.7)	1000 (4.3)	1210 (2.2)
36.2	893 (2.1)	875 (2.5)	842 (4.0)	944 (2.1)
45.9	791 (1.9)	780 (2.3)	696 (3.8)	712 (2.1)
54.9	683 (2.6)	682 (3.0)	549 (5.4)	568 (2.9)
62.7	582 (2.7)	588 (3,1)	573 (5.0)	516 (2.9)
71.8	510 (2.7)	485 (3.2)	460 (5.3)	411 (3.0)
82.8	426 (2.7)	401 (3.3)	326 (6.0)	335 (3.2)
96.2	327 (2.9)	299 (3.6)	275 (6.0)	255 (3.4)
113.0	219 (3.3)	210 (4.0)	162 (7.4)	154 (4.1)
133.0	131 (3.9)	126 (4.7)	99.5 (8.7)	88.9 (5.1)
159.0	59.8 (5.3)	52.4 (6.8)	40.9(13.0)	36.1 (8.0)
194.0	22.3 (7.9)	21.0(10.0)	17.3(19.0)	12.5(14.0)
239.0	6.1(15.0)	5.6(20.0)		
		60 deg		
10.5	908 (8.2)	819 (8.9)	1360 (6.5)	1930 (4.9)
13.0	765 (7.4)	799 (7.2)	1230 (5.6)	1300 (5.1)
16.2	777 (6.5)	702 (6.8)	888 (6.1)	999 (5.3)
20.3	699 (6.2)	690 (6.2)	797 (5.9)	789 (5.5)
25.5	584 (5.9)	617 (5.6)	605 (6.0)	590 (5.6)
32.3	540 (5.0)	560 (4.8)	516 (5.2)	463 (5.0)
41.3	402 (4.7)	421 (4.5)	375 (5.0)	346 (4.7)
53.5	319 (4.7)	311 (4.6)	298 (5.0)	255 (4.8)
65.8	251 (6.5)	213 (6.9)	226 (7.0)	168 (7.6)
77.2	220 (6.6)	174 (7.3)	177 (7.5)	130 (8.3)
91.7	146 (7.3)	107 (8.5)	112 (8.6)	80.8(10.0)
110.0	68.7(10.0)	74.4 (9.4)	59.8(11.0)	58.6(11.0)
135.0	37.4(12.0)	34.9(13.0)	28.8(14.0)	15.9(25.0)
169.0	19.2(15.0)	13.1(19.0)	11.8(21.0)	
217.0	4.2(31.0)			
		90 deg		
13.2	574 (3.9)	550 (3.7)	964 (3.8)	1160 (2.2)
17.8	417 (4.0)	366 (4.1)	579 (4.5)	640 (2.7)
23.8	377 (3.7)	307 (3.9)	496 (4.4)	458 (2.8)
31.8	250 (3.5)	168 (4.2)	319 (4.3)	262 (2.9)
42.3	143 (3.8)	110 (4.3)	173 (4.9)	155 (3.2)
56.2	86.8 (4.4)	56.9 (5.4)	111 (5.6)	87.4 (3.9)
69.4	47.0 (7.7)	34.7 (9.0)	56.8(10.0)	49.1 (7.1)
81.6	25.6 (9.8)	20.5(11.0)	39.8(12.0)	30.6 (8.7)
96.7	12.9(14.0)	13.5(13.0)	29.9(13.0)	17.0(12.0)
115.0	6.9(18.0)	6.0(20.0)	11.9(21.0)	9.4(17.0)
139.0			4.7(33.0)	

Table 1.2.3 (Continued.)

Energy (MeV)	Neutron yield (Neutrons/10^6/alphas/MeV/sr)			
	Carbon	Water	Steel	Lead
		120 deg		
13.2	393 (4.7)	330 (4.8)	792 (3.0)	1190 (2.1)
17.8	283 (4.9)	234 (5.0)	420 (3.7)	622 (2.7)
23.8	182 (5.5)	150 (5.5)	290 (4.0)	330 (3.4)
31.8	91.1 (6.1)	68.8 (6.5)	148 (4.4)	173 (3.7)
42.3	39.6 (8.0)	32.7 (8.1)	72.8 (5.3)	74.6 (5.1)
56.2	15.3(12.0)	11.6(13.0)	28.2 (7.9)	33.5 (7.6)
69.4	11.0(18.0)	6.0(25.0)	12.9(16.0)	13.1(19.0)
81.6			6.9(21.0)	10.2(20.0)
		150 deg		
12.8	347 (2.7)	222 (3.3)	648 (1.9)	1080 (1.2)
17.1	218 (3.0)	148 (3.5)	348 (2.3)	483 (1.8)
22.8	133 (3.5)	81.3 (4.4)	192 (2.9)	255 (2.3)
30.4	55.7 (4.4)	38.5 (5.2)	83.8 (3.6)	108 (3.1)
40.7	21.7 (6.1)	15.0 (7.4)	31.8 (5.1)	40.9 (4.7)
54.7	7.5(10.0)	6.0(11.0)	9.4 (9.6)	12.0(10.0)
68.7				4.0(30.0)

Percent uncertainties (in parenthes) are statistical only. The yields include neutrons produced by the interactions of primary neutrons and secondary chraged particles as well as the effects of neutron scattering in the thick targets.

Table 1.2.4 Low-energy neutron yields from 710 MeV alphas stopping in a lead target.

Energy (MeV)	Neutron yield (Neutrons/10^6/alphas/MeV/sr)		
	0 degree	90 degree	135 degree
3.39	31,600(2.6)	17,800(3.2)	19,000 (2.7)
3.91	23,500(2.6)	13,400(3.2)	15,100 (2.6)
4.52	17,600(2.7)	9,100(3.4)	11,300 (2.7)
5.27	13,500(3.8)	6,670(3.6)	8,120 (2.8)
6.18	10,200(3.0)	4,880(3.9)	5,780 (3.1)
7.32	7,900(3.1)	3,590(4.1)	4,030 (3.4)
8.79	5,750(3.7)	2,490(4.6)	2,920 (3.7)
10.6	4,230(3.8)	1,670(5.2)	1,870 (4.3)
13.1	3,470(3.8)	1,180(5.8)	1,210 (5.1)
16.3	2,510(3.8)	772(6.1)	709 (5.7)
20.9	2,080(3.3)	491(6.4)	399 (6.4)
27.3	1,700(3.2)	298(7.2)	208 (8.0)
37.1	1,690(2.7)	230(7.2)	136 (8.8)
52.9	1,690(2.3)	141(8.2)	80.1(10.0)

Table 1.2.5 Low-energy neutron yields at 45 degree from 710 MeV alphas stopping in carbon, water, steel, and lead targets.

Energy (MeV)	Neutron yield (neutrons/10^6/alphas/MeV/sr)			
	Carbon	Water	Steel	Lead
3.39	3,040(7.0)	2,420(7.9)	10,100(4.6)	35,900(2.2)
3.91	2,960(6.0)	2,320(6.7)	7,200(4.7)	26,900(2.2)
4.52	3,120(5.0)	2,050(6.3)	5,930(4.6)	21,100(2.2)
5.27	2,370(5.2)	1,880(5.8)	4,600(4.7)	15,500(2.4)
6.18	2,040(5.2)	1,630(5.8)	4,040(4.5)	11,700(2.5)
7.32	1,810(5.0)	1,400(5.6)	3,000(4.8)	8,510(2.7)
8.79	1,440(5.2)	1,180(5.6)	2,490(4.9)	5,900(3.0)
10.60	1,410(4.8)	1,230(5.0)	2,060(5.0)	4,670(3.1)
13.10	1,440(4.4)	1,400(4.3)	1,620(5.2)	3,350(3.4)
16.30	1,220(4.0)	1,160(4.0)	1,230(5.0)	2,400(3.4)
20.90	974(3.7)	959(3.6)	1,000(4.5)	1,620(3.4)
27.30	866(3.4)	858(3.3)	760(4.5)	1,240(3.4)
37.10	760(3.2)	792(3.0)	694(4.0)	1,090(3.2)
52.90	681(3.0)	658(3.0)	601(3.8)	802(3.3)

Table 1.2.6 Scale uncertainties.

Source	Percent uncertainty		
Number of alphas	2		
Efficiency	5		
Background	7		
Target:	Steel/Lead	Carbon	Water
Solid-angle[a]	1(3)	4(6)	6(9)
Total[a]	9(9)	10(11)	11(13)

[a] Numbers in parentheses are for the NE213 counter.

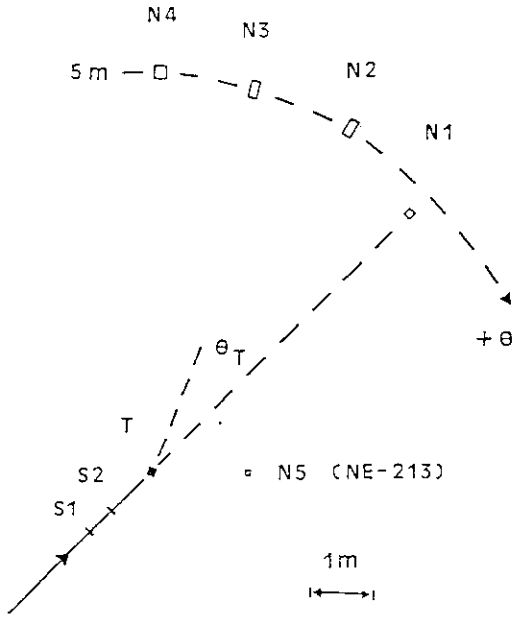

Fig. 1.2.1 Plan view of experimental arrangement.

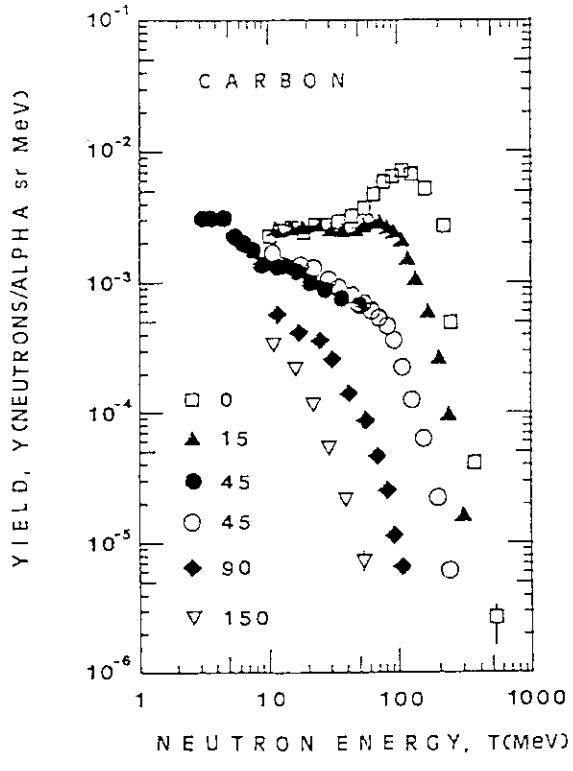

Fig. 1.2.2 Neutron yield spectra at laboratory angles of 0, 15, 45, 90, and 150 deg from 710 MeV alphas stopping in a carbon target.

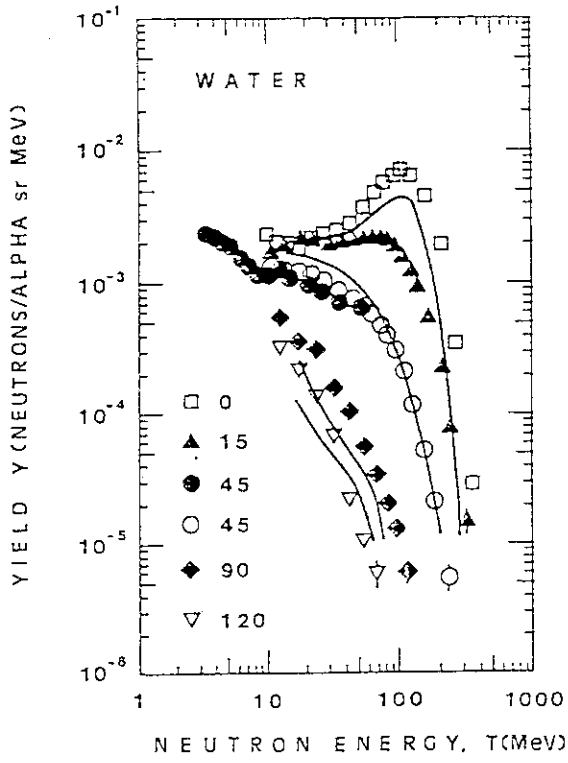

Fig. 1.2.3 Neutron yield spectra at laboratory angles of 0, 15, 45, 90, and 120 deg from 710 MeV alphas stopping in a water target.

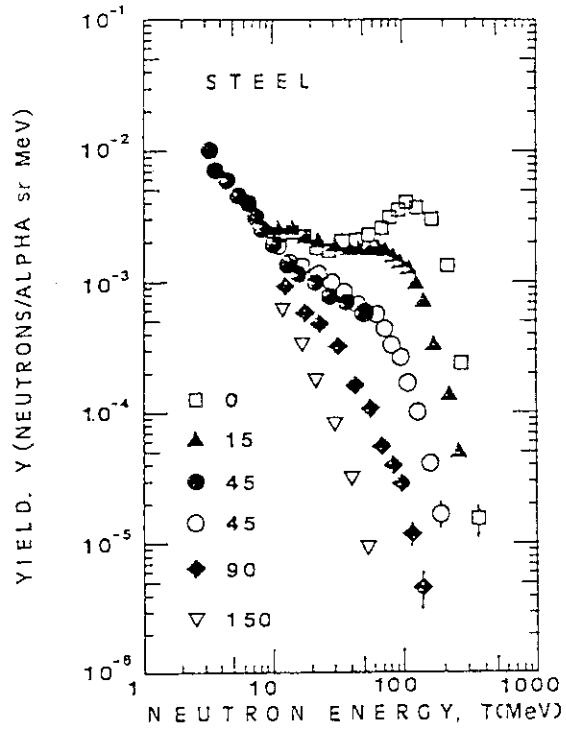

Fig. 1.2.4 Neutron yield spectra at laboratory angles of 0, 15, 45, 90, and 150 deg from 710 MeV alphas stopping in a steel target.

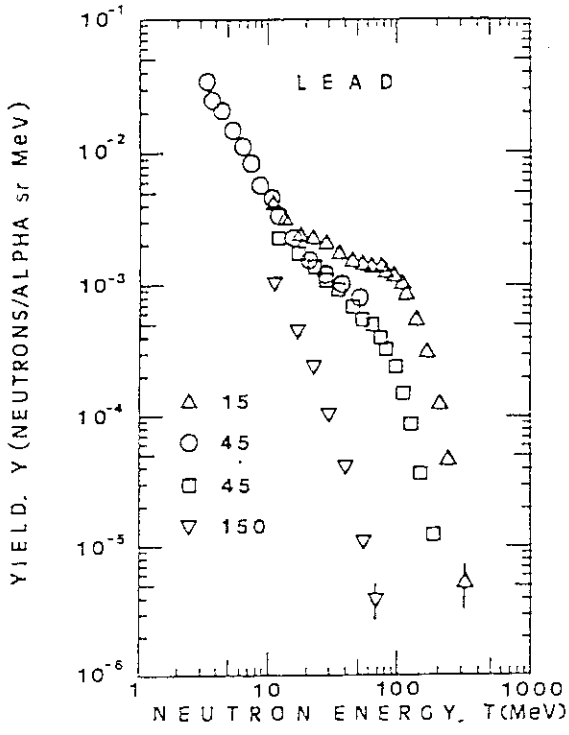

Fig. 1.2.5 Neutron yield spectra at laboratory angles of 15, 45, and 150 deg from 710 MeV alphas stopping in a lead target.

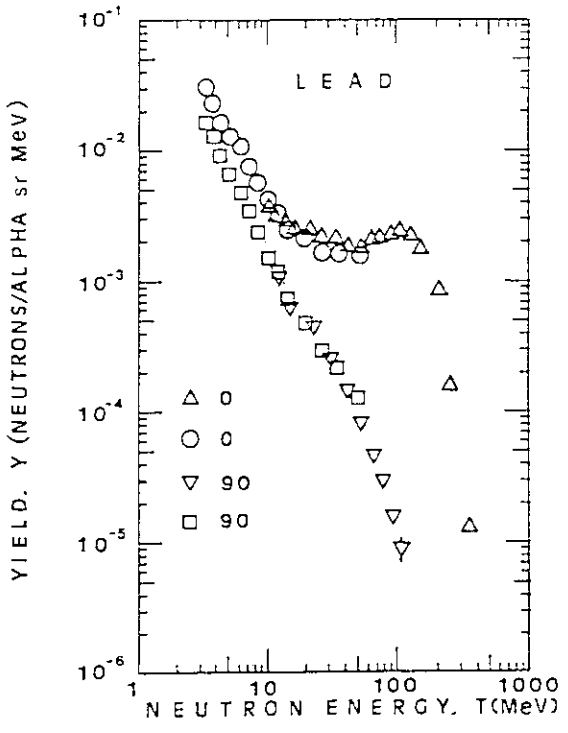

Fig. 1.2.6 Neutron yield spectra at laboratory angles of 0 and 90 deg from 710 MeV alphas stopping in a lead target obtained by NE-213 counter.

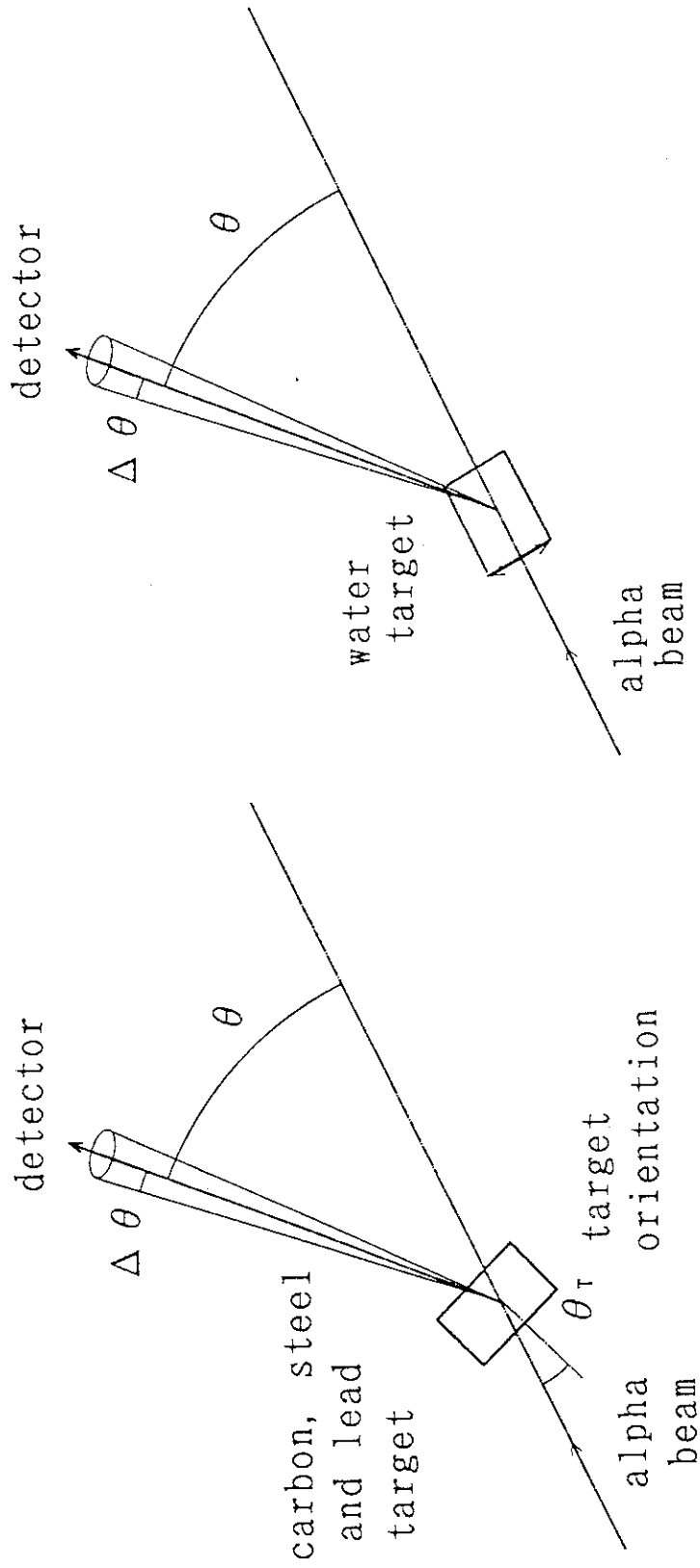

Fig. 1.2.7 Modeled configuration.

1.3 Photoproduction of High-Energy Neutrons in Thick Lead Targets by Electrons in the Energy Range 150 to 270 MeV

(Summary)

1) Accelerator(Organization)	:	Electron Linac (Mainz University)
2) Projectile(Energy)	:	Electron (150 – 266MeV)
3) Target Material	:	Lead
4) Shielding Material	:	No Shield
5) Geometry	:	Rectangular Block
6) Instruments	:	NE102A Scintillation Counter (Recoil Proton Detection and Time-of-Flight Method)
7) Measured Quantities	:	Absolute Neutron Yields

1. Experimental Arrangement

The schematic arrangement and the diagrammatic view of the target and collimator setup are shown in Figs. 1.3.1 and 1.3.2. The undeflected electron beam from the Mainz Electron Linac is focused on the lead target to a diameter of about 1 cm. Neutrons emitted from the target at an angle of 90 degree pass variable-aperture lead collimator of 50 cm length with the aperture of 4 cm. In addition they pass a lead collimator of 100 cm length with a fixed aperture diameter of 5 cm. In front of these collimators lead absorbers of 12 cm thickness was placed, to improve the γ/n ratio.

The neutrons produced in the target, after having passed the lead collimator, impacted on two polyethylene or carbon converters which can be positioned in the neutron beam for proton recoil counter telescope and protn time-of-flight method. In order to reduce the back ground and the losses by multiple scattering, the converter and the flight path are placed in a helium-filled chamber.

For the neutron time-of-flight measurements neutrons are led to the neutron detector placed at a distance of 24.6 m from the target through the lead collimators descrived above and a 3 m thick wall of concrete with an aperture of 20 cm diameter.

2. Method of Measurement and Instrument

Three kinds of methods were applied to measure the neutron spectra: proton recoil

counter terescope, proton time-of-flight method and neutron time-of-flight method. The telescope is placed at an angle of 30 degree and consists of nine plastic scintillation counters (NE102A: 0.022 cm thick) in a compact one-after-another arrangement with five aluminum absorbers between the last six counters. In the proton time-of-flight equipment, the energy of the recoil proton was determined by the measurement of their transit time between two scintillation counter pairs 200 cm apart consisted of Naton 136 plastic scintillators 0.05 cm thick with an area of 7 x 7 cm. In the neutron time-of-flight measurements the detector uesd is a NE102A scintillator, 5 cm thick and with an area of 10 x 10 cm.

3. Target Geometry and Beam Conditions

The target was composed of eight lead sheets with a thickness of 0.3 cm each (4.3 radiation lengths) and a diameter of 6.8 cm, placed one behind the other with a spacing of 0.2 cm for water cooling as shown in Fig. 1.3.2.

An average electron current was 30-40 μA, and the pulse length was 3 μsec with repetition rate of 100 Hz for the recoil proton measurment. For the neutron time-of-flight measurements linac pulses of 4.5 nsec FWHM was uesd with a repetition rate of 300 Hz and an average current of 0.3 μA. The electron energy was checked at intervals of 1.5 h with the three-magnetic energy-analyzing system, and the beam current was monitored by a calibrated secondary emission monitor placed 1 m in front of the target.

4. Measured Results

The neutron production cross sections for six primary electron energies between 150 and 266 MeV are shown in Fig. 1.3.3 and tabulated in Table 1.3.1. The standard deviation of experimental data for En less than 100 MeV is less than 10 %. The total error is estimated to ±20 %, mainly due to systematic errors of current monitoring, the uncertainties in the determination of detector efficiency, the neutron attenuation losses and the errors in the energy calibration. The absolute agreement among the measurements is better than ±15 %.

5. Model for Calculation

a. Source Condition

Mono-directional monoenergetic electron having the energy between 150 and 266

MeV centered at lead target.

b. Calculation Geometry

Figure 1.3.4 shows the modeled configuration. The target was hitted by electron beam perpendicularly.

6. Normalization Between Calculation and Measurement

All absolute experimental data for 90 degree neutrons are given in unit of μbarn/MeV/steradian/incident electron.

Reference

1. von Eyss H. J. and Luhrs G.: "Photoproduction of High-Energy Neutrons in Thick Targets by Electrons in the Energy Range 150 to 270 MeV," Z.Physik, 262,393-412(1973).

Table 1.3.1 Photoneutron spectra produced by electrons on a thick lead target (4.3 X_0 thickness) .

Energy (MeV)	Neutron Flux (μbarn/MeV/Sr/electron)		
	Ee: 266 MeV	Ee: 234 MeV	Ee: 202 MeV
1.63E+02*	4.39942E-02	1.80780E-02	
1.52E+02	8.35744E-02	3.84935E-02	
1.42E+02	1.43835E-01	6.72295E-02	1.60999E-02
1.33E+02	2.31008E-01	1.10382E-01	3.11847E-02
1.25E+02	3.34895E-01	1.75431E-01	5.25583E-02
1.18E+02	4.49671E-01	2.55339E-01	8.99364E-02
1.11E+02	6.12612E-01	3.59606E-01	1.55602E-01
1.05E+02	8.20678E-01	4.99239E-01	2.29091E-01
1.00E+02	1.05933E+00	6.68149E-01	3.22812E-01
9.45E+01	1.25508E+00	8.28189E-01	4.18532E-01
9.00E+01	1.53964E+00	1.04231E+00	5.52387E-01
8.54E+01	1.80051E+00	1.26483E+00	6.75030E-01
8.16E+01	2.07545E+00	1.44197E+00	7.74247E-01
7.83E+01	2.29783E+00	1.63174E+00	8.92539E-01
7.49E+01	2.48840E+00	1.78025E+00	1.05586E+00
7.11E+01	2.68458E+00	1.91391E+00	1.16895E+00
6.81E+01	2.82334E+00	2.05012E+00	1.25676E+00
6.52E+01	2.92599E+00	2.18008E+00	1.39665E+00
6.25E+01	3.14637E+00	2.28477E+00	1.55818E+00
6.00E+01	3.24904E+00	2.38550E+00	1.63293E+00
5.79E+01	3.44360E+00	2.58459E+00	1.79544E+00
5.54E+01	3.62225E+00	2.80009E+00	1.90976E+00
5.31E+01	3.85289E+00	3.02264E+00	2.09211E+00
5.12E+01	4.14414E+00	3.26263E+00	2.35174E+00
5.00E+01	4.49133E+00	3.58839E+00	2.63427E+00
4.79E+01	4.90229E+00	4.01860E+00	2.82321E+00
4.60E+01	5.65483E+00	4.27573E+00	3.17416E+00
4.48E+01	5.86414E+00	4.75430E+00	3.49082E+00
4.32E+01	6.40164E+00	5.22880E+00	3.72788E+00
4.20E+01	6.83687E+00	5.68796E+00	4.22255E+00
4.05E+01	7.63068E+00	6.16494E+00	4.59283E+00
3.94E+01	8.27058E+00	7.29493E+00	
3.70E+01	9.36423E+00	8.22924E+00	
3.46E+01	1.07997E+01	9.08223E+00	
3.27E+01	1.17883E+01	1.05911E+01	
3.08E+01	1.30587E+01	1.13934E+01	
2.85E+01	1.53966E+01	1.43519E+01	
2.63E+01	1.90439E+01		
2.45E+01	2.56377E+01	1.94574E+01	
2.24E+01	2.98993E+01	2.59985E+01	

* Read as 1.63×10^2 .

Table 1.3.1 (Continued.)

Energy (MeV)	Neutron Flux (μbarn/MeV/sr/electron)		
	Ee: 182 MeV	Ee: 170 MeV	Ee: 150 MeV
1.25E+02*	2.61483E-02	1.26787E-02	
1.18E+02	4.42499E-02	2.21771E-02	1.08719E-02
1.12E+02	7.27364E-02	4.44515E-02	2.03979E-02
1.05E+02	1.24019E-01	6.12491E-02	3.36498E-02
1.00E+02	1.63587E-01	9.35798E-02	5.19841E-02
9.46E+01	2.21439E-01	1.60205E-01	8.76350E-02
9.00E+01	3.08895E-01	2.27616E-01	1.34486E-01
8.60E+01	4.04805E-01	3.16318E-01	1.80137E-01
8.20E+01	5.02081E-01	3.76771E-01	2.44947E-01
7.77E+01	6.04592E-01	4.76028E-01	3.03930E-01
7.47E+01	7.17517E-01	6.10513E-01	3.70063E-01
7.13E+01	8.30221E-01	6.34735E-01	4.54154E-01
6.80E+01	9.60700E-01	7.29135E-01	5.41191E-01
6.50E+01	1.06771E+00	7.80941E-01	6.01450E-01
6.30E+01	1.15257E+00	9.27591E-01	6.83185E-01
6.00E+01	1.27621E+00	1.11799E+00	7.73926E-01
5.80E+01	1.41369E+00	1.28956E+00	8.73079E-01
5.53E+01	1.58294E+00	1.25992E+00	9.28463E-01
5.30E+01	1.65907E+00	1.38566E+00	1.11100E+00
5.18E+01	1.90007E+00	1.54620E+00	1.20412E+00
5.00E+01	2.16753E+00	1.80980E+00	1.29039E+00
4.77E+01	2.40102E+00	2.13437E+00	1.54414E+00
4.65E+01	2.67980E+00	2.30478E+00	1.86179E+00
4.45E+01	3.03495E+00	2.67782E+00	1.99525E+00
4.30E+01	3.31325E+00	2.78727E+00	2.29376E+00
4.20E+01		3.08854E+00	2.58850E+00
4.05E+01	4.11276E+00	3.52343E+00	2.86776E+00
3.85E+01	4.86696E+00		3.11912E+00
3.60E+01	5.75904E+00		3.49294E+00
3.40E+01	6.42581E+00		4.24225E+00
3.20E+01	7.33088E+00		5.09481E+00
3.00E+01	8.39424E+00		5.94103E+00
2.75E+01	1.06528E+01		6.80506E+00
2.67E+01			8.57207E+00
2.48E+01	1.40245E+01		1.06810E+01
2.24E+01	2.00953E+01		1.47018E+01

* Read as 1.25×10^2 .

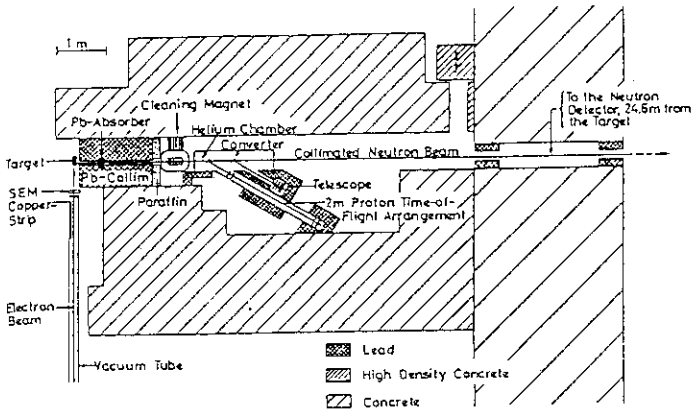

Fig. 1.3.1 Experimental arrangement.

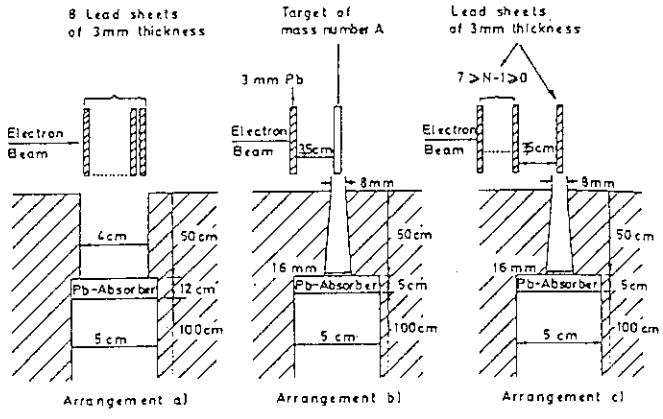

Fig. 1.3.2 Diagrammatic veiw of the target and collimator setup.

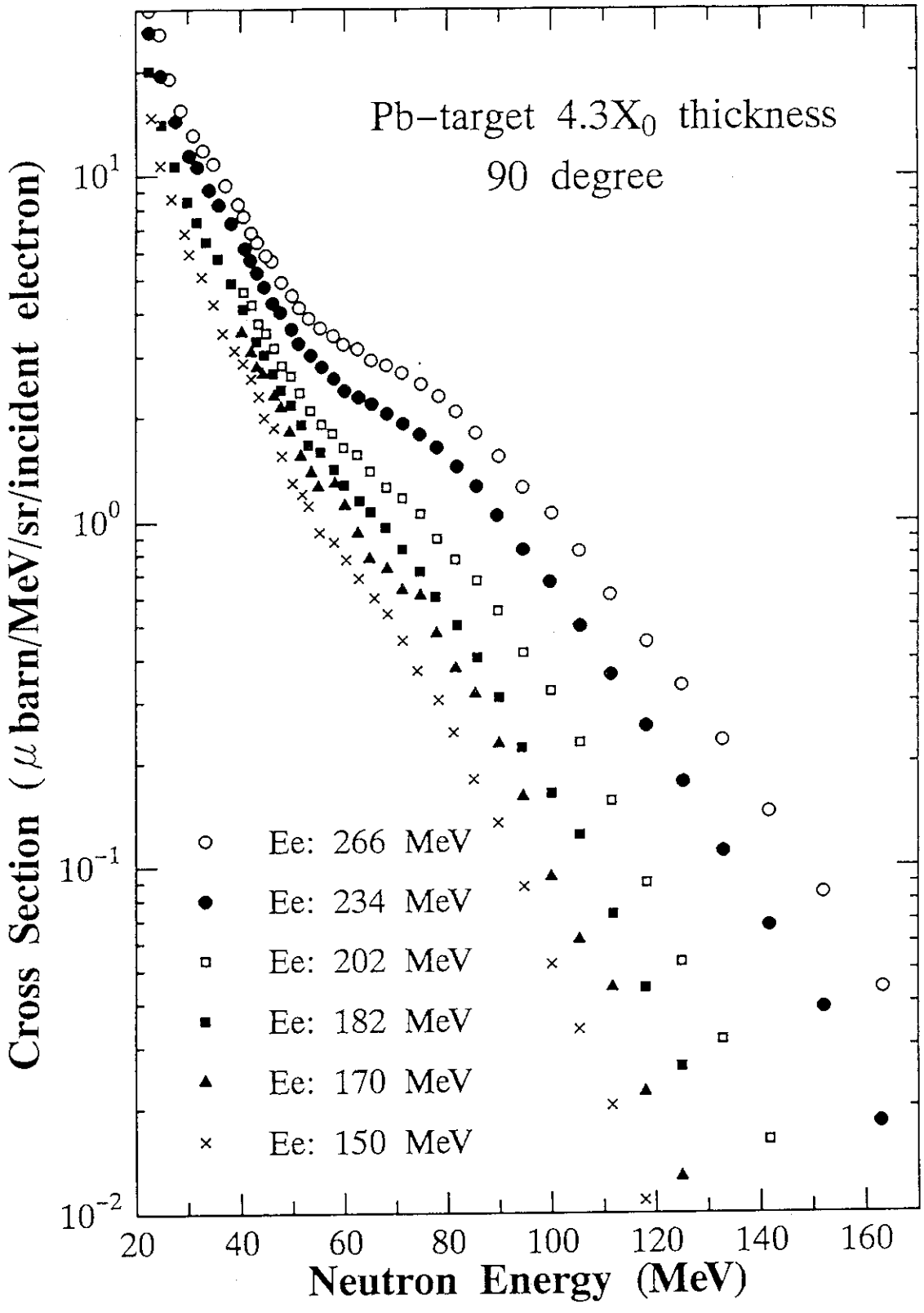

Fig. 1.3.3 Photoneutron spectra produced by electrons on a thick lead target (4.3 X_0 thickness) with primary energies of 150, 170, 182, 202, 234 and 266 MeV.

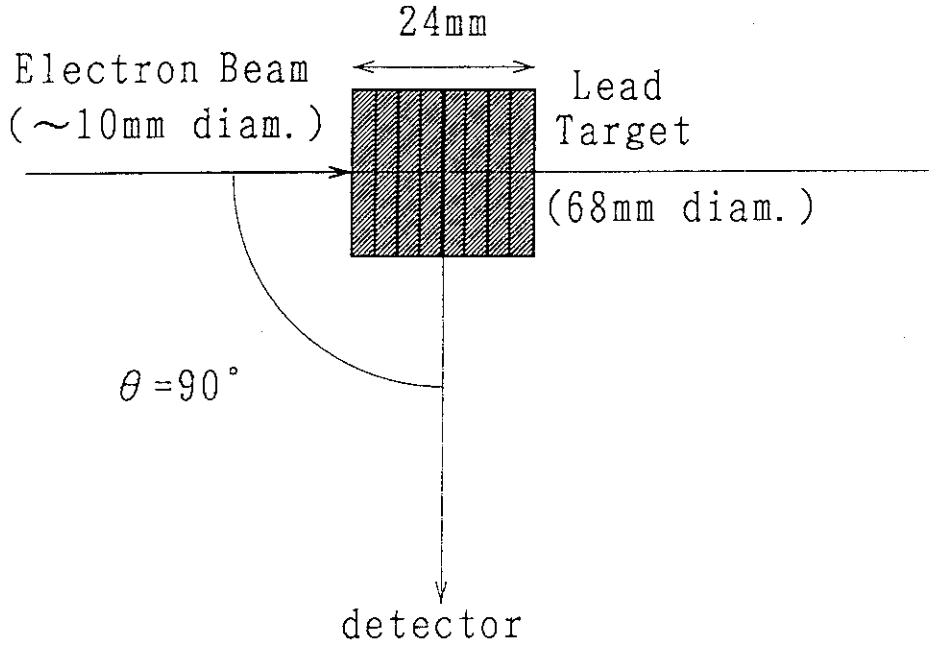

Fig. 1.3.4 Modeled configuration.

2. Secondary Neutron and Photon Transmission Problems

2.1 Transmission Through Shielding Materials of Neutrons and Photons Generated by Intermediate-Energy Protons No.1

(Summary)

1) Accelerator (Organization) : FM cyclotron (INS the Univ. of Tokyo)
2) Projectile (Energy) : P (52MeV)
3) Target (Thickness) : Carbon (2.145cmt)
4) Shielding material : Graphite, Iron, Water and Ordinary Concrete
5) Geometry : Slab
6) Instruments : NE213 Liquid Scintillator, FERDO Unfolding
7) Measured Quantities : Neutron and Photon Energy Spectra

1. Experimental Arrangement

Figure 2.1.1 shows the geometrical arrangement of experiment and Table 2.1.1 gives the dimension of assemblies. A 52 MeV proton beam from the FM cyclotron of the Institute for Nuclear Study at the University of Tokyo irradiated a 2.145-cm-thick graphite target in front of the slab assemblies.

2. Method of Measurement and Instrument

A 51-mm-diam x 51-mm-long NE213 scintillation detector placed in contact with the rear face of the slabs. The pulse height distributions were unfolded to neutron and photon energy spectra by the revised FERDO unfolding code. The number of protons incident on the target was monitored by a current integrator connected to the target.

3. Target Geometry, Beam Conditions and Neutron Source

The 52 MeV proton beam was extracted into the air through a 0.15-mm-thick stainless-steel window of the beam transporting duct and injected to the center of a 2.145-cm-thick graphite target placed 5 cm from the window. The diameter of proton beam was about 5 mm at the injecting point. The beam intensity was 1 to 2 nA. The source neutron spectra from the graphite target are given by the measurement performed with the same detection system at 0, 15, 30 and 70 degree as shown in Fig. 2.1.2 and Table 2.1.2, and the source photon spectrum at 0 degree is also given in Fig. 2.1.3 and

Table 2.1.3.

4. Measured Results

The absolute energy spectra of neutrons and photons at the detector located in contact with the rear face of the assemblies are shown in Figs. 2.1.4 through 2.1.11, and tabulated in Tables 2.1.4 through 2.1.11.

5. Model for Calculation

a. Source Condition

For the codes which can treat an incident proton such as HETC and NMTC, mono−directional 52 MeV proton centered at a graphite target. For neutron and photon transport codes, source neutron and photon spectra given in Figs. 2.1.2 and 2.1.3.

b. Calculation Geometry

Rectangular slab geometry as shown in Fig. 2.1.1.

c. Compositions of Material

Atomic densities given in Table 2.1.1.

6. Normalization Between Calculation and Measurement

Experimental data are given in absolute values in unit of n/cm^2/MeV/proton except for neutron and photon spectra with the 21.4− and 42.8−cm−thick graphite and the 19.3−cm−thick iron assemblies which are normalized to their integrated flux above 2 MeV as calculated by the MMCR−U code.

References

1. Shin K., Uwamino Y., Yoshida M., Hyodo T. and Nakamura T.: "Penetration of Secondary Neutrons and Photons from a Graphite Assembly Exposed to 52−MeV Protons," Nucl. Sci. Eng., 71, 294−300 (1979).
2. Uwamino Y., Nakamura T. and Shin K.: "Penetration Through Shielding Materials of Secondary Neutrons and Photons Generated by 52−MeV Protons," Nucl. Sci. Eng., 80, 360−369 (1982).

Table 2.1.1 Dimensions and Densities of the Assemblies Used in the Experiment and in the Calculation

Material	Width (cm)	Height (cm)	Thickness (cm)	Distance[a] (cm)	Density ($g \cdot cm^{-3}$)	Atomic Density ($atom \cdot cm^{-3}$) (A)[b]		(B)[b]	
Graphite	90.0	54.0	21.4	24.0	1.68	Carbon	8.43+22[c]	Carbon	8.43+22
	90.0	54.0	42.8	45.5					
	90.0	54.0	64.5	67.0					
	90.0	54.0	9.6	345.0					
	90.0	54.0	21.4	345.0					
	90.0	54.0	42.8	345.0					
Iron	52.0	50.0	19.3	21.8	7.14	Iron	7.70+22	Iron	7.70+22
	52.0	50.0	38.6	41.1					
	52.0	50.0	57.9	60.4					
Water	80.0	55.0	60.0	66.5	1.00	Hydrogen	6.68+22	Hydrogen	6.68+22
	80.0	55.0	101.0	112.0		Oxygen	3.34+22	Oxygen	3.34+22
Ordinary concrete	75.0	60.0	46.0	52.5	2.3	Hydrogen	5.95+21	Hydrogen	5.95+21
	75.0	60.0	69.0	75.5		Oxygen	4.46+22	Oxygen	4.48+22
	75.0	60.0	115.0	121.5		Sodium	1.52+20	Silicon	2.00+22
						Magnesium	5.26+20	Calcium	1.52+21
						Aluminum	1.17+21	Iron	7.38+20
						Silicon	1.83+22		
						Sulfur	3.98+19		
						Potassium	2.35+19		
						Calcium	1.50+21		
						Iron	7.38+20		

[a]Distance between the front surface of the carbon target and the detector.
[b]See text, (A) was measured and (B) was used in the calculation.
[c]Read as 8.43×10^{22}.

Table 2.1.2 Neutron Source Spectra.

Energy (MeV)	Neutron Flux (1/sr/MeV/proton)				
Angle	0 deg.	15 deg.	30 deg.	45 deg.	75 deg.
2.0	5.78E-05*		7.11E-05		5.66E-05
3.0	4.62E-05		6.75E-05		3.47E-05
4.0	5.40E-05	8.36E-05	7.02E-05	4.35E-05	3.82E-05
5.0	4.35E-05	8.29E-05	7.18E-05	4.36E-05	3.84E-05
6.0	4.30E-05	5.36E-05	5.32E-05	3.99E-05	2.51E-05
7.0	3.34E-05	5.90E-05	4.75E-05	3.49E-05	2.66E-05
8.0	4.25E-05	5.75E-05	5.66E-05	5.26E-05	3.09E-05
9.0	3.89E-05	5.49E-05	5.24E-05	4.60E-05	1.95E-05
10.0	3.03E-05	5.21E-05	4.24E-05	3.43E-05	1.47E-05
11.0	3.08E-05	4.89E-05	3.93E-05	3.04E-05	1.51E-05
12.0	3.20E-05	5.42E-05	3.57E-05	2.92E-05	1.28E-05
13.0	2.66E-05	4.04E-05	3.76E-05	2.84E-05	1.10E-05
14.0	2.99E-05	4.76E-05	3.66E-05	2.65E-05	1.01E-05
15.0	2.41E-05	4.63E-05	3.65E-05	2.33E-05	8.76E-06
16.0	2.57E-05	4.45E-05	3.61E-05	2.27E-05	8.58E-06
17.0	2.36E-05	2.99E-05	3.01E-05	2.06E-05	9.17E-06
18.0	2.30E-05	3.73E-05	2.74E-05	2.10E-05	7.26E-06
19.0	2.04E-05	3.50E-05	3.01E-05	1.88E-05	6.39E-06
20.0	2.38E-05	4.07E-05	3.08E-05	1.99E-05	5.06E-06
21.0	2.38E-05	3.77E-05	2.75E-05	1.91E-05	6.25E-06
22.0	2.06E-05	3.22E-05	2.61E-05	1.68E-05	6.72E-06
23.0	1.88E-05	3.08E-05	2.34E-05	1.42E-05	
24.0	1.67E-05	2.99E-05	1.89E-05	1.32E-05	
25.0	1.39E-05	2.45E-05	1.70E-05	1.14E-05	
26.0	1.18E-05	2.06E-05	1.63E-05	7.69E-06	
27.0	9.83E-06	1.63E-05	1.56E-05	5.69E-06	
28.0	7.91E-06	1.17E-05		4.37E-06	
29.0	6.36E-06	8.86E-06		3.08E-06	
30.0	5.09E-06	6.61E-06		2.46E-06	
31.0	4.25E-06	4.81E-06		1.40E-06	
32.0	3.52E-06	3.25E-06			
33.0	2.75E-06	1.91E-06			
34.0					

* Read as 5.78×10^{-5}.

Table 2.1.3 Photon Source Spectrum.

Energy (MeV)	Photon Flux (1/sr/MeV/proton)
0.7	1.38E-03*
0.9	4.69E-04
1.1	5.36E-04
1.4	3.57E-04
1.7	3.98E-04
1.9	7.02E-04
2.1	4.15E-04
2.4	2.79E-04
2.7	2.55E-04
2.9	2.58E-04
3.1	2.60E-04
3.4	3.19E-04
3.7	3.05E-04
3.9	4.18E-04
4.1	9.83E-04
4.4	1.10E-03
4.7	7.12E-04
4.9	3.34E-04
5.1	1.71E-04
5.4	1.36E-04
5.7	1.30E-04
5.9	1.05E-04
6.1	1.18E-04
6.4	1.53E-04
6.7	1.62E-04
6.9	1.05E-04
7.1	5.04E-05
7.4	5.71E-05
7.7	9.22E-05
7.9	8.30E-05
8.1	2.86E-05
8.4	6.48E-05
8.7	1.04E-04
8.9	5.41E-05
9.1	4.46E-05
9.4	5.83E-05
9.7	9.55E-05
9.9	8.39E-05
10.1	

* Read as 1.38×10^{-3}.

Table 2.1.4 Neutron Spectra Transmitted Through Graphite Assemblies.

Energy (MeV)	Neutron Flux (1/cm²/MeV/proton)	Neutron Flux (1/cm²/MeV/proton)	Neutron Flux (1/cm²/MeV/proton)
Thickness	21.4 cm	42.8 cm	64.5 cm
2.5	9.07E-08*	1.18E-08	2.24E-09
3.5	6.91E-08	7.73E-09	1.42E-09
4.5	7.74E-08	9.21E-09	1.68E-09
5.5	7.08E-08	8.48E-09	1.48E-09
6.5	6.44E-08	7.86E-09	1.33E-09
7.5	4.64E-08	5.45E-09	8.61E-10
8.5	3.97E-08	3.90E-09	6.55E-10
9.5	3.96E-08	3.62E-09	5.09E-10
10.5	3.53E-08	3.54E-09	4.69E-10
11.5	3.16E-08	3.09E-09	4.41E-10
12.5	3.01E-08	2.73E-09	3.67E-10
13.5	2.76E-08	2.41E-09	3.59E-10
14.5	2.79E-08	2.22E-09	2.66E-10
15.5	2.61E-08	2.28E-09	2.85E-10
16.5	2.47E-08	2.20E-09	3.25E-10
17.5	2.30E-08	2.36E-09	3.70E-10
18.5	2.39E-08	2.47E-09	3.50E-10
19.5	2.52E-08	2.47E-09	3.24E-10
20.5	2.46E-08	2.33E-09	3.05E-10
21.5	2.32E-08	2.21E-09	2.99E-10
22.5	2.23E-08	2.16E-09	3.30E-10
23.5	2.15E-08	2.00E-09	3.17E-10
24.5	1.95E-08	1.88E-09	2.88E-10
25.5	1.73E-08	1.72E-09	2.39E-10
26.5	1.51E-08	1.49E-09	2.02E-10
27.5	1.18E-08	1.18E-09	1.68E-10
28.5	9.61E-09	9.32E-10	1.47E-10
29.5	7.47E-09	7.30E-10	1.19E-10
30.5	5.85E-09	5.48E-10	8.72E-11
31.5	4.22E-09	4.41E-10	5.72E-11
32.5	3.06E-09	3.43E-10	3.65E-11
33.5	2.14E-09	2.61E-10	2.69E-11
34.5	1.48E-09	1.85E-10	2.67E-11

* Read as 9.07×10^{-8}.

Table 2.1.5 Neutron Spectra Transmitted Through Iron Assemblies.

Energy (MeV)	Neutron Flux (1/cm²/MeV/proton)	Neutron Flux (1/cm²/MeV/proton)	Neutron Flux (1/cm²/MeV/proton)
Thickness	19.3 cm	38.6 cm	57.9 cm
2.5	9.09E-08*	3.00E-09	
3.5	4.02E-08	1.53E-09	9.11E-11
4.5	3.46E-08	9.13E-10	4.98E-11
5.5	2.36E-08	6.46E-10	3.85E-11
6.5	1.80E-08	4.28E-10	1.93E-11
7.5	1.36E-08	3.05E-10	1.56E-11
8.5	1.22E-08	3.11E-10	5.49E-12
9.5	1.30E-08	3.18E-10	1.37E-11
10.5	1.19E-08	2.92E-10	1.24E-11
11.5	1.12E-08	2.77E-10	8.00E-12
12.5	1.17E-08	2.75E-10	1.26E-11
13.5	1.09E-08	2.95E-10	1.05E-11
14.5	1.17E-08	3.10E-10	1.66E-11
15.5	1.15E-08	3.00E-10	1.42E-11
16.5	1.09E-08	2.96E-10	1.11E-11
17.5	9.66E-09	3.05E-10	8.56E-12
18.5	9.79E-09	2.93E-10	8.00E-12
19.5	9.73E-09	2.74E-10	9.43E-12
20.5	9.59E-09	2.71E-10	1.20E-11
21.5	9.40E-09	2.77E-10	1.33E-11
22.5	8.90E-09	2.52E-10	1.33E-11
23.5	8.09E-09	2.26E-10	1.36E-11
24.5	6.87E-09	2.03E-10	1.30E-11
25.5	5.45E-09	1.87E-10	1.16E-11
26.5	4.41E-09	1.56E-10	1.09E-11
27.5	3.50E-09	1.23E-10	1.10E-11
28.5	2.56E-09	9.09E-11	1.03E-11
29.5	1.72E-09	6.22E-11	8.90E-12
30.5	1.08E-09	4.25E-11	6.60E-12
31.5	7.46E-10	3.31E-11	5.50E-12
32.5	6.60E-10	2.97E-11	4.94E-12
33.5	7.07E-10	2.96E-11	5.08E-12
34.5	6.88E-10	2.79E-11	5.12E-12
35.5			4.12E-12

* Read as 9.09×10^{-8}.

Table 2.1.6 Neutron Spectra Transmitted Through Water Assemblies.

Energy (MeV)	Neutron Flux (1/cm²/MeV/proton)	Neutron Flux (1/cm²/MeV/proton)
Thickness	60 cm	101 cm
2.5	9.53E-10*	1.11E-10
3.5	8.36E-10	6.25E-11
4.5	7.19E-10	5.01E-11
5.5	7.04E-10	4.40E-11
6.5	5.61E-10	3.78E-11
7.5	4.60E-10	2.47E-11
8.5	4.35E-10	2.74E-11
9.5	5.06E-10	2.97E-11
10.5	4.53E-10	2.21E-11
11.5	3.98E-10	1.74E-11
12.5	4.17E-10	1.82E-11
13.5	3.69E-10	1.90E-11
14.5	4.63E-10	2.32E-11
15.5	4.63E-10	2.29E-11
16.5	4.23E-10	2.09E-11
17.5	4.35E-10	2.01E-11
18.5	4.47E-10	1.90E-11
19.5	4.35E-10	2.09E-11
20.5	4.66E-10	2.37E-11
21.5	4.96E-10	2.44E-11
22.5	4.79E-10	2.37E-11
23.5	4.38E-10	2.39E-11
24.5	4.15E-10	2.32E-11
25.5	3.61E-10	2.15E-11
26.5	3.28E-10	1.99E-11
27.5	2.88E-10	1.69E-11
28.5	2.23E-10	1.23E-11
29.5	1.63E-10	7.93E-12
30.5	1.11E-10	5.25E-12
31.5	8.12E-11	4.42E-12
32.5	6.34E-11	4.51E-12
33.5	5.37E-11	4.51E-12
34.5	5.15E-11	4.24E-12

* Read as 9.53×10^{-10}.

Table 2.1.7 Neutron Spectra Transmitted Through Ordinary Concrete Assemblies.

Energy (MeV)	Neutron Flux (1/cm²/MeV/proton)	Neutron Flux (1/cm²/MeV/proton)	Neutron Flux (1/cm²/MeV/proton)
Thickness	46 cm	69 cm	115 cm
2.5	8.13E-09*	1.76E-09	1.05E-10
3.5	4.86E-09	8.63E-10	5.05E-11
4.5	3.47E-09	6.74E-10	3.10E-11
5.5	3.28E-09	5.60E-10	2.45E-11
6.5	2.56E-09	4.74E-10	1.79E-11
7.5	1.82E-09	3.02E-10	1.11E-11
8.5	1.57E-09	2.21E-10	9.38E-12
9.5	1.47E-09	2.32E-10	6.70E-12
10.5	1.20E-09	1.86E-10	4.98E-12
11.5	1.02E-09	1.29E-10	4.75E-12
12.5	1.03E-09	1.38E-10	3.35E-12
13.5	9.98E-10	1.42E-10	3.30E-12
14.5	9.98E-10	1.71E-10	2.91E-12
15.5	1.03E-09	1.72E-10	3.27E-12
16.5	1.02E-09	1.56E-10	3.34E-12
17.5	9.56E-10	1.53E-10	3.43E-12
18.5	9.69E-10	1.61E-10	3.67E-12
19.5	9.62E-10	1.72E-10	3.82E-12
20.5	9.68E-10	1.68E-10	3.67E-12
21.5	9.54E-10	1.55E-10	3.47E-12
22.5	9.28E-10	1.48E-10	3.69E-12
23.5	8.42E-10	1.50E-10	3.89E-12
24.5	7.04E-10	1.52E-10	4.08E-12
25.5	5.81E-10	1.34E-10	3.68E-12
26.5	4.76E-10	1.12E-10	2.74E-12
27.5	3.79E-10	9.05E-11	1.96E-12
28.5	2.75E-10	6.51E-11	1.62E-12
29.5	1.94E-10	5.08E-11	1.44E-12
30.5	1.26E-10	4.37E-11	1.36E-12
31.5	8.73E-11	3.51E-11	1.31E-12
32.5	7.55E-11		1.08E-12
33.5	7.87E-11		
34.5	7.65E-11		
35.5	6.40E-11		

* Read as 8.13×10^{-9}.

Table 2.1.8 Photon Spectra Transmitted Through Graphite Assemblies.

Energy (MeV)	Photon Flux (1/cm²/MeV/proton)	Photon Flux (1/cm²/MeV/proton)	Photon Flux (1/cm²/MeV/proton)
Thickness	21.4 cm	42.8 cm	64.5 cm
0.75	1.02E-06*	1.26E-07	2.97E-08
1.00	2.86E-07	4.50E-08	1.09E-08
1.25	4.14E-07	5.73E-08	1.57E-08
1.50	3.26E-07	4.86E-08	1.41E-08
1.75	3.58E-07	7.14E-08	1.45E-08
2.00	3.36E-07	5.28E-08	1.53E-08
2.25	2.69E-07	5.16E-08	1.48E-08
2.50	1.98E-07	3.45E-08	9.16E-09
2.75	1.91E-07	3.47E-08	8.84E-09
3.00	1.99E-07	3.28E-08	8.24E-09
3.25	2.11E-07	3.52E-08	8.39E-09
3.50	2.17E-07	3.71E-08	8.90E-09
3.75	2.34E-07	3.75E-08	8.94E-09
4.00	2.71E-07	3.77E-08	9.23E-09
4.25	5.98E-07	7.89E-08	1.63E-08
4.50	8.74E-07	1.11E-07	2.12E-08
4.75	5.72E-07	7.34E-08	1.44E-08
5.00	2.17E-07	2.99E-08	5.76E-09
5.25	7.41E-08	1.10E-08	2.49E-09
5.50	3.06E-08	4.84E-09	1.69E-09
5.75	2.19E-08	4.16E-09	1.35E-09
6.00	3.99E-08	6.77E-09	1.10E-09
6.25	5.16E-08	7.04E-09	1.49E-09
6.50	4.14E-08	5.14E-09	2.23E-09
6.75	3.97E-08	6.59E-09	1.79E-09
7.00	4.95E-08	6.53E-09	7.02E-10
7.25	4.81E-08	5.97E-09	1.16E-09
7.50	1.89E-08	1.31E-09	4.75E-10
7.75	1.01E-08	1.24E-09	9.04E-10
8.00	1.37E-08	4.71E-09	8.09E-10
8.25	3.56E-08	5.13E-09	6.81E-10
8.50	3.53E-08	3.36E-09	1.05E-09
8.75	2.91E-08	6.01E-09	1.48E-09
9.00	3.24E-08	8.78E-09	1.89E-09
9.25	2.78E-08	5.33E-09	1.43E-09
9.50	1.53E-08	1.13E-09	4.05E-10
9.75	3.79E-08	5.27E-09	1.20E-09
10.00	8.66E-08	1.45E-08	3.36E-09

* Read as 1.02×10^{-6}.

Table 2.1.9 Photon Spectra Transmitted Through Iron Assemblies.

Energy (MeV)	Photon Flux (1/cm²/MeV/proton)	Photon Flux (1/cm²/MeV/proton)	Photon Flux (1/cm²/MeV/proton)
Thickness	19.3 cm	38.6 cm	57.9 cm
0.75	7.76E-07*	4.02E-08	4.36E-09
1.00	1.24E-07	3.46E-09	8.93E-10
1.25	2.52E-07	9.88E-09	1.79E-09
1.50	1.39E-07	6.80E-09	1.60E-09
1.75	1.50E-07	8.91E-09	1.61E-09
2.00	1.27E-07	7.62E-09	1.91E-09
2.25	1.01E-07	5.76E-09	2.09E-09
2.50	8.41E-08	2.87E-09	1.16E-09
2.75	6.86E-08	2.34E-09	8.12E-10
3.00	6.49E-08	2.05E-09	6.40E-10
3.25	5.94E-08	2.14E-09	6.80E-10
3.50	5.47E-08	2.02E-09	6.57E-10
3.75	5.00E-08	1.87E-09	6.09E-10
4.00	5.84E-08	1.80E-09	5.17E-10
4.25	5.91E-08	1.54E-09	4.99E-10
4.50	4.10E-08	1.53E-09	5.48E-10
4.75	2.60E-08	1.47E-09	5.26E-10
5.00	2.05E-08	1.46E-09	4.44E-10
5.25	1.71E-08	1.49E-09	4.28E-10
5.50	1.58E-08	1.47E-09	5.21E-10
5.75	1.92E-08	1.46E-09	4.76E-10
6.00	2.00E-08	1.41E-09	4.57E-10
6.25	1.53E-08	1.08E-09	4.99E-10
6.50	9.61E-09	8.62E-10	5.90E-10
6.75	9.80E-09	9.73E-10	5.66E-10
7.00	1.36E-08	1.75E-09	4.08E-10
7.25	1.17E-08	1.47E-09	2.83E-10
7.50	4.73E-09	8.82E-10	3.68E-10
7.75	5.95E-09	5.56E-10	6.16E-10
8.00	9.95E-09	5.99E-10	8.69E-10
8.25	9.54E-09	5.40E-10	8.74E-10
8.50	6.31E-09	3.62E-10	6.79E-10
8.75	7.21E-09	3.42E-10	5.89E-10
9.00	7.76E-09	2.83E-10	5.03E-10
9.25	4.86E-09	2.37E-10	2.81E-10
9.50	1.13E-09	1.65E-10	8.51E-11
9.75	4.78E-09	1.79E-10	1.46E-10
10.00	1.35E-08	4.15E-10	2.92E-10

* Read as 7.76×10^{-7}.

Table 2.1.10 Photon Spectra Transmitted Through Water Assemblies.

Energy (MeV)	Photon Flux (1/cm²/MeV/proton)	Photon Flux (1/cm²/MeV/proton)
Thickness	60 cm	101 cm
0.25	1.44E-07*	
0.50	4.72E-08	
0.75	3.98E-08	9.94E-09
1.00	3.99E-08	3.22E-09
1.25	3.39E-08	4.90E-09
1.50	3.31E-08	4.14E-09
1.75	3.34E-08	4.53E-09
2.00	4.37E-08	5.35E-09
2.25	3.92E-08	4.45E-09
2.50	1.67E-08	2.33E-09
2.75	1.57E-08	2.32E-09
3.00	1.42E-08	2.18E-09
3.25	1.42E-08	2.10E-09
3.50	1.48E-08	2.24E-09
3.75	1.59E-08	2.26E-09
4.00	1.62E-08	2.31E-09
4.25	3.07E-08	3.58E-09
4.50	3.80E-08	4.06E-09
4.75	2.28E-08	2.63E-09
5.00	9.14E-09	1.30E-09
5.25	5.15E-09	7.80E-10
5.50	4.03E-09	6.07E-10
5.75	4.89E-09	7.46E-10
6.00	5.47E-09	9.90E-10
6.25	5.05E-09	8.89E-10
6.50	5.23E-09	6.07E-10
6.75	5.62E-09	5.96E-10
7.00	3.58E-09	4.42E-10
7.25	1.27E-09	4.19E-10
7.50	2.57E-10	2.32E-10
7.75	2.19E-09	1.30E-10
8.00	2.30E-09	2.95E-10
8.25	2.84E-10	2.78E-10
8.50	1.20E-10	1.31E-10
8.75	2.34E-09	2.64E-10
9.00	2.94E-09	4.30E-10
9.25	1.45E-09	2.69E-10
9.50	5.68E-10	4.71E-11
9.75	2.09E-09	2.95E-10
10.00	4.92E-09	7.70E-10

* Read as 1.44×10^{-7}.

Table 2.1.11 Photon Spectra Transmitted Through Ordinary Concrete Assemblies.

Energy (MeV)	Photon Flux (1/cm²/MeV/proton)	Photon Flux (1/cm²/MeV/proton)	Photon Flux (1/cm²/MeV/proton)
Thickness	46 cm	69 cm	115 cm
0.25			3.05E-09
0.50			1.06E-09
0.75	9.98E-08*	4.21E-08	8.67E-10
1.00	3.22E-08	5.93E-09	8.81E-10
1.25	5.11E-08	1.50E-08	8.70E-10
1.50	4.28E-08	1.26E-08	8.71E-10
1.75	4.47E-08	1.39E-08	8.32E-10
2.00	3.47E-08	1.03E-08	8.56E-10
2.25	3.03E-08	8.02E-09	7.23E-10
2.50	2.37E-08	6.10E-09	4.73E-10
2.75	2.43E-08	6.07E-09	4.27E-10
3.00	1.97E-08	4.50E-09	3.76E-10
3.25	1.98E-08	4.50E-09	3.98E-10
3.50	2.04E-08	5.07E-09	4.35E-10
3.75	1.84E-08	4.77E-09	3.67E-10
4.00	1.95E-08	4.03E-09	3.04E-10
4.25	2.75E-08	4.50E-09	2.98E-10
4.50	2.56E-08	5.24E-09	3.05E-10
4.75	1.62E-08	4.36E-09	3.16E-10
5.00	9.88E-09	3.30E-09	2.87E-10
5.25	8.11E-09	2.22E-09	2.44E-10
5.50	7.85E-09	1.82E-09	2.13E-10
5.75	8.96E-09	2.43E-09	2.25E-10
6.00	9.22E-09	2.86E-09	2.57E-10
6.25	7.73E-09	2.09E-09	2.32E-10
6.50	6.98E-09	1.23E-09	1.75E-10
6.75	6.31E-09	1.75E-09	1.52E-10
7.00	4.39E-09	2.18E-09	1.65E-10
7.25	2.42E-09	1.30E-09	1.88E-10
7.50	2.21E-09	4.62E-10	1.89E-10
7.75	2.91E-09	5.53E-10	1.34E-10
8.00	2.15E-09	9.92E-10	8.00E-11
8.25	9.53E-10	6.72E-10	4.24E-11
8.50	1.73E-09	6.67E-11	3.05E-11
8.75	2.60E-09	4.08E-10	4.71E-11
9.00	2.06E-09	8.29E-10	4.78E-11
9.25	1.50E-09	4.83E-10	3.05E-11
9.50	8.72E-10	1.51E-10	1.51E-11
9.75	1.82E-09	4.71E-10	2.65E-11
10.00	4.66E-09	9.63E-10	5.30E-11

* Read as 9.98×10^{-8}.

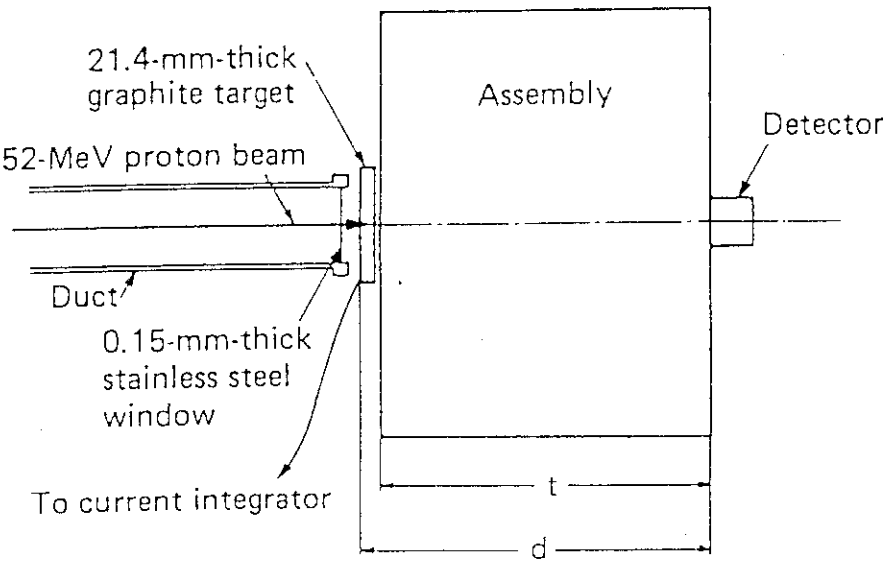

Fig. 2.1.1 Experimental arrangement.

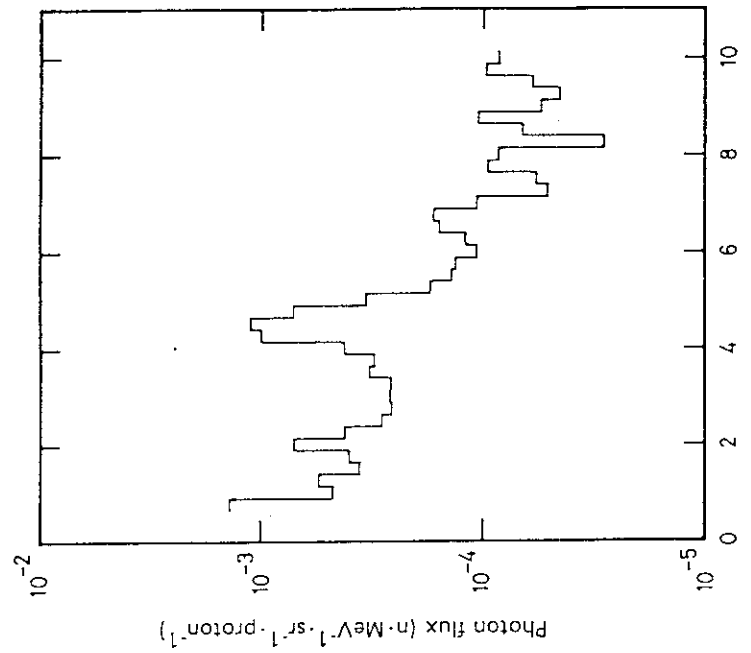

Fig. 2.1.3 Photon source spectrum from the 2.14-cm-thick carbon target located on the 52 MeV proton beam axis.

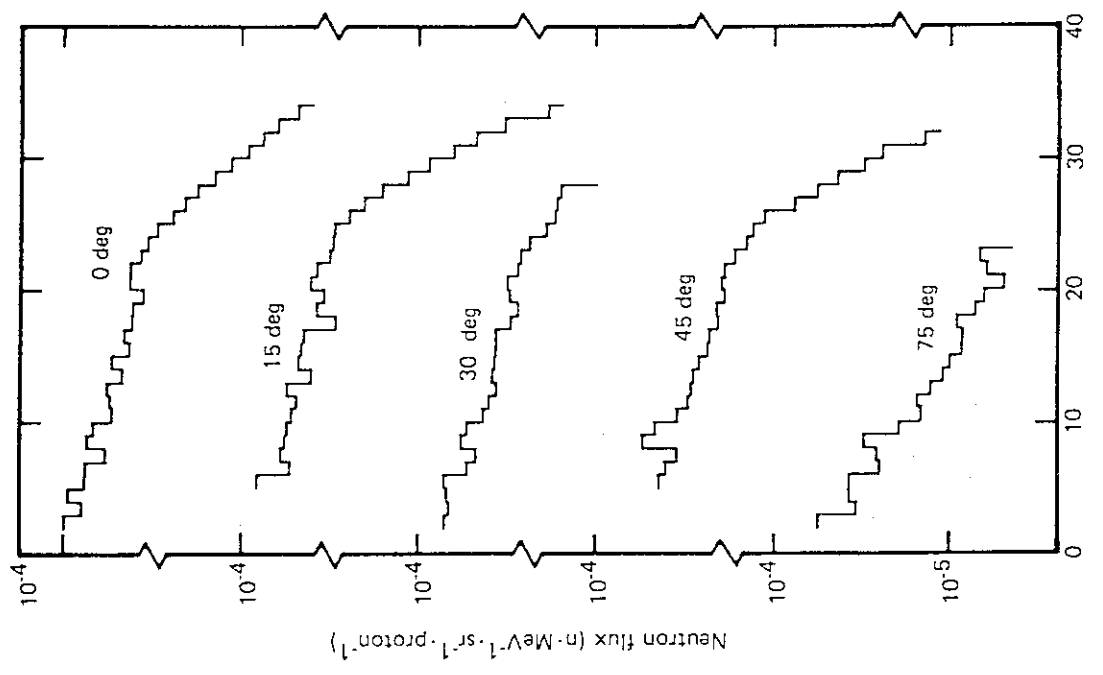

Fig. 2.1.2 Neutron source spectra from the 2.14-cm-thick carbon target at 0, 15, 30, 45, and 75 degree to the 52 MeV proton beam axis.

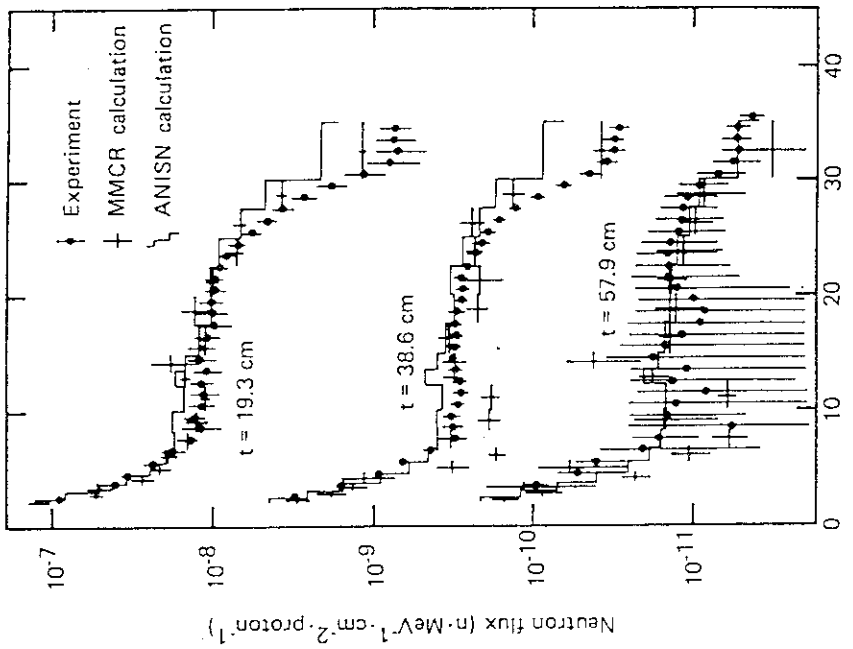

Fig. 2.1.5 Neutron spectra transmitted through iron assemblies. The spectra measured with the 38.6- and 57.9-cm-thick sample is given in absolute values; that of 19.3-cm thickness is normalized to its integrated flux above 2 MeV as calculated by the MMCR-U code.

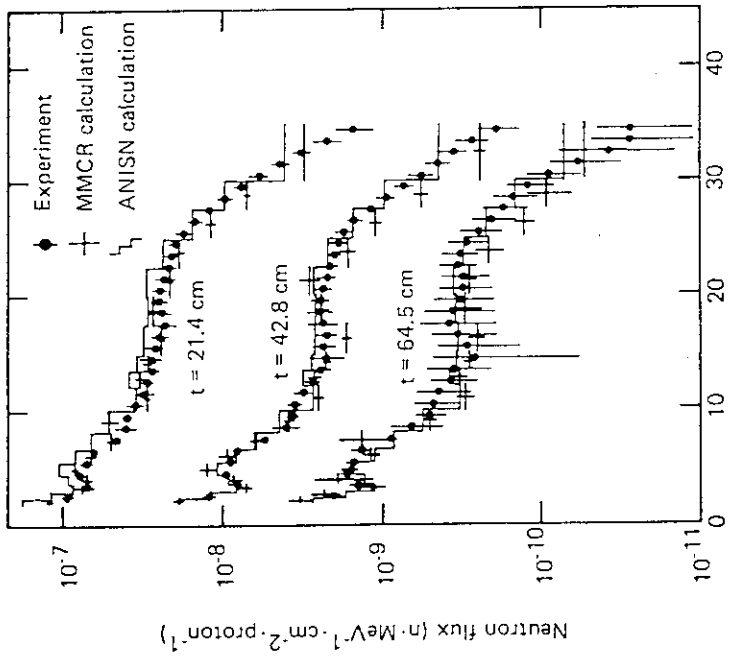

Fig. 2.1.4 Neutron spectra transmitted through graphite assemblies. The spectrum measured with the 64.5-cm-thick sample is given in absolute values; those of 21.4- and 42.8-cm thicknesses are normalized to their integrated flux above 2 MeV as calculated by the MMCR-U code.

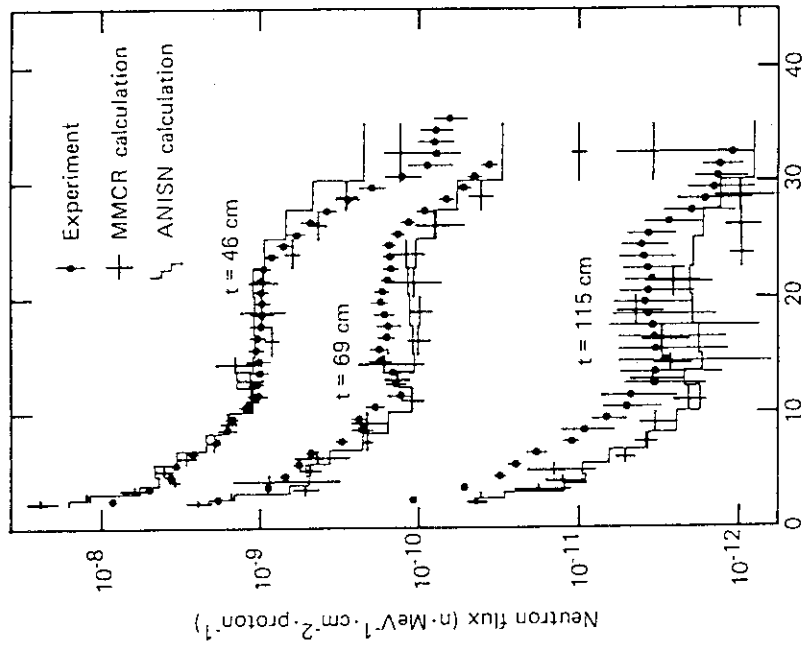

Fig. 2.1.7 Neutron spectra transmitted through ordinary concrete assemblies.

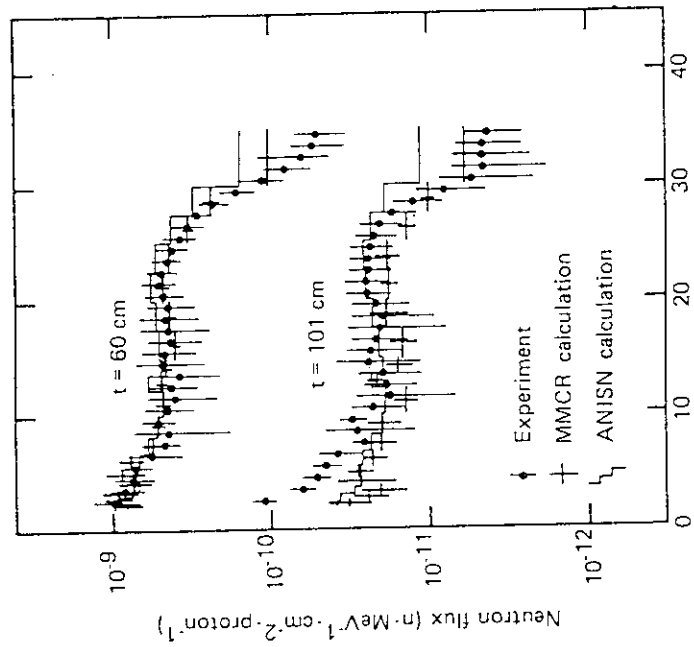

Fig. 2.1.6 Neutron spectra transmitted through water assemblies.

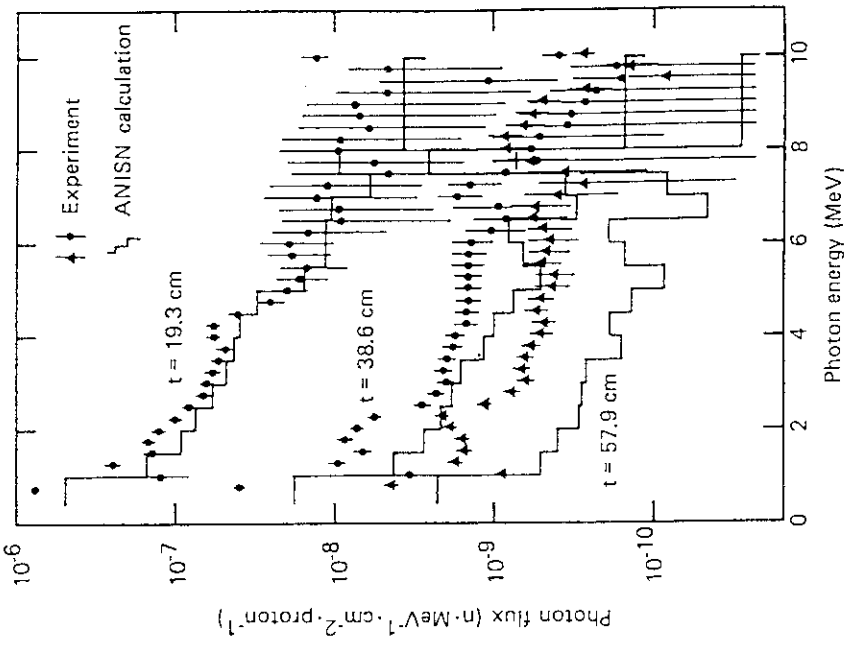

Fig. 2.1.9 Photon spectra transmitted through iron assemblies. The spectra measured with the 38.6- and 57.9-cm-thick sample is given in absolute values; that of 19.3-cm thickness is normalized by the same factor as in the neutron spectra.

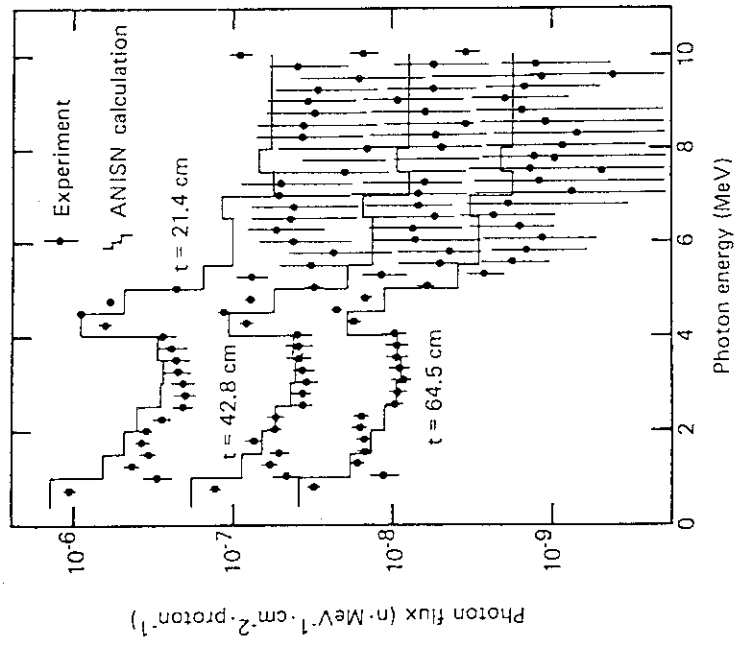

Fig. 2.1.8 Photon spectra transmitted through graphite assemblies. The spectrum measured with the 64.5-cm-thick sample is given in absolute values; those of 21.4- and 42.8-cm thicknesses are normalized by the same factors as in the neutron spectra.

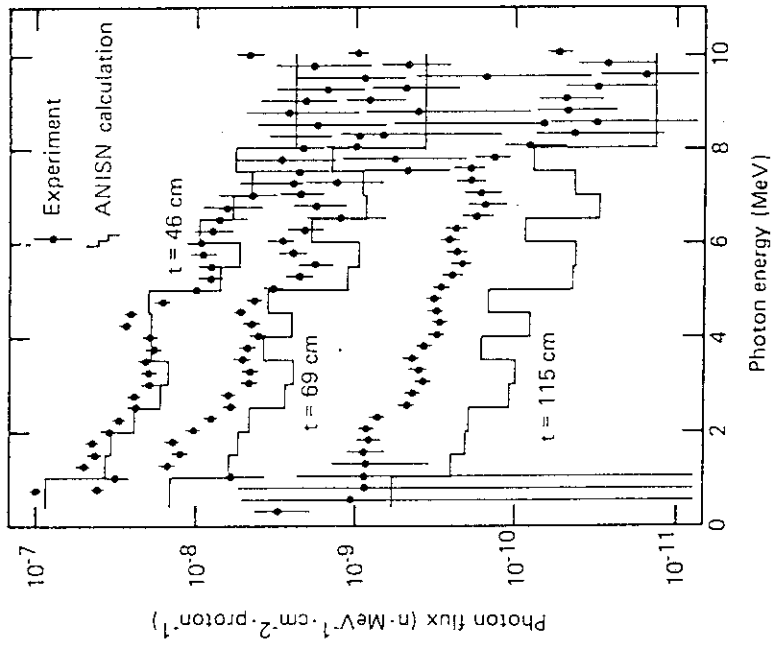

Fig. 2.1.11 Photon spectra transmitted through ordinary concrete assemblies.

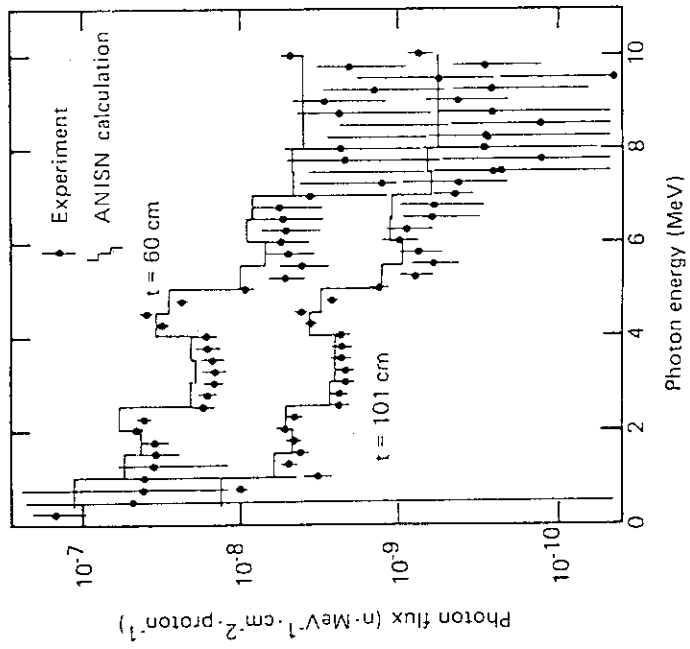

Fig. 2.1.10 Photon spectra transmitted through water assemblies.

2.2 Transmission Through Shielding Materials of Neutrons and Photons Generated by Intermediate-Energy Protons No.2

(Summary)

1)	Accelerator (Organization)	: AVF cyclotron (Osaka Univ.)
2)	Projectile (Energy)	: P (65MeV)
3)	Target (Thickness)	: Copper (1.0cmt)
4)	Shielding material	: Graphite, Iron, Lead and Concrete
5)	Geometry	: Slab
6)	Instruments	: NE213 Liquid Scintillator, FERDO-U Unfolding
7)	Measured Quantities	: Neutron and Photon Energy Spectra

1. Experimental Arrangement

Figure 2.2.1 shows the experimental arrangement and Table 2.2.1 gives the dimension of assemblies. A 65 MeV proton beam from the AVF cyclotron of Osaka University irradiated a 1.0-cm-thick copper target. Neutrons generated in the forward direction were passed to an experimental room through a 7.5-cm-diam x 50-cm-long iron-lined concrete collimator.

2. Method of Measurement and Instrument

A 76-mm-diam x 76-mm-long NE213 scintillation detector placed just behind the shield system. The pulse height distributions were unfolded to neutron and photon energy spectra by the FERDO-U code.

3. Neutron and Photon Sources

Neutron source spectrum is given in Fig. 2.2.2 and Table 2.2.2. The spectrum above 4.5 MeV was converted from the measured flux at 538 cm from the copper target at 0 degree, and the evaporation spectrum below 4.5 MeV was calculated by the following equation.

$$S(E) = CE\exp(-E/T), \qquad (2.2.1)$$

where

$T = 2.5$ MeV : nuclear temperature,

$C = 8.25 \times 10^{-4}$: a constant fitted to the measurement from 4.5 to

10 MeV,

E : neutron energy in the laboratory frame.

Figure 2.2.3 and Table 2.2.3 show the corresponding photon source spectrum above 1.8 MeV at 383 cm point from the target.

4. Measured Results

The absolute energy spectra of neutrons and photons transmitted through the shield materials are shown in Figs. 2.2.4 through 2.2.11 and tabulated in Tables 2.2.4 through 2.2.8.

5. Model for Calculation

a. Source Condition

For the codes which can treat an incident proton such as HETC and NMTC, mono-direction 65 MeV proton centered at a copper target. For neutron and photon transport codes, source spectra of neutron and photon given in Tables 2.2.2 and 2.2.3 and in Figs. 2.2.2 and 2.2.3.

b. Calculation Geometry

Rectangular slab geometry as shown in Fig. 2.2.1 and Table 2.2.1.

c. Compositions of Material

Atomic densities given in Table 2.2.9.

6. Normalization between Calculation and Measurement

All absolute experimental data are given in unit of n/cm^2/MeV/proton and the source neutron and photon spectra are also shown in unit of n/sr/MeV/proton and n/cm^2/MeV/proton, respectively.

Reference

1. Shin K., Ishii Y., Miyahara K., Uwamino Y., Sakai H. and Numata S.: "Transmission of Intermediate-Energy Neutrons and Associated Gamma Rays Through Iron, Lead, Graphite, and Concrete Shields," Nucl. Sci. Eng., 109, 380-390 (1991).

Table 2.2.1 Dimensions of the Shield Assemblies.

Material	a (cm)	Thickness (cm)	Width × Height (cm)
Iron	5	20, 40, 50	40 × 40
Lead	5	10, 20, 30	40 × 40
Concrete	5	20, 50, 100	40 × 40
Graphite	7.5	30, 60, 90	52 × 40

Table 2.2.2 Neutron Source Spectrum

Energy (MeV)	Neutron Flux (1/sr/MeV/proton)	Energy (MeV)	Neutron Flux (1/sr/MeV/proton)
4.0	5.84E-04*	27.0	6.82E-05
4.5	5.28E-04	28.0	6.76E-05
5.0	4.67E-04	29.0	6.84E-05
5.5	4.02E-04	30.0	6.71E-05
6.0	3.88E-04	31.0	6.32E-05
6.5	3.13E-04	32.0	5.81E-05
7.0	2.14E-04	33.0	5.29E-05
8.0	1.68E-04	34.0	4.82E-05
9.0	1.60E-04	35.0	4.46E-05
10.0	1.38E-04	36.0	4.34E-05
11.0	1.20E-04	37.0	4.22E-05
12.0	1.15E-04	38.0	4.11E-05
13.0	1.03E-04	39.0	4.06E-05
14.0	1.00E-04	40.0	3.55E-05
15.0	9.62E-05	42.0	3.09E-05
16.0	9.59E-05	44.0	2.59E-05
17.0	9.64E-05	46.0	2.28E-05
18.0	9.30E-05	48.0	1.89E-05
19.0	8.91E-05	50.0	1.66E-05
20.0	8.80E-05	52.0	1.45E-05
21.0	8.70E-05	54.0	1.12E-05
22.0	7.80E-05	56.0	6.36E-06
23.0	7.06E-05	58.0	2.76E-06
24.0	6.70E-05	60.0	8.88E-07
25.0	6.63E-05	64.0	1.73E-07
26.0	7.01E-05	68.0	

* Read as 5.84×10^{-4}.

Table 2.2.3 Photon Source Spectrum at 383 cm from target

Energy (MeV)	Photon Flux (1/cm²/MeV/proton)
1.9	2.63E-08*
2.1	1.55E-08
2.4	1.40E-08
2.7	1.07E-08
2.9	8.77E-09
3.1	7.48E-09
3.4	6.84E-09
3.7	6.11E-09
3.9	5.03E-09
4.1	4.40E-09
4.4	4.03E-09
4.7	3.81E-09
4.9	3.44E-09
5.1	2.85E-09
5.4	2.36E-09
5.7	2.05E-09
5.9	1.94E-09
6.1	1.58E-09
6.4	1.38E-09
6.7	1.35E-09
6.9	1.39E-09
7.1	1.12E-09
7.4	7.01E-10
7.7	7.36E-10
7.9	1.05E-09
8.1	8.90E-10
8.4	4.41E-10
8.7	3.92E-10
8.9	5.49E-10
9.1	5.07E-10
9.4	

* Read as 2.63×10^{-8}.

Table 2.2.4 Transmission Neutron Spectra behind Iron

Energy (MeV)	Neutron Flux (1/cm²/MeV/proton)	Energy (MeV)	Neutron Flux (1/cm²/MeV/proton)	Energy (MeV)	Neutron Flux (1/cm²/MeV/proton)
Thickness	20 cm		40 cm		60 cm
5.0	8.18E-11*	6.0	8.19E-13	6.0	2.84E-13
6.0	6.16E-11	7.0	1.75E-12	7.0	2.50E-13
7.0	4.89E-11	9.0	9.27E-13	8.0	3.69E-13
8.0	3.32E-11	11.0	6.20E-13	9.0	1.57E-13
9.0	2.75E-11	12.0	7.70E-13	10.0	1.90E-13
10.0	2.24E-11	13.0	1.21E-12	11.0	1.02E-13
11.0	2.56E-11	14.0	7.92E-13	12.0	6.56E-14
13.0	2.77E-11	15.0	7.34E-13	13.0	3.89E-14
15.0	2.66E-11	16.0	1.05E-12	14.0	1.07E-13
18.0	3.11E-11	18.0	1.05E-12	15.0	1.39E-13
20.0	2.91E-11	20.0	1.25E-12	16.0	1.18E-13
22.0	3.02E-11	22.0	1.33E-12	17.0	1.04E-13
24.0	2.83E-11	24.0	1.00E-12	18.0	1.27E-13
26.0	2.58E-11	26.0	8.17E-13	20.0	9.94E-14
28.0	2.63E-11	28.0	7.98E-13	22.0	1.90E-13
30.0	2.57E-11	30.0	8.72E-13	23.0	2.71E-13
31.0	2.28E-11	31.0	9.28E-13	24.0	2.26E-13
33.0	2.10E-11	33.0	8.39E-13	25.0	1.51E-13
35.0	2.10E-11	35.0	7.26E-13	26.0	1.20E-13
37.0	1.97E-11	36.0	5.91E-13	27.0	1.39E-13
40.0	1.75E-11	37.0	5.16E-13	28.0	1.82E-13
41.0	1.57E-11	40.0	6.70E-13	30.0	2.14E-13
43.0	1.33E-11	41.0	6.65E-13	31.0	2.13E-13
45.0	1.20E-11	43.0	5.66E-13	33.0	1.57E-13
47.0	1.13E-11	45.0	4.95E-13	35.0	1.17E-13
49.0	1.03E-11	47.0	3.73E-13	37.0	9.62E-14
51.0	8.82E-12	49.0	4.15E-13	40.0	9.81E-14
53.0	7.07E-12	51.0	4.19E-13	41.0	9.18E-14
55.0	5.07E-12	53.0	3.30E-13	43.0	7.95E-14
57.0	3.11E-12	55.0	2.37E-13	45.0	8.11E-14
59.0	1.50E-12	57.0	1.48E-13	47.0	6.79E-14
		59.0	8.39E-14	49.0	8.58E-14
				51.0	1.01E-13
				53.0	7.01E-14
				55.0	4.45E-14
				57.0	2.78E-14

* Read as 8.18×10^{-11}.

Table 2.2.5 Transmission Neutron Spectra behind Lead

Energy (MeV)	Neutron Flux (1/cm²/MeV/proton)	Energy (MeV)	Neutron Flux (1/cm²/MeV/proton)	Energy (MeV)	Neutron Flux (1/cm²/MeV/proton)
Thickness	10 cm		20 cm		30 cm
5.0	6.08E-10*	5.0	1.17E-10	7.0	2.02E-11
7.0	5.23E-10	7.0	1.03E-10	9.0	1.60E-11
8.0	4.06E-10	9.0	7.24E-11	11.0	1.60E-11
9.0	3.18E-10	11.0	7.45E-11	13.0	1.47E-11
11.0	2.97E-10	13.0	6.27E-11	15.0	1.17E-11
13.0	2.50E-10	15.0	5.12E-11	17.0	1.11E-11
15.0	2.16E-10	17.0	5.35E-11	19.0	1.15E-11
17.0	2.31E-10	19.0	4.88E-11	21.0	1.26E-11
19.0	2.19E-10	21.0	5.17E-11	23.0	1.11E-11
21.0	1.95E-10	23.0	4.54E-11	25.0	1.03E-11
23.0	1.82E-10	25.0	4.74E-11	27.0	1.18E-11
25.0	1.66E-10	27.0	5.36E-11	29.0	1.17E-11
27.0	1.65E-10	29.0	4.48E-11	31.0	1.08E-11
29.0	1.68E-10	31.0	4.03E-11	34.0	1.08E-11
31.0	1.59E-10	34.0	3.83E-11	36.0	1.10E-11
33.0	1.47E-10	36.0	4.16E-11	39.0	1.01E-11
35.0	1.36E-10	39.0	3.83E-11	41.0	8.14E-12
37.0	1.28E-10	41.0	2.67E-11	43.0	7.55E-12
39.0	1.12E-10	43.0	2.76E-11	45.0	6.62E-12
41.0	9.92E-11	45.0	2.86E-11	47.0	6.34E-12
43.0	8.16E-11	47.0	2.39E-11	49.0	5.42E-12
45.0	7.75E-11	49.0	1.78E-11	51.0	4.19E-12
47.0	7.07E-11	51.0	1.53E-11	53.0	3.21E-12
49.0	5.82E-11	53.0	1.32E-11	55.0	2.36E-12
51.0	5.02E-11	55.0	1.19E-11	57.0	1.39E-12
53.0	4.30E-11	57.0	8.00E-12	59.0	6.14E-13
55.0	3.14E-11	59.0	3.77E-12		
57.0	1.88E-11	61.0	6.85E-13		
59.0	1.03E-11				
61.0	3.08E-12				

* Read as 6.08×10^{-10}.

Table 2.2.6 Transmission Neutron Spectra behind Graphite

Energy (MeV)	Neutron Flux (1/cm²/MeV/proton)	Energy (MeV)	Neutron Flux (1/cm²/MeV/proton)	Energy (MeV)	Neutron Flux (1/cm²/MeV/proton)
Thickness	30 cm		60 cm		90 cm
6.0	2.80E-10*	6.0	1.84E-11	7.0	1.35E-12
7.0	3.74E-10	7.0	2.03E-11	8.0	1.56E-12
8.0	2.66E-10	8.0	2.35E-11	9.0	1.33E-12
9.0	1.71E-10	9.0	7.10E-12	10.0	9.03E-13
10.0	1.30E-10	10.0	6.36E-12	11.0	5.65E-13
11.0	1.12E-10	11.0	5.51E-12	12.0	3.72E-13
12.0	8.21E-11	12.0	7.29E-12	13.0	2.85E-13
13.0	6.65E-11	13.0	4.21E-12	14.0	2.50E-13
14.0	5.32E-11	14.0	2.85E-12	15.0	2.46E-13
15.0	5.20E-11	15.0	4.06E-12	16.0	2.64E-13
16.0	5.43E-11	16.0	4.03E-12	17.0	2.94E-13
17.0	5.39E-11	17.0	2.63E-12	18.0	2.98E-13
18.0	5.12E-11	18.0	1.62E-12	19.0	2.88E-13
19.0	4.83E-11	19.0	2.84E-12	20.0	2.53E-13
20.0	4.39E-11	20.0	4.41E-12	21.0	2.08E-13
21.0	4.33E-11	21.0	4.57E-12	22.0	1.69E-13
22.0	4.92E-11	22.0	3.50E-12	23.0	1.43E-13
23.0	4.99E-11	23.0	2.35E-12	24.0	1.23E-13
24.0	4.54E-11	24.0	1.53E-12	25.0	1.07E-13
25.0	4.16E-11	25.0	1.65E-12	26.0	8.92E-14
26.0	4.25E-11	26.0	2.65E-12	27.0	7.08E-14
27.0	4.50E-11	27.0	3.27E-12	28.0	6.21E-14
28.0	4.70E-11	28.0	3.17E-12	29.0	6.21E-14
29.0	4.66E-11	29.0	3.10E-12	30.0	7.43E-14
30.0	4.69E-11	30.0	3.12E-12	31.0	9.55E-14
31.0	4.66E-11	31.0	3.06E-12	32.0	1.22E-13
32.0	4.46E-11	32.0	2.99E-12	33.0	1.47E-13
33.0	4.33E-11	33.0	2.88E-12	34.0	1.72E-13
34.0	4.32E-11	34.0	2.84E-12	35.0	1.89E-13
35.0	4.54E-11	35.0	2.92E-12	36.0	2.03E-13
36.0	4.92E-11	36.0	3.03E-12	37.0	2.21E-13
37.0	4.84E-11	37.0	3.25E-12	38.0	2.32E-13
38.0	4.60E-11	38.0	3.29E-12	39.0	2.50E-13
39.0	3.98E-11	39.0	3.13E-12	41.0	2.55E-13
41.0	3.39E-11	41.0	3.08E-12	43.0	2.55E-13
43.0	3.07E-11	43.0	2.86E-12	45.0	2.58E-13
45.0	3.06E-11	45.0	2.46E-12	47.0	2.54E-13
47.0	3.06E-11	47.0	2.13E-12	49.0	2.41E-13
49.0	2.72E-11	49.0	2.06E-12	51.0	2.21E-13
51.0	2.49E-11	51.0	1.68E-12	53.0	1.64E-13
53.0	1.68E-11	53.0	1.02E-12		
55.0	9.40E-12	55.0	5.12E-13		
57.0	4.91E-12				
59.0	2.60E-12				
61.0	9.20E-13				

* Read as 2.80×10^{-10}.

Table 2.2.7 Transmission Neutron Spectra behind Concrete

Energy (MeV)	Neutron Flux (1/cm²/MeV/proton)	Energy (MeV)	Neutron Flux (1/cm²/MeV/proton)	Energy (MeV)	Neutron Flux (1/cm²/MeV/proton)
Thickness	20 cm		50 cm		100 cm
5.0	2.05E-10*	5.0	6.50E-12	12.0	4.08E-14
6.0	2.83E-10	6.0	1.15E-11	13.0	7.85E-14
7.0	2.03E-10	7.0	9.96E-12	14.0	9.51E-14
8.0	1.92E-10	8.0	8.50E-12	16.0	9.01E-14
9.0	1.40E-10	9.0	6.20E-12	18.0	9.31E-14
10.0	1.39E-10	10.0	5.68E-12	20.0	1.02E-13
12.0	1.19E-10	12.0	4.72E-12	22.0	9.62E-14
13.0	1.03E-10	13.0	4.18E-12	23.0	8.43E-14
14.0	8.88E-11	14.0	3.79E-12	24.0	6.65E-14
15.0	9.34E-11	15.0	3.88E-12	25.0	4.94E-14
17.0	1.05E-10	17.0	3.71E-12	26.0	3.60E-14
19.0	9.49E-11	19.0	3.61E-12	27.0	2.84E-14
20.0	8.17E-11	20.0	4.05E-12	28.0	2.43E-14
22.0	7.48E-11	22.0	4.53E-12	30.0	2.11E-14
23.0	7.40E-11	23.0	4.26E-12	31.0	1.86E-14
24.0	7.93E-11	24.0	3.33E-12	32.0	1.74E-14
26.0	7.39E-11	25.0	2.56E-12	33.0	1.75E-14
28.0	6.82E-11	27.0	3.15E-12	35.0	1.98E-14
29.0	6.41E-11	28.0	3.69E-12	36.0	2.25E-14
30.0	6.18E-11	29.0	4.05E-12	37.0	2.61E-14
32.0	6.62E-11	31.0	3.68E-12	38.0	2.97E-14
33.0	6.79E-11	33.0	3.06E-12	40.0	3.21E-14
35.0	6.67E-11	35.0	3.45E-12	41.0	3.56E-14
36.0	6.43E-11	36.0	3.63E-12	43.0	3.92E-14
38.0	6.04E-11	38.0	3.63E-12	45.0	4.01E-14
39.0	5.53E-11	40.0	3.12E-12	47.0	4.11E-14
41.0	5.15E-11	41.0	2.96E-12	49.0	4.04E-14
43.0	4.39E-11	43.0	3.09E-12	51.0	5.06E-14
45.0	4.02E-11	45.0	3.06E-12	53.0	3.99E-14
47.0	3.84E-11	47.0	3.05E-12	55.0	2.88E-14
49.0	3.34E-11	49.0	2.97E-12	57.0	1.83E-14
51.0	2.77E-11	51.0	2.38E-12		
53.0	2.15E-11	53.0	1.78E-12		
55.0	1.64E-11	55.0	1.44E-12		
57.0	9.67E-12	57.0	8.60E-13		
59.0	4.89E-12	59.0	3.95E-13		
		61.0	9.40E-14		

* Read as 2.05×10^{-10}.

Table 2.2.8 Gamma-Ray Spectra behind Various Shields

Energy (MeV)	Photon Flux (1/MeV/cm²/proton)				
	Iron	Lead	Graphite	Concrete	
Thickness	20 cm	10 cm	30 cm	20 cm	50 cm
1.9				3.65E-09	
2.1	1.81E-10*	5.03E-10	7.75E-09	2.52E-09	1.71E-10
2.4	2.23E-10	3.88E-10	5.70E-09	2.41E-09	1.50E-10
2.7	1.73E-10	4.70E-10	4.98E-09	1.98E-09	1.79E-10
2.9	1.29E-10	3.91E-10	2.46E-09	1.71E-09	1.48E-10
3.1	1.06E-10	2.74E-10	2.68E-09	1.56E-09	1.38E-10
3.4	1.03E-10	1.91E-10	2.29E-09	1.50E-09	1.45E-10
3.7	1.09E-10	1.58E-10	2.25E-09	1.32E-09	1.33E-10
3.9	8.93E-11	1.66E-10	2.00E-09	1.21E-09	1.29E-10
4.1	7.49E-11	1.43E-10	1.85E-09	1.06E-09	1.14E-10
4.4	7.32E-11	1.32E-10	1.63E-09	9.35E-10	1.11E-10
4.7	7.35E-11	1.96E-10	1.46E-09	9.03E-10	1.04E-10
4.9	5.18E-11	2.63E-10	1.43E-09	8.11E-10	9.49E-11
5.1	5.05E-11	1.66E-10	1.35E-09	7.08E-10	7.88E-11
5.4	4.97E-11	9.52E-11	1.09E-09	6.10E-10	8.36E-11
5.7	4.34E-11	1.01E-10	9.59E-10	5.35E-10	8.41E-11
5.9	3.43E-11	8.33E-11	8.38E-10	4.86E-10	5.40E-11
6.1	3.33E-11	5.61E-11	7.18E-10	4.24E-10	4.89E-11
6.4	3.84E-11	5.51E-11	6.07E-10	3.88E-10	5.47E-11
6.7	3.82E-11	8.76E-11	5.66E-10	3.65E-10	4.91E-11
6.9	3.01E-11	9.83E-11	5.85E-10	3.25E-10	3.25E-11
7.1	2.02E-11	2.98E-11	4.97E-10	2.60E-10	2.29E-11
7.4	2.36E-11	5.52E-11	3.38E-10	1.96E-10	2.59E-11
7.7	3.48E-11	8.42E-11	2.25E-10	1.66E-10	1.96E-11
7.9	3.48E-11	1.12E-10	2.22E-10	1.59E-10	1.23E-11
8.1	2.16E-11	4.47E-11	2.76E-10	1.41E-10	1.88E-11
8.4	1.63E-11	8.46E-12	2.70E-10	1.03E-10	1.11E-11
8.7	2.20E-11	5.43E-11	1.63E-10	9.23E-11	
8.9	1.85E-11	9.49E-11	1.52E-10	1.07E-10	
9.1			1.92E-10	9.07E-11	
9.4			1.12E-10		

* Read as 1.81×10^{-10}.

Table 2.2.9 Atomic Composition of the Shields

Shield	Element	Atomic Density ($1/cm^3$)
Concrete	Hydrogen	1.70E+22[a]
	Oxygen	4.26E+22
	Sodium	7.44E+20
	Magnesium	3.77E+20
	Aluminum	2.29E+21
	Silicon	1.25E+22
	Calcium	3.50E+21
	Iron	4.44E+20
Iron	Iron	8.48E+22
Lead	Lead	3.30E+22
Graphite	Carbon	8.67E+22

[a]Read as 1.70×10^{22}.

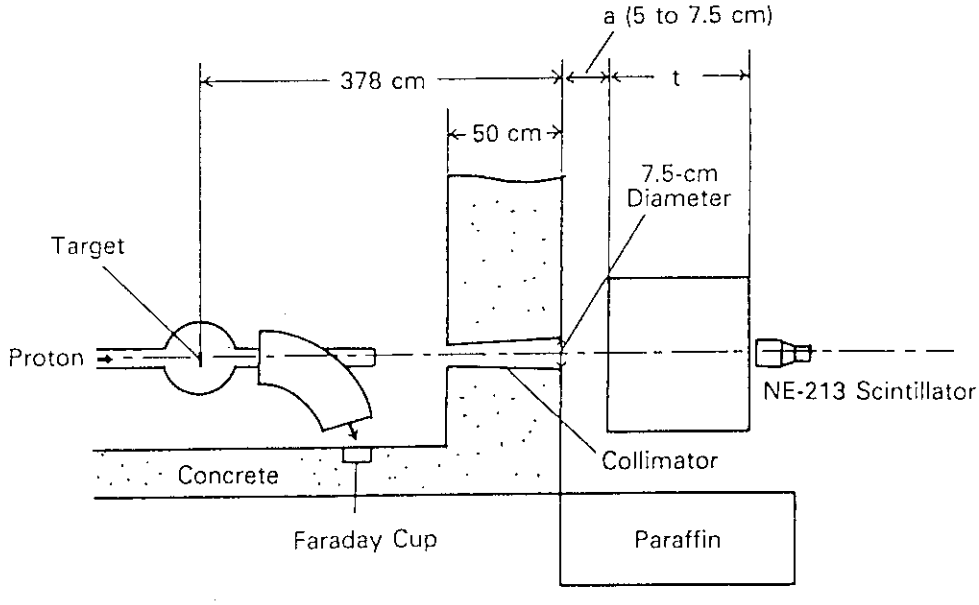

Fig. 2.2.1 Experimental setup for neutron penetration measurements.

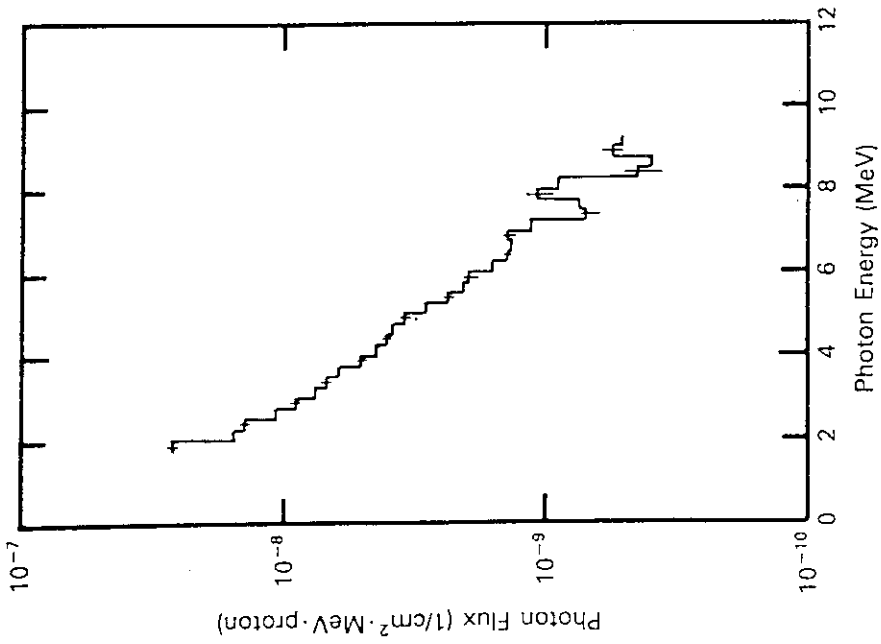

Fig. 2.2.3 Photon source spectrum at 383 cm from target.

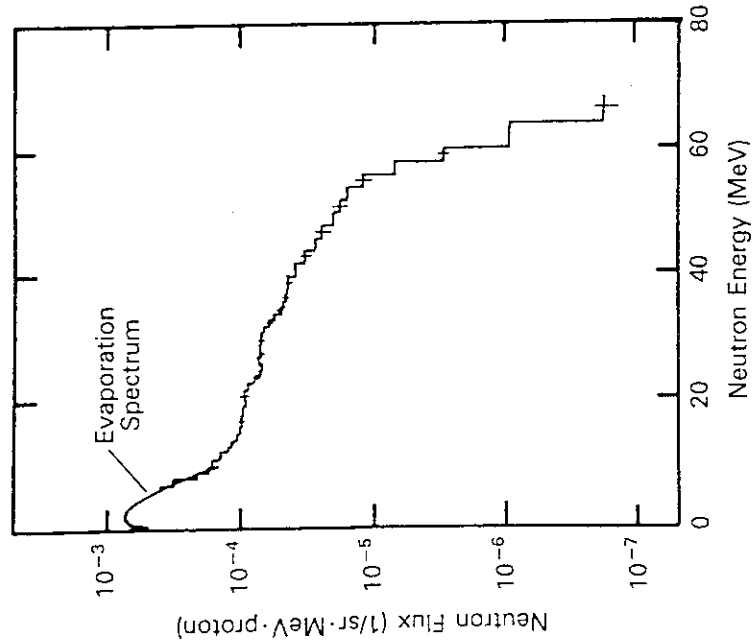

Fig. 2.2.2 Neutron source spectrum.

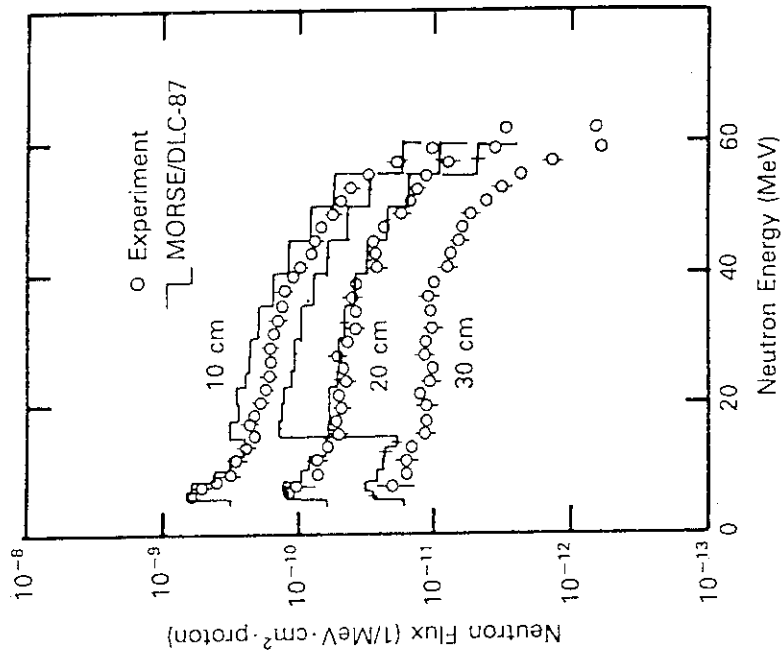

Fig. 2.2.5 Neutron spectra transmitted through the lead shields.

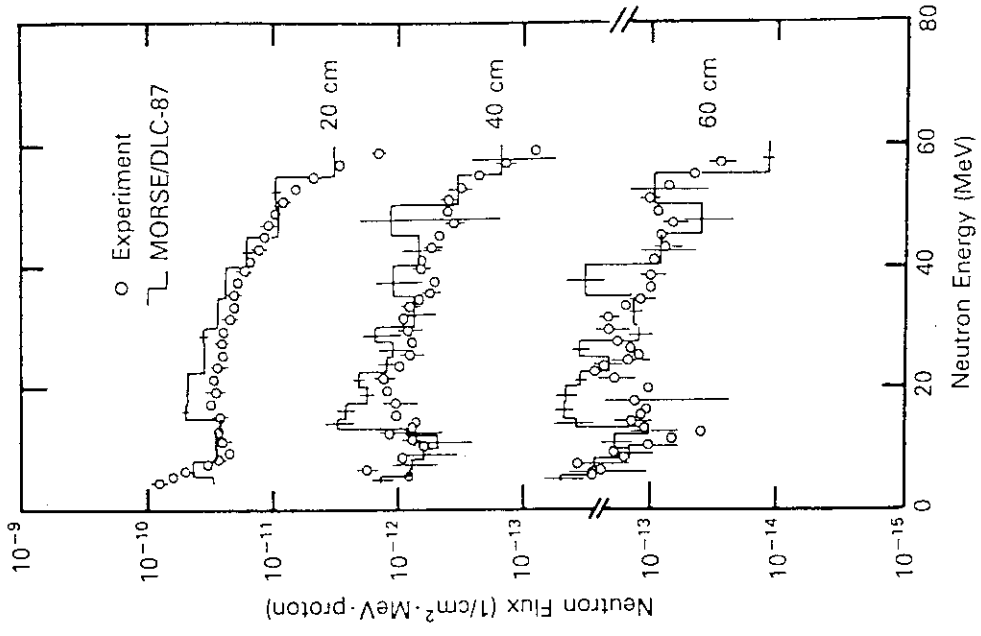

Fig. 2.2.4 Neutron spectra transmitted through the iron shields.

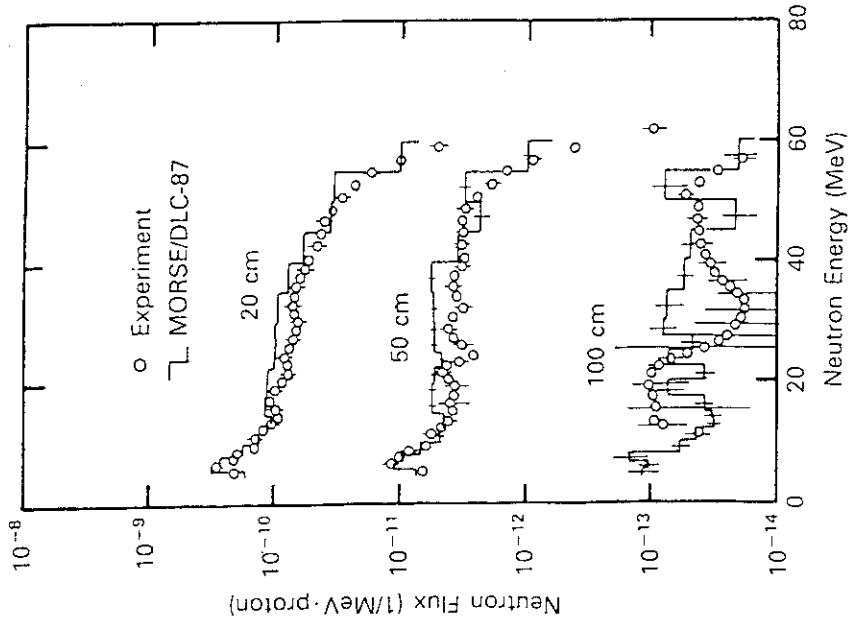

Fig. 2.2.7 Neutron spectra transmitted through the concrete shields.

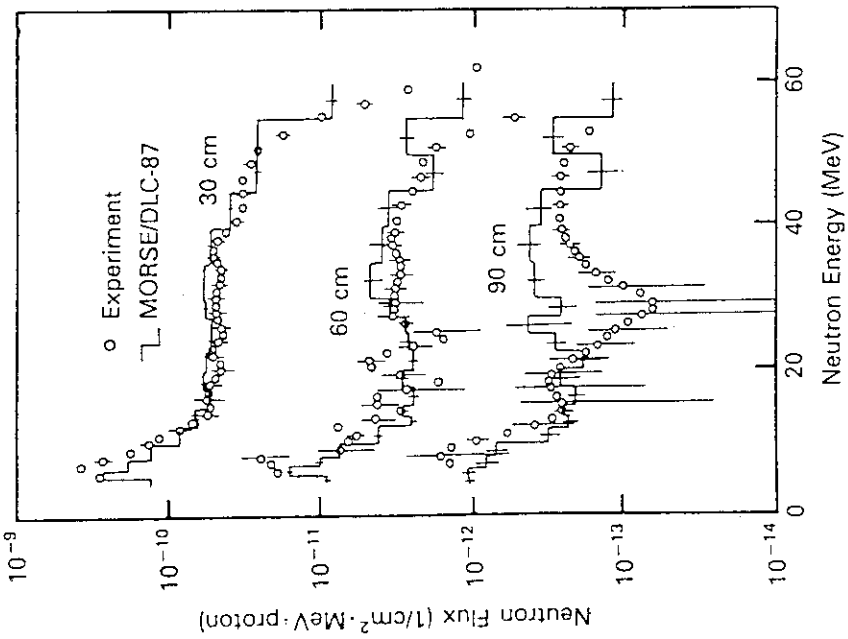

Fig. 2.2.6 Neutron spectra transmitted through the graphite shields.

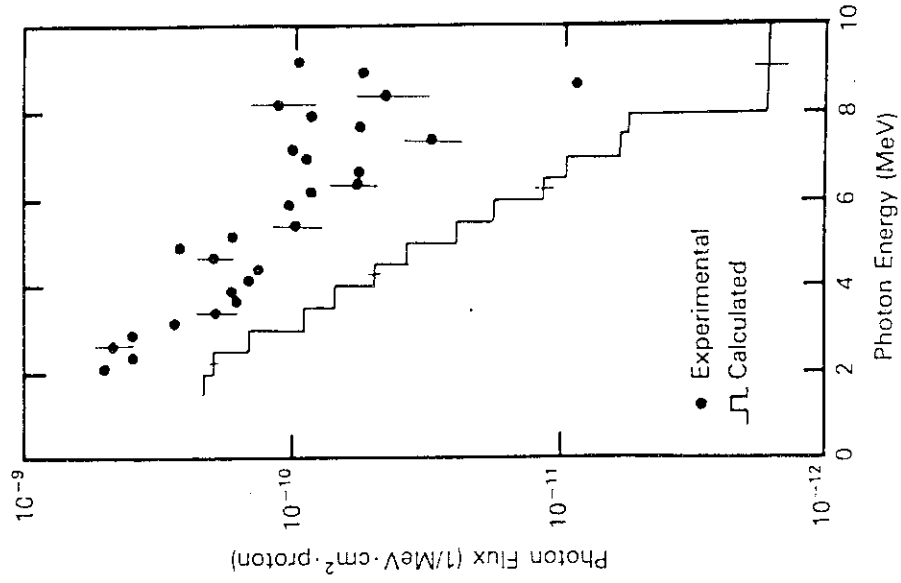

Fig. 2.2.9 Photon spectrum behind the 10-cm lead shield.

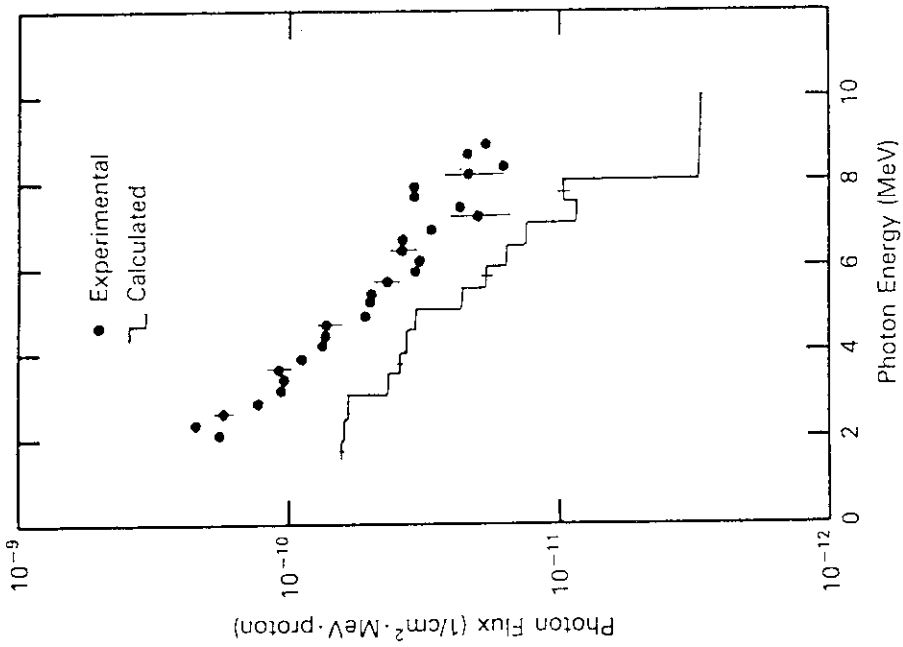

Fig. 2.2.8 Photon spectrum behind the 20-cm iron shield.

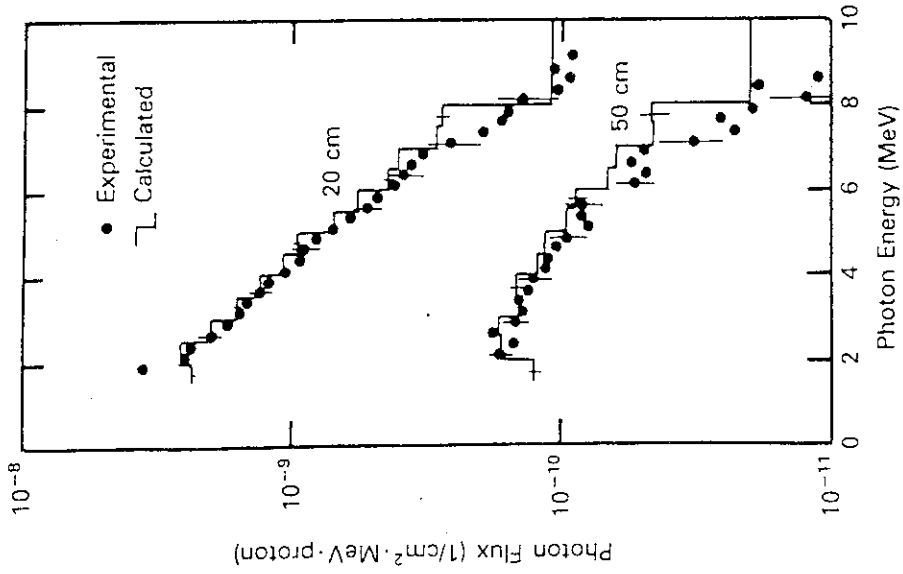

Fig. 2.2.11 Photon spectra behind the 20- and 50-cm concrete shields.

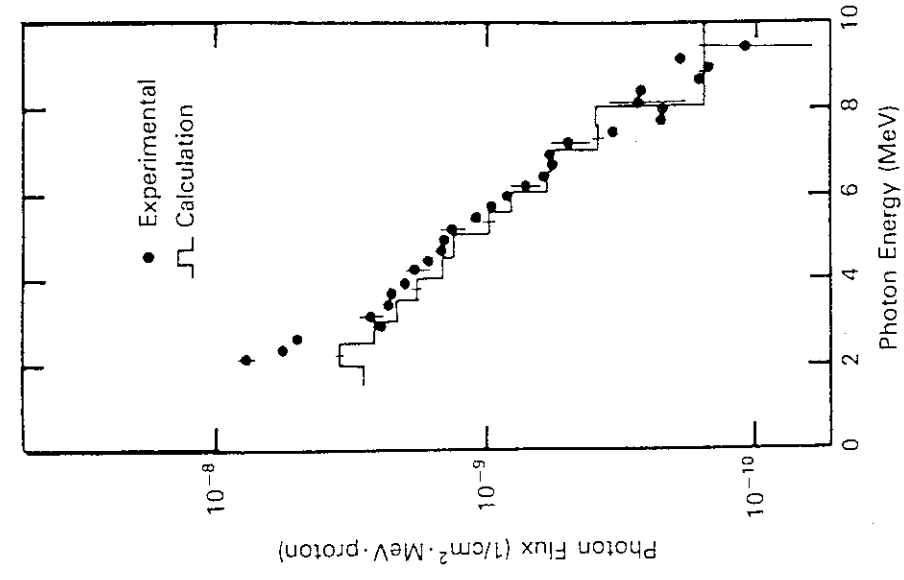

Fig. 2.2.10 Photon spectrum behind the 30-cm graphite shield.

2.3 Secondary Neutron Fluxes inside and around Iron Beam Stop for 500 MeV Protons

(Summary)

1) Accelerator (Organization) : Proton Synchrotron (KEK booster)
2) Projectile (Energy) : P (500MeV)
3) Target (Thickness) : Iron
4) Shielding material : Iron and Concrete
5) Geometry : Beam Dump, Forward and Lateral Shield
6) Instruments : Activation Detector
7) Measured Quantities : Saturated Activities

1. Experimental Arrangement

Cross-sectional plane view of beam stop and plan view of the beam dump room are shown in Figs. 2.3.1 and 2.3.2, respectively. The front shield is 2-m-thick and the side one 1.5-m-thick. The beam stop was irradiated by 500 MeV proton accelerated by proton synchrotron in KEK.

2. Methods of Measurement and Instrument

Sample disks of iron and activation foils of Al, Cu and Au, were packed in iron pipes of 55.0 cm long and 2.0 cm inner diameter and put into the hole bored in the beam stop. Activities were measured with a 40 cm^3 Ge(Li) gamma-ray detector. Saturated activity distributions of Fe$\Rightarrow{}^{48}$V, Fe$\Rightarrow{}^{52}$Mn, Fe$\Rightarrow{}^{54}$Mn and Fe$\Rightarrow{}^{56}$Co were measured in the beam stop. Distribution of ^{27}Al(n,x)^{24}Na, Cu$\Rightarrow{}^{58}$Co and ^{197}Au(n,γ)^{198}Au were also measured in the beam stop. Saturated activities of ^{12}C(n,2n)^{11}C, ^{27}Al(n,spallation)^{18}F and ^{27}Al(n,x)^{24}Na were measured at 0, 65, 80, 90 and 100 degree around the beam stop shown in Fig. 2.3.2.

3. Target Geometry and Beam Conditions

The beam profile was expected to be about 6.0 cm (FWHM) in the horizontal and 3.0 cm (FWHM) in the vertical direction, and the beam direction to be nearly parallel within 4 mrad (FWHM). The absolute beam intensity was monitored using a total beam charge collector and three monitors with ferrite core, which were calibrated within 4 % accuracy.

In the dump room experiment the origin was set at 5 cm from the entrance point

toward the beam direction. The beam intensity 3.8 x 10^{12} protons/sec was monitored using a ferrite core, and its horizontal width was 30 mm (FWHM) and vertical one 15 mm.

4. Measured Results

The measured distribution of saturated activities in the beam stop are shown in Figs. 2.3.3 through 2.3.5 and Tables 2.3.1 and 2.3.2. The saturated activities around the beam stop are given in Table 2.3.3.

5. Model for Calculation

a. Source Condition

500 MeV proton of mono-direction along the Z-axis, which injects at the origin in Figs. 2.3.6. and 2.3.7

b. Calculation Geometry

Three-dimensional calculation model as shown in Figs. 2.3.6. and 2.3.7. The cross-sectional plane view along YZ-plane is the same as one along XZ-plane.

c. Compositions of Material

Densities and atomic composition given in Table 2.3.4.

6. Normalization Between Calculation and Measurement

The measured results are normalized to one incident proton for measurements in the beam stop and one incident proton per second for ones around the beam stop.

References

1. Arakita Y., Hirayama H., Inagaki T. and Miyajima M.: "Study of an Iron Beam Stop for 500 MeV Protons," Nucl. Instrum. Methods, 164, 255-265 (1979).
2. Ban S., Hirayama H. and Katoh K.: "Measurement of Secondary Neutron Fluxes around Beam Stop for 500 MeV Protons," ibid., 184, 409-412 (1981).

Table 2.3.1 Saturated avtivity distributions of ^{48}V, ^{52}Mn, ^{54}Mn and ^{56}Co in beam stop.

R (cm)	Z (cm) -2.5	12.5	27.5	40.0	52.5	67.5	82.5
	Fe → ^{48}V						
0.0		5.22E-29	2.48E-30	1.06E-30	2.30E-31	5.94E-32	2.07E-32
7.0	6.92E-30*		2.12E-30	1.06E-30	2.28E-31	6.23E-32	2.02E-32
14.0	6.87E-32	9.95E-31	6.17E-31	6.11E-31	1.58E-31	5.23E-32	2.30E-32
28.0		6.51E-32	8.68E-32		7.38E-32	3.68E-32	1.49E-32
44.0		5.41E-33	1.79E-32	1.72E-32	2.27E-32		
	Fe → ^{52}Mn						
0.0		4.23E-29	3.19E-30	6.11E-31	2.85E-31	7.87E-32	2.68E-32
7.0	4.88E-30	1.88E-29	2.76E-30	5.74E-31	2.73E-31	7.69E-32	2.28E-32
14.0	2.16E-31	1.65E-30	9.30E-31	3.58E-31	2.16E-31	7.15E-32	2.38E-32
28.0	8.68E-33	1.50E-31	2.02E-31	6.07E-32	1.15E-31	3.67E-32	1.51E-32
44.0		2.18E-32	2.81E-32		2.33E-32	1.12E-32	7.14E-33
	Fe → ^{54}Mn						
0.0		5.88E-28	6.73E-29	1.26E-29	6.21E-30	1.70E-30	6.84E-31
7.0	8.18E-29	2.80E-28	5.75E-29	1.24E-29	5.88E-30	2.07E-30	6.28E-31
14.0	1.77E-29	4.19E-29	1.79E-29	8.86E-30	5.17E-30	1.44E-30	6.93E-31
28.0	9.25E-30	1.20E-29	7.45E-30	2.09E-30	3.05E-30	1.02E-30	
44.0	4.93E-30	7.57E-30	2.08E-30	1.30E-30	8.24E-31		
56.0		6.03E-30	1.49E-30	1.11E-30	6.02E-31	4.41E-31	
	Fe → ^{56}Co (Relative to ^{54}Mn)						
0.0		5.88E-28					
1.5	2.36E-28						
2.0		2.45E-28					
3.0	1.60E-28	1.71E-28					
4.0	6.19E-29	7.08E-29					
5.0	3.03E-29	4.09E-29					
6.0	8.32E-30	2.21E-29					
7.0		1.34E-29					

* Read as 6.92×10^{-30} (n/proton).

Table 2.3.2 Saturated activity distributions of ^{24}Na, ^{58}Co, and ^{198}Au in beam stop.

R (cm)	Z (cm) -2.5	12.5	27.5	40.0	52.5	67.5	82.5	97.5
	$^{27}Al(n,x)^{24}Na$							
0.0		1.82E-28	7.43E-30	1.46E-30	6.24E-31	4.07E-31	8.16E-32	2.49E-32
7.0	1.08E-29*	2.53E-29	5.52E-30	1.78E-30	5.58E-31	2.78E-31	8.51E-32	1.77E-32
14.0	2.03E-30	4.87E-30	3.04E-30	9.32E-31	3.20E-31	2.22E-31	6.07E-32	2.43E-32
28.0	3.26E-31	6.79E-31	6.68E-31	4.22E-31	1.14E-31	8.47E-32	2.87E-32	
	$Cu \rightarrow {}^{58}Co$							
0.0		1.21E-27	2.96E-29	5.49E-30	2.28E-30	8.58E-31		
7.0	1.29E-29	7.50E-29	2.01E-29	4.46E-30	1.98E-30	5.84E-31		
14.0	1.49E-30	8.05E-30	5.73E-30	2.54E-30	1.30E-30	4.67E-31		
28.0	2.79E-31	9.70E-31	1.25E-30	8.12E-31	7.71E-31	2.54E-31		
	$^{197}Au(n,\gamma)^{198}Au$							
0.0		4.33E-27	3.69E-27	2.23E-27	2.21E-28	1.47E-28	1.20E-28	3.45E-29
7.0	3.00E-27	4.15E-27	2.82E-27	2.46E-27	2.16E-28	1.58E-28	8.93E-29	3.39E-29
14.0		3.68E-27	2.19E-27	2.74E-27	2.42E-28	1.39E-28	1.15E-28	
28.0	2.03E-27	2.79E-27	1.34E-27	1.77E-27	1.80E-28	1.05E-28	6.14E-29	2.27E-29
44.0	4.69E-28	7.36E-28		6.04E-28	7.23E-29	2.83E-29	3.19E-29	1.22E-29
54.0	2.18E-28	2.47E-28	2.54E-28	2.32E-28	1.97E-29	1.84E-29	2.10E-29	

* Read as 1.08×10^{-29} (n/proton).

Table 2.3.3 Experimental and calculated results of saturated activities.

Position	$^{11}C\ s^{-1}$ per proton/s		$^{18}F\ s^{-1}$ per proton/s		$^{24}Na\ s^{-1}$ per proton/s
	Exp.	Cal.	Exp.	Cal.	Exp.
0° I [a]	1.96E-33 [c]	5.0 ± 0.6E-33 [d]	3.84E-34	1.1 ± 0.1E-33	2.99E-33
65° I	1.08E-33	9.2 ± 0.8E-33			
80° I	1.04E-33	6.9 ± 1.0E-33	1.73E-34	8.0 ± 1.7E-34	2.14E-33
90° I	1.18E-33	3.4 ± 0.7E-33	1.64E-34	4.1 ± 1.2E-34	2.13E-33
100° I	8.71E-34	1.1 ± 0.4E-33			
0° O [b]	1.15E-35	4.3 ± 0.9E-35	1.85E-36	1.0 ± 0.2E-35	1.46E-35
65° O	1.11E-35	6.9 ± 2.0E-35			
80° O	9.86E-36	3.8 ± 1.4E-35	1.74E-36	2.9 ± 2.0E-36	1.70E-35
90° O	7.25E-36	3.3 ± 1.3E-35	1.18E-36		1.43E-35
100° O	4.40E-36				

[a] Inside the concrete shield. [b] Outside. [c] 1.96×10^{-33}. [d] $(5.0 \pm 0.6) \times 10^{-33}$.

Table 2.3.4 Densities and composition.

Material	Density
Fe	7.8 g/cm³
Concrete	2.35 g/cm³
H	1.2%
O	54%
Si	31%
Ca	9.7%
Al	4.1%

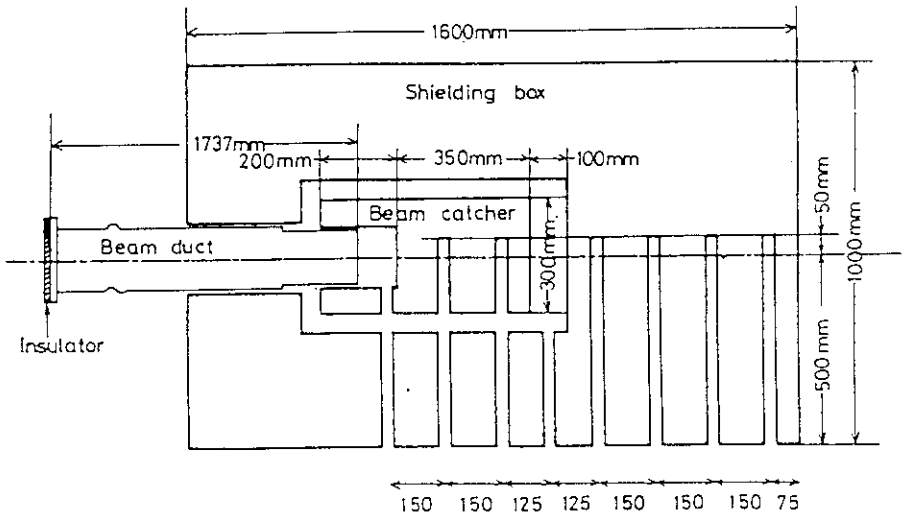

Fig. 2.3.1 Cross-sectional plan view of beam stop.

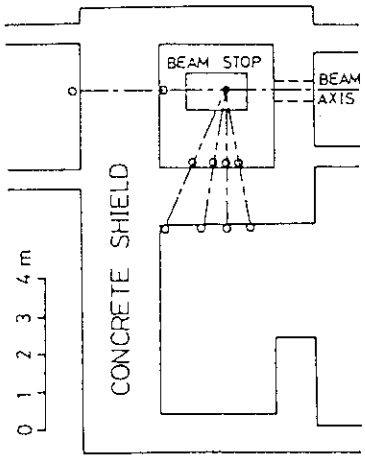

Fig. 2.3.2 Plan view of beam dump room. Open circles denote measurement points for directions 0, 65, 80, 90 and 100 degree. Black circle denotes the origin for each direction.

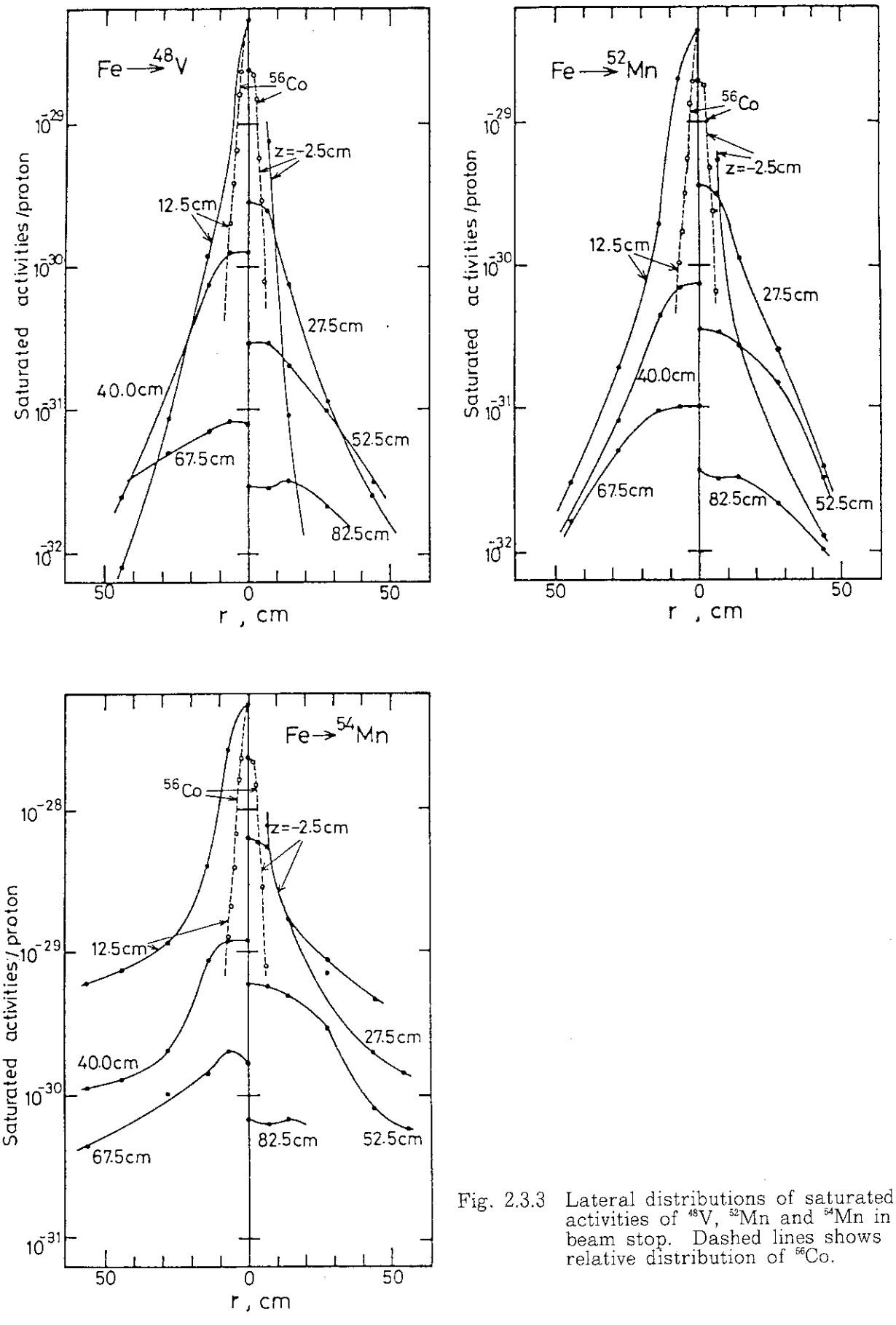

Fig. 2.3.3 Lateral distributions of saturated activities of ^{48}V, ^{52}Mn and ^{54}Mn in beam stop. Dashed lines shows relative distribution of ^{56}Co.

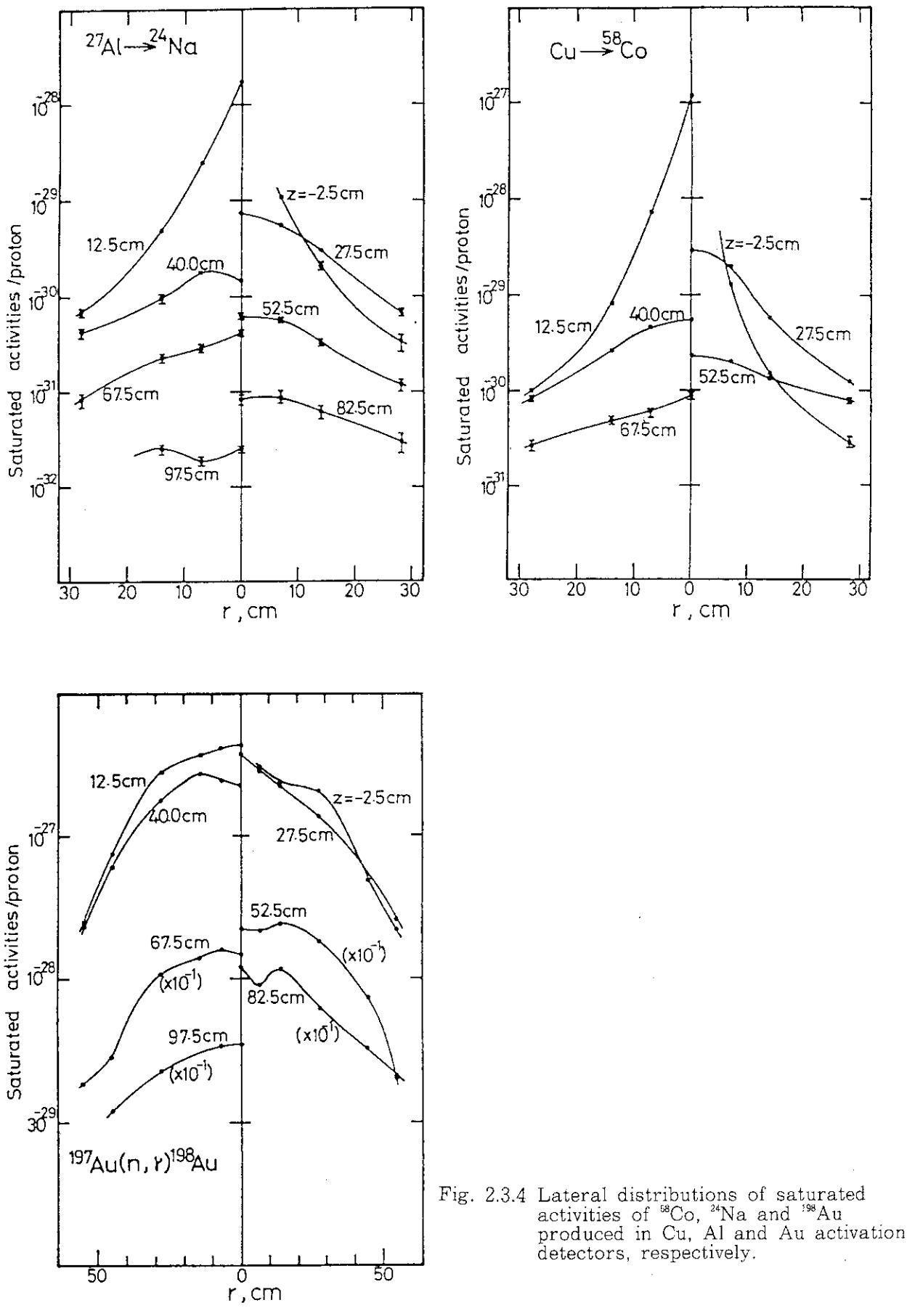

Fig. 2.3.4 Lateral distributions of saturated activities of ^{58}Co, ^{24}Na and ^{198}Au produced in Cu, Al and Au activation detectors, respectively.

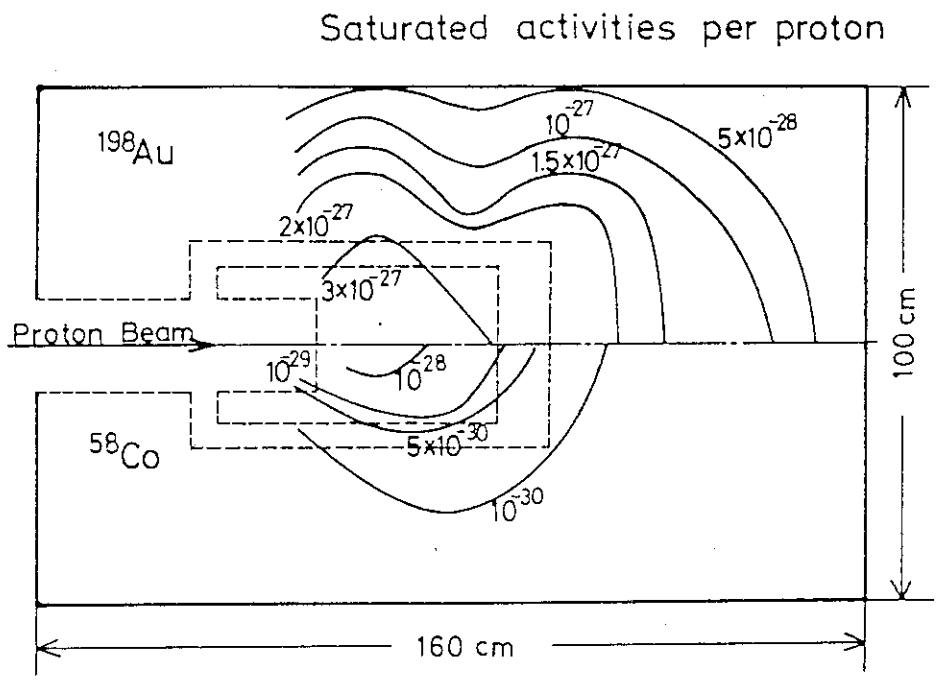

Fig. 2.3.5 Iso-activity-contours of ^{58}Co and ^{198}Au in beam stop.

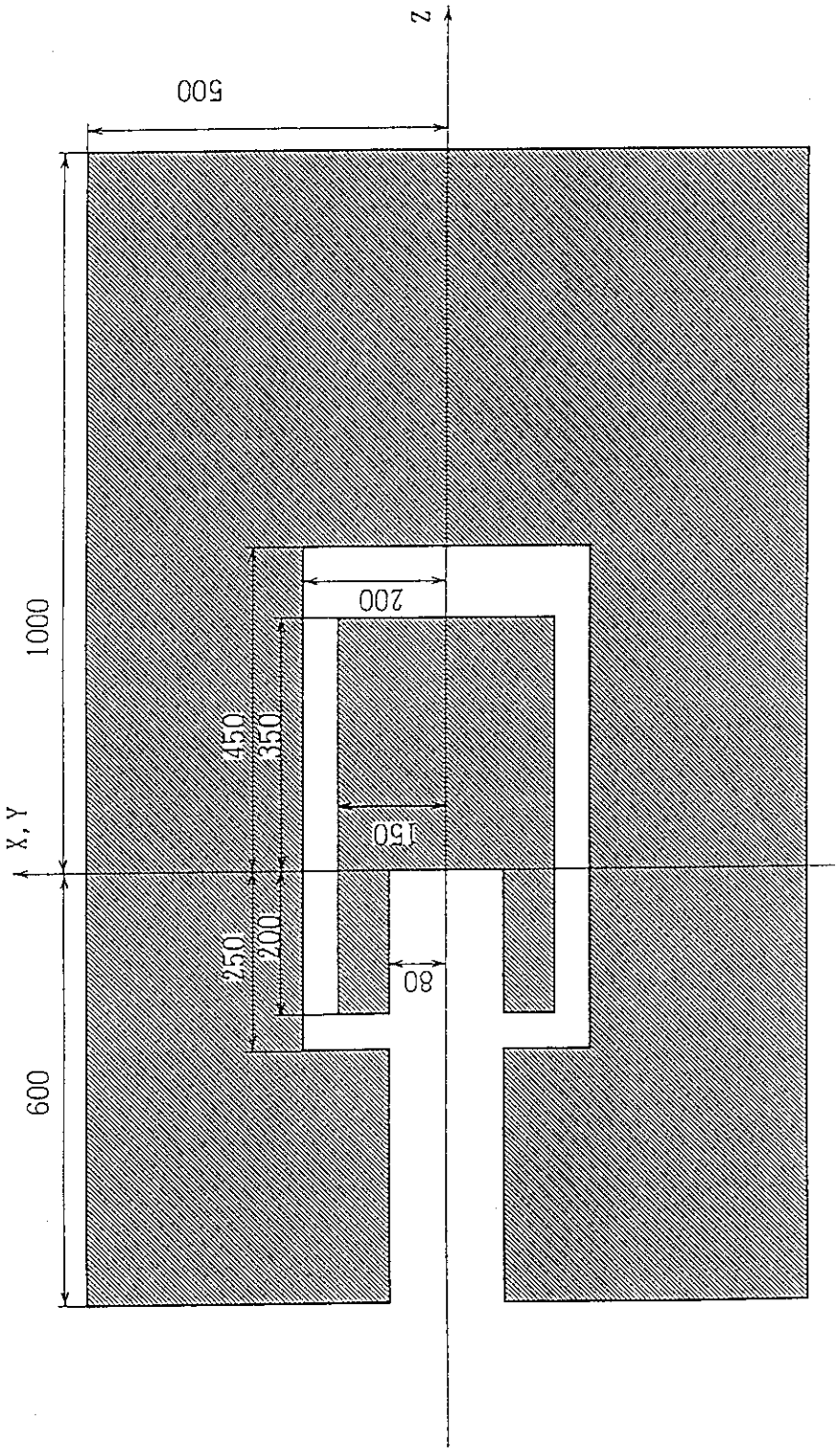

Fig. 2.3.6 Calculational model inside beam stop. The unit in figure is shown in millimeter.

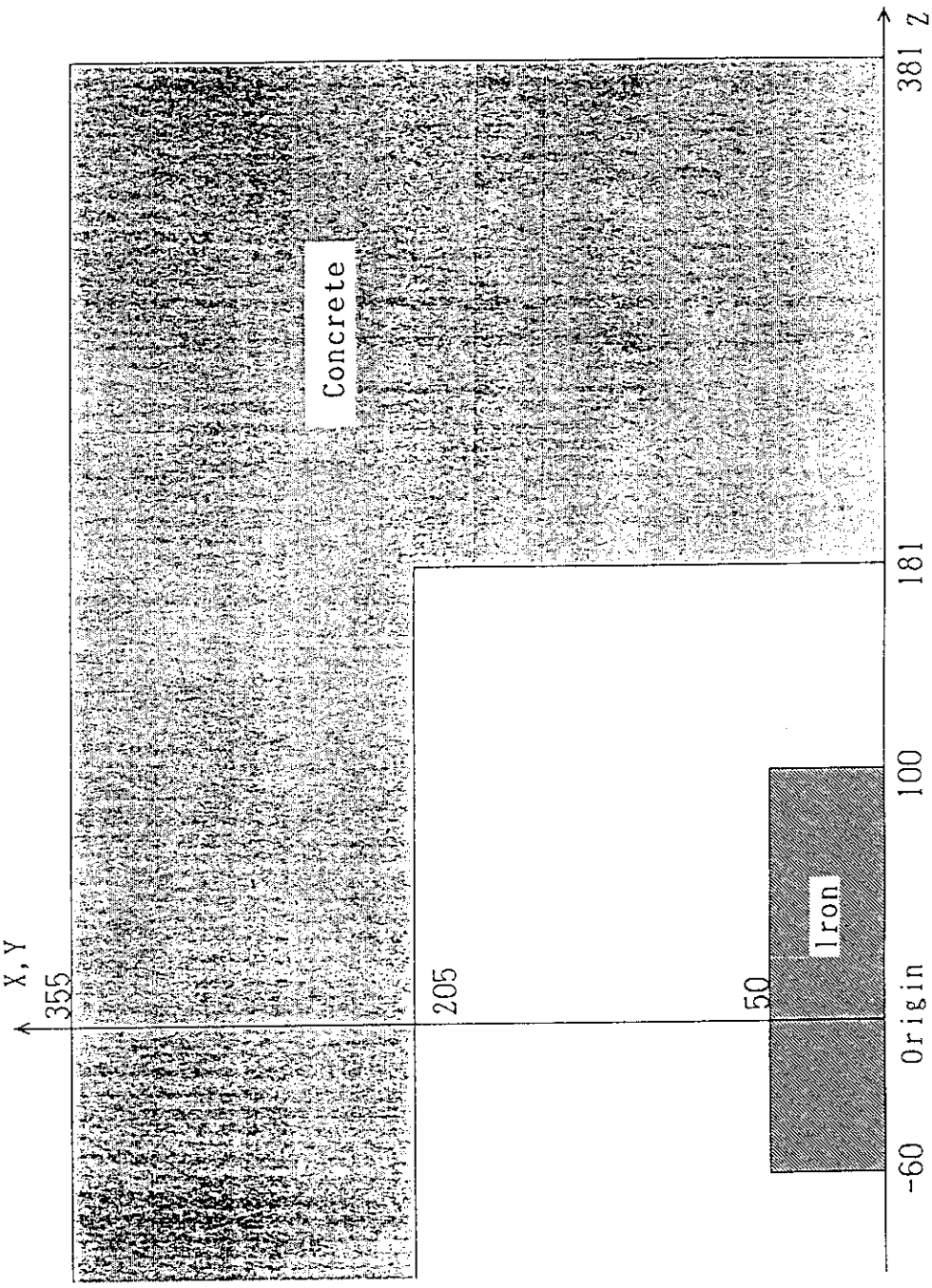

Fig. 2.3.7 Calculational model around beam stop. The unit in figure is shown in centimeter. The origin of angles in Fig. 2.3.2 and Table 2.3.3 is set at (0,0,5) .

Appendix Reaction Cross Sections for Benchmark Problems

The reaction cross sections for the benchmark calculations are prepared up to 500 MeV for neutron and 300 MeV for photon as follows. The quantities in the file (J4276.MEDIUM02.DATA) of computer FACOM－M/780 are available for whoever contacts to T. Fukahori (Nuclear Data Center, JAERI).

1) $^{197}Au(n,\gamma)^{198}Au$ (Fig. A.1)

The cross section was referred from ENDF/B－VI[A.1] up to 30 MeV, and extrapolated by a log－log manner above the energy up to 500 MeV. The data are in a member of the file (SHAU197N), and its ID number is MAT=7925, MF=3, MT=102.

2) $^{12}C(n,2n)^{11}C$ (Fig. A.2)

The cross section was calculated by the ALICE－F code[A.2]. The data is held in a member of the file (SHC012N), and its ID number is MAT=612, MF=3, MT=16.

3) $^{27}Al(n,x)^{24}Na$, $^{27}Al(n,x)^{18}F$ (Figs. A.3 and A.4)

The $^{27}Al(n,x)^{24}Na$ cross section was referred from JENDL－3[A.3] up to 20 MeV, and calculated by the ALICE－F code above the energy as the production cross section of ^{24}Na. The (n,x) cross section was also calculated by the ALICE－F code for all energy region. These data are contained in a member of the file (SHAL027N), and ID numbers are MAT=1327, MF=3, MT=107, 800.

4) $Fe(n,x)^{48}V,^{52,54}Mn$ (Figs. A.5, A.6 and A.7)

The cross section of ^{54}Fe was referred from JENDL－3 below 20 MeV and calculated by the ALICE－F code over the energy. For the cross section of ^{56}Fe, high energy file in the ENDF/B－VI file was referred, which was produced by the ENDF/B－VI file and the calculation by the ALICE－P code[A.4] basically. The cross section of Fe was deduced with relative isotopic abundance as follows,

$$\sigma(Fe) = \sigma(^{54}Fe)\times 0.058 + \sigma(^{56}Fe)\times 0.918. \qquad (A.1)$$

The data are in a member of the file (SHFE000N), and ID numbers are MAT=2600, MF=3, MT=800, 801, 802.

5) Cu(n,x)^{58}Co (Fig. A.8)

The cross sections of ^{63,65}Cu were calculated by the ALICE−F code as the production cross section of ^{58}Co , and the cross section of Cu was derived from the following equation with relative isotopic abundance,

$$\sigma(\mathrm{Cu}) = \sigma(^{63}\mathrm{Cu})\times 0.692 + \sigma(^{65}\mathrm{Cu})\times 0.308. \qquad (A.2)$$

The data are included in a member of the file (SHCU000N), and its ID number is MAT=2900, MF=3, MT=800.

6) ^{208}Pb(γ,n)^{207}Pb

The photo−absorption cross section of ^{208}Pb up to 300 MeV was calculated by utilizing a code[A.5] considering the giant dipole resonance and quasi−deuteron reactions. The branching ratio of each isotope production was calculated by the ALICE−F code as the reaction of the neutron absorption of ^{207}Pb. The reaction cross section and double−differential cross section generating neutron are in a member of the file (SHPB208G) and ID number are MAT=8208, MF=3, 6, MT=201. Figures A.9, A.10 and A.11 show the double−differential neutron production cross sections toward 30.0, 90.0 and 150.0 degree at the photon incident energy of 150 and 266 MeV.

A group−wise data file (J3931.REACTXX.DATA(CROS66)) is also available , which was obtained by averaging the cross sections in the DLC−119/HILO86[A.6] type energy intervals up to 400 MeV. The average cross sections were calculated by MACS−N code system[A.7] weighting with 1/E spectrum above 0.3224 eV and maxwellian spectrum from 0.3224 to 1.0 x 10^{-5} eV.

References

A.1. BNL/NNDC, ENDF/B−VI (1990).

A.2. T. Fukahori, et al., JAERI−M 92−039, 114 (1992).

A.3. K. Shibata, et al., JAERI−1319 (1990).

A.4. S. Pearlstein, J. Astrophys., 346, 1049 (1989).

A.5. S. Igarashi, Private communication.

A.6. R.G. Alsmiller Jr., ORNL/TM−9801 (1986).

A.7. A. Hasegawa, Private communication.

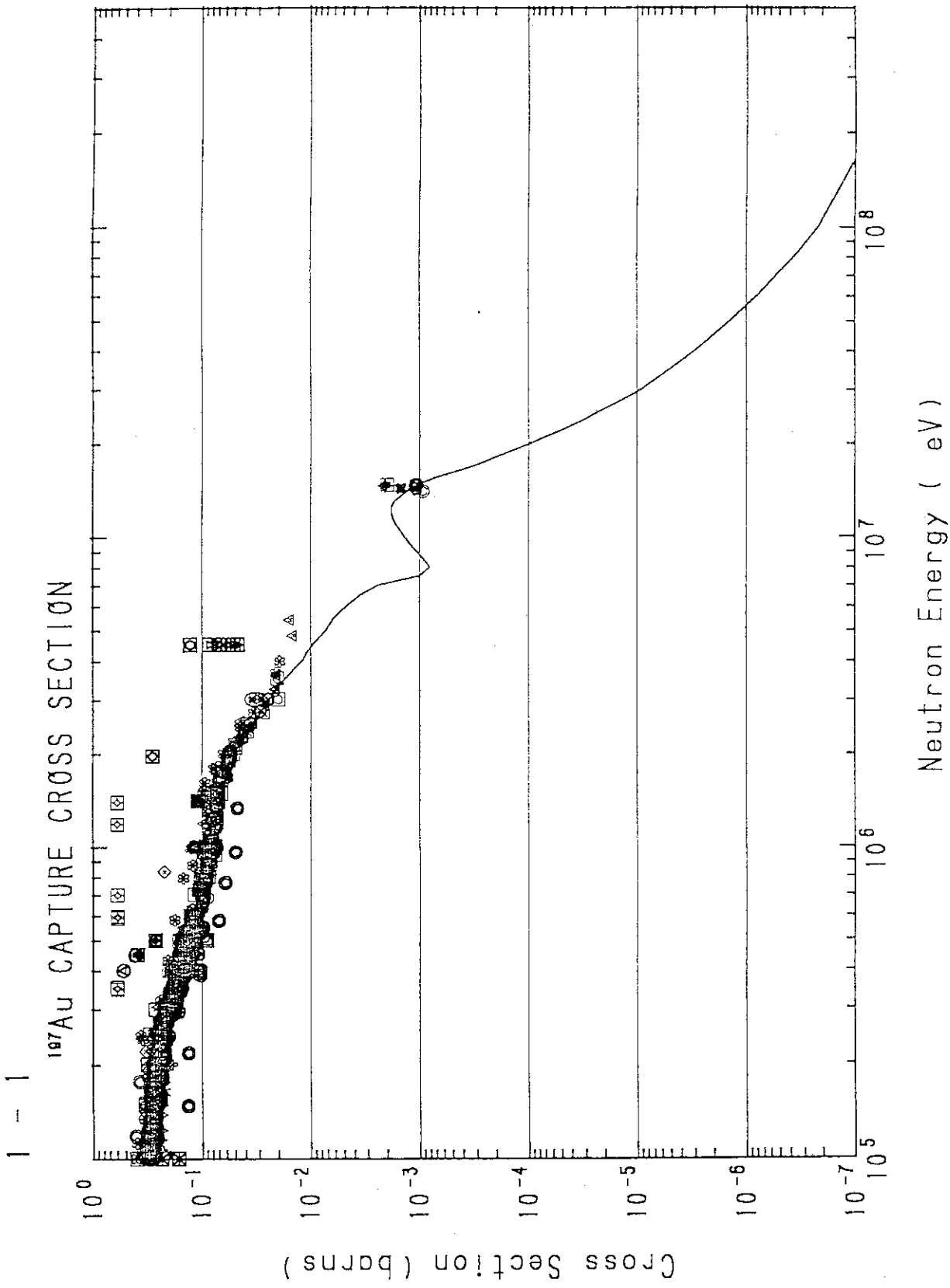

Fig. A.1 $^{197}Au(n,\gamma)^{198}Au$ cross section.

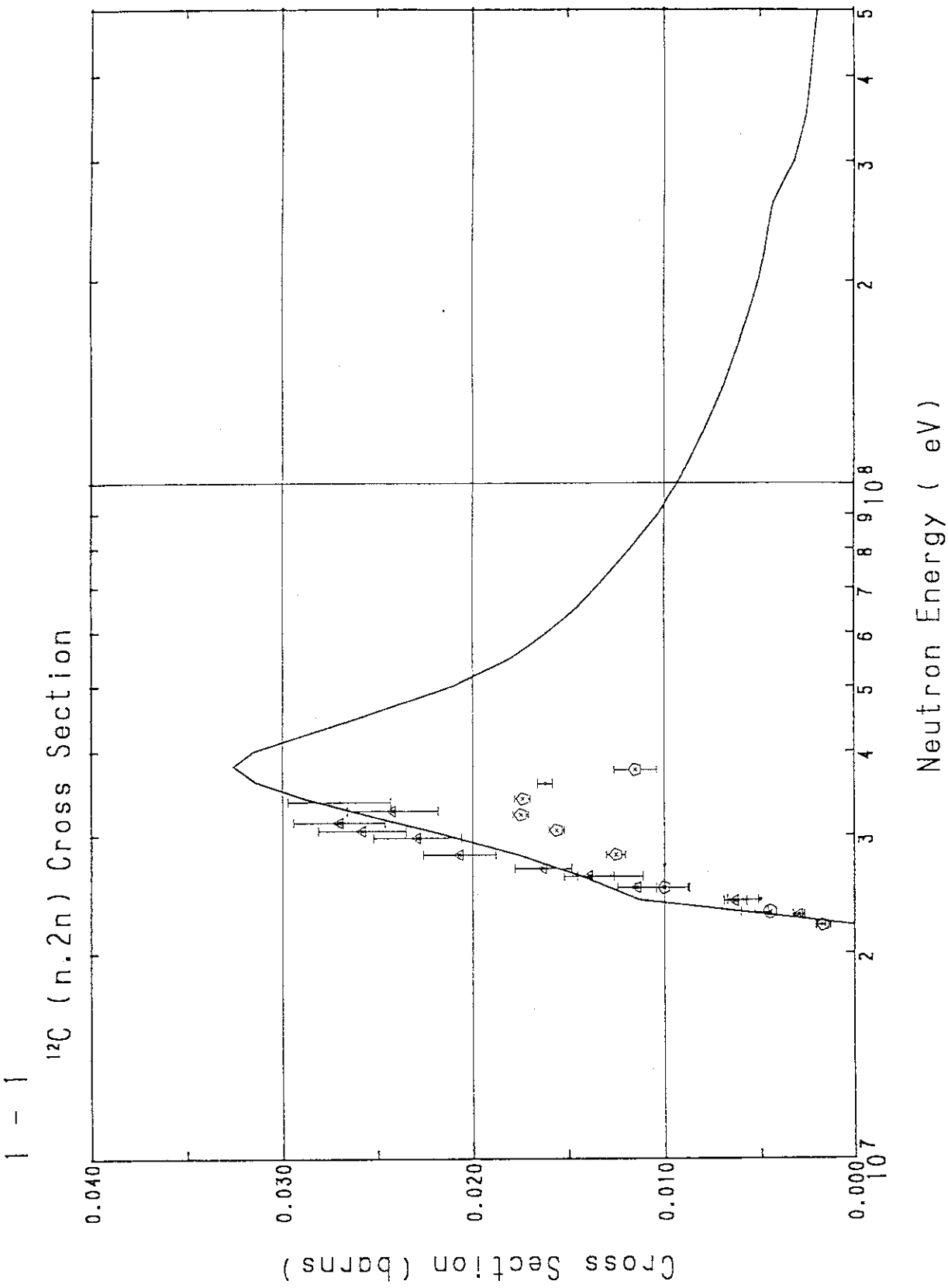

Fig. A.2 ^{12}C(n,2n)^{11}C cross section.

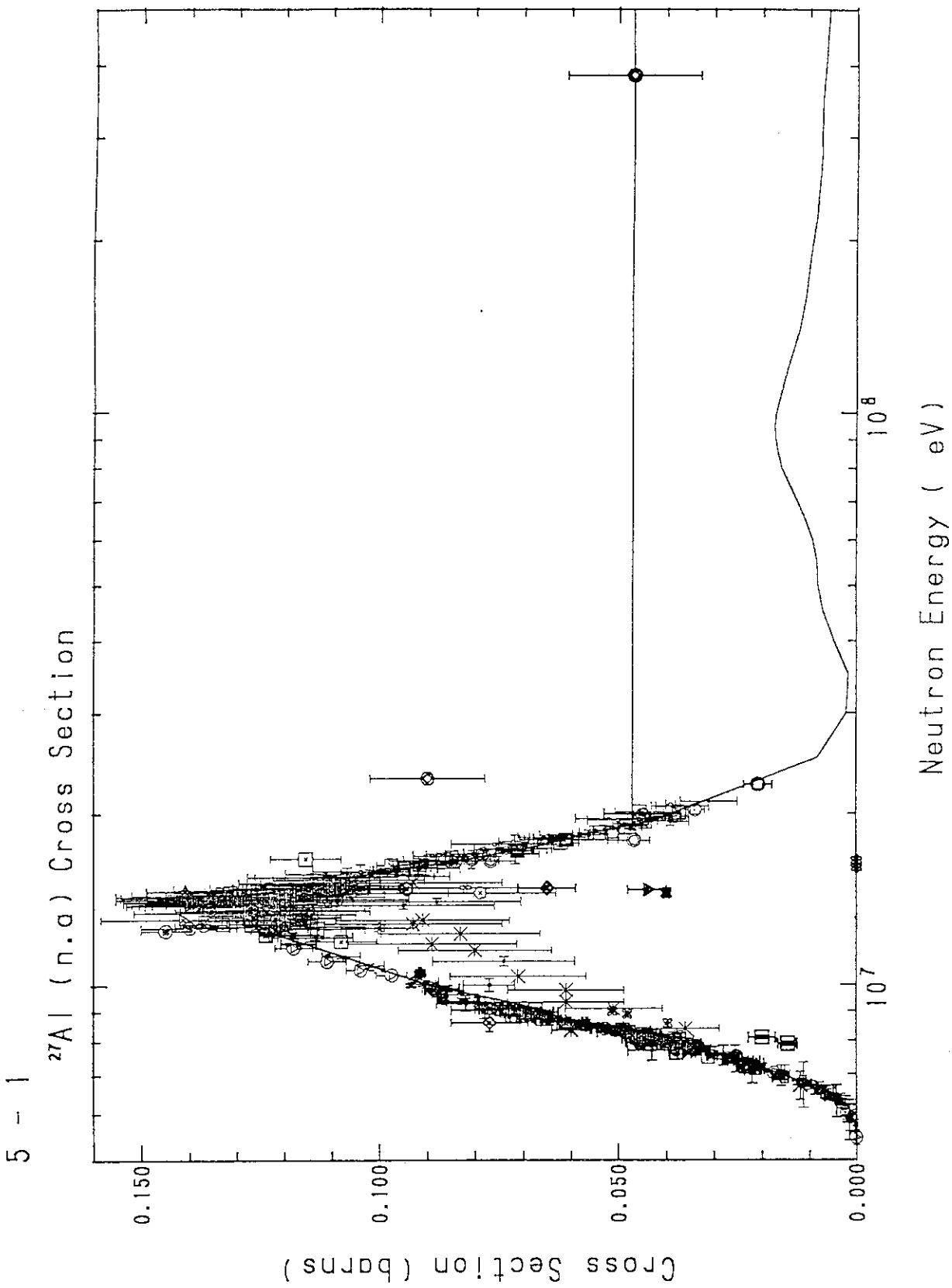

Fig. A.3 $^{27}Al(n,x)^{24}Na$ cross section.

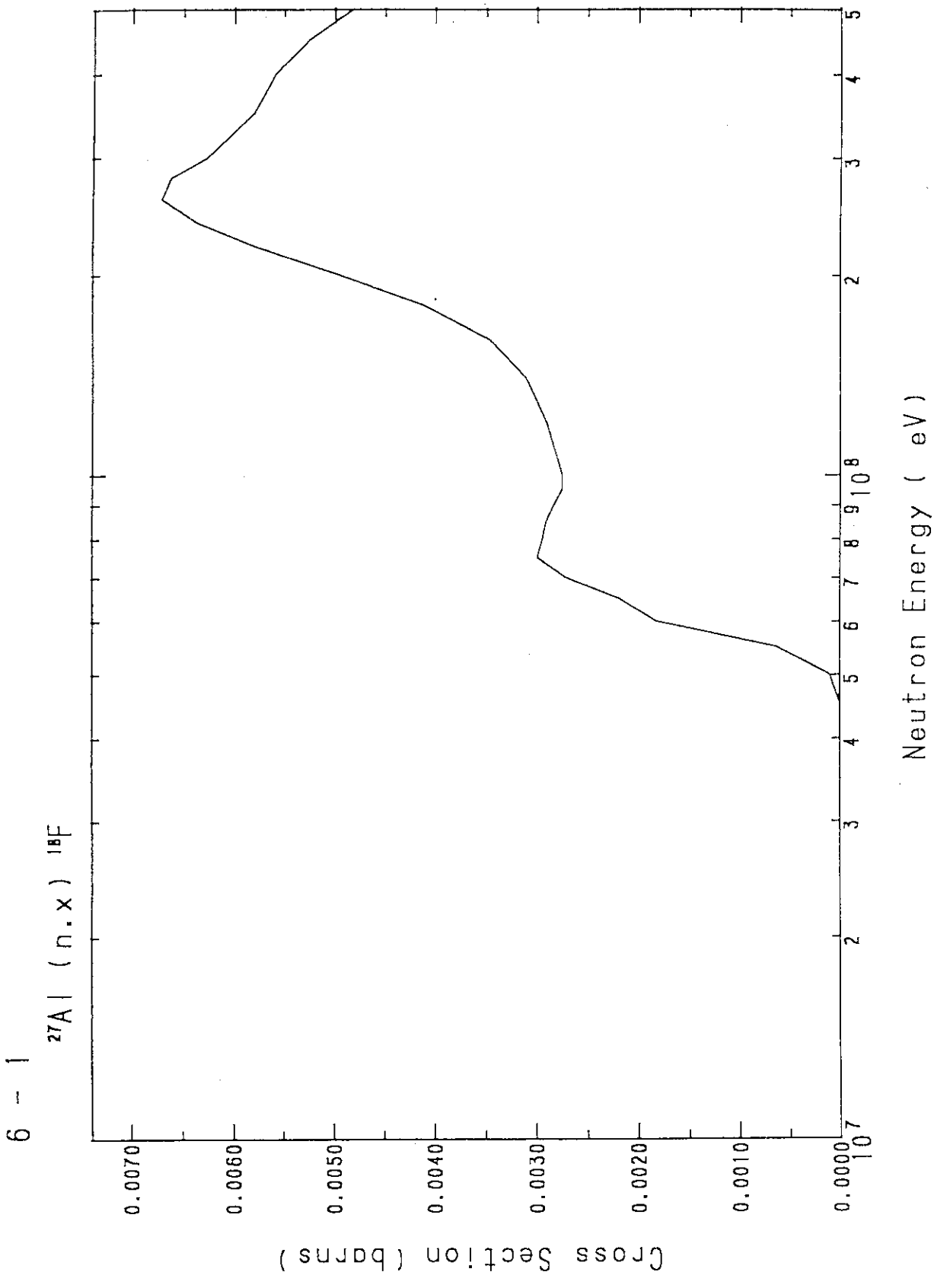

Fig. A.4 ^{27}Al(n,x)^{18}F cross section.

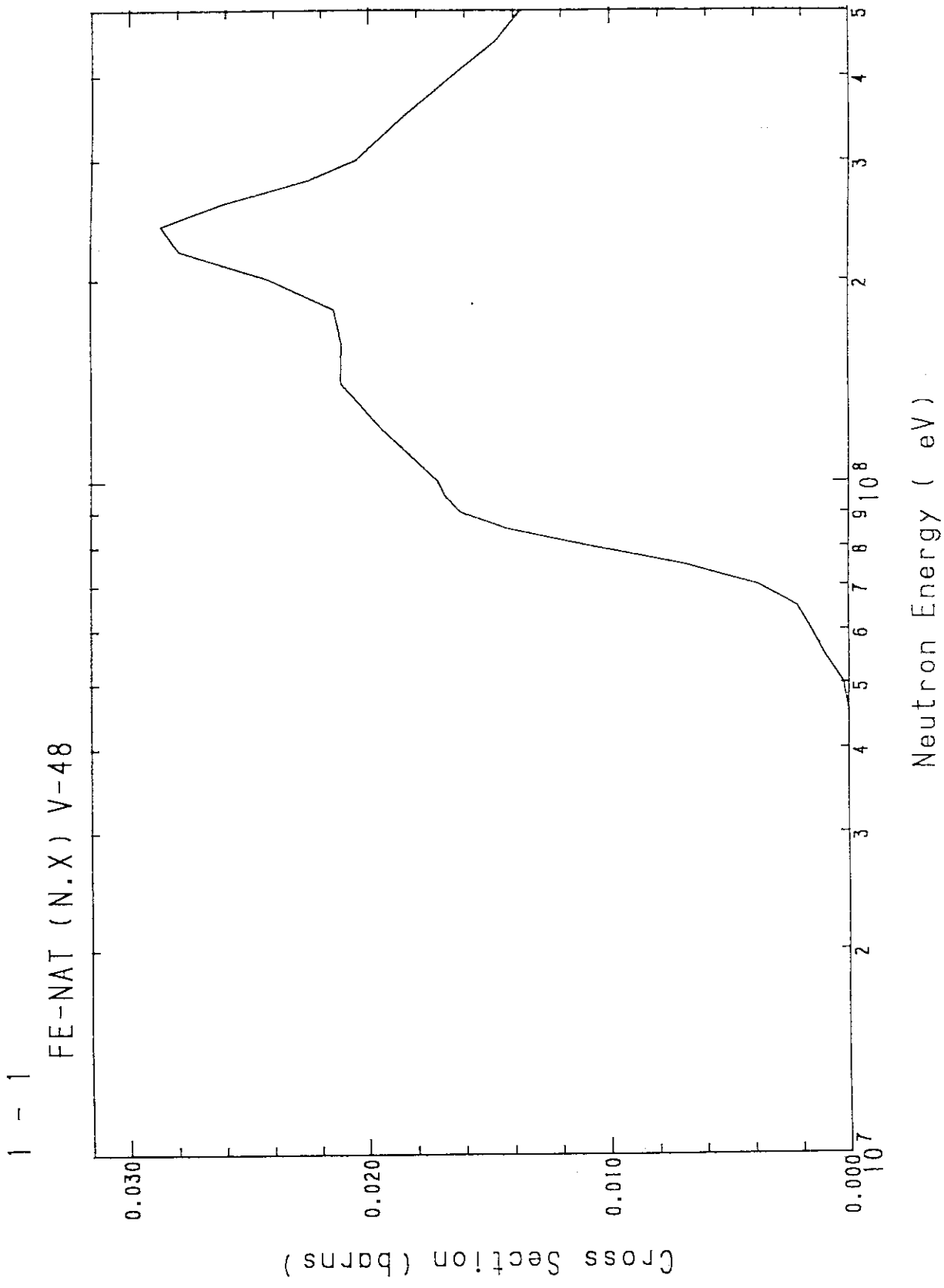

Fig. A.5 Fe(n,x)^{48}V cross section.

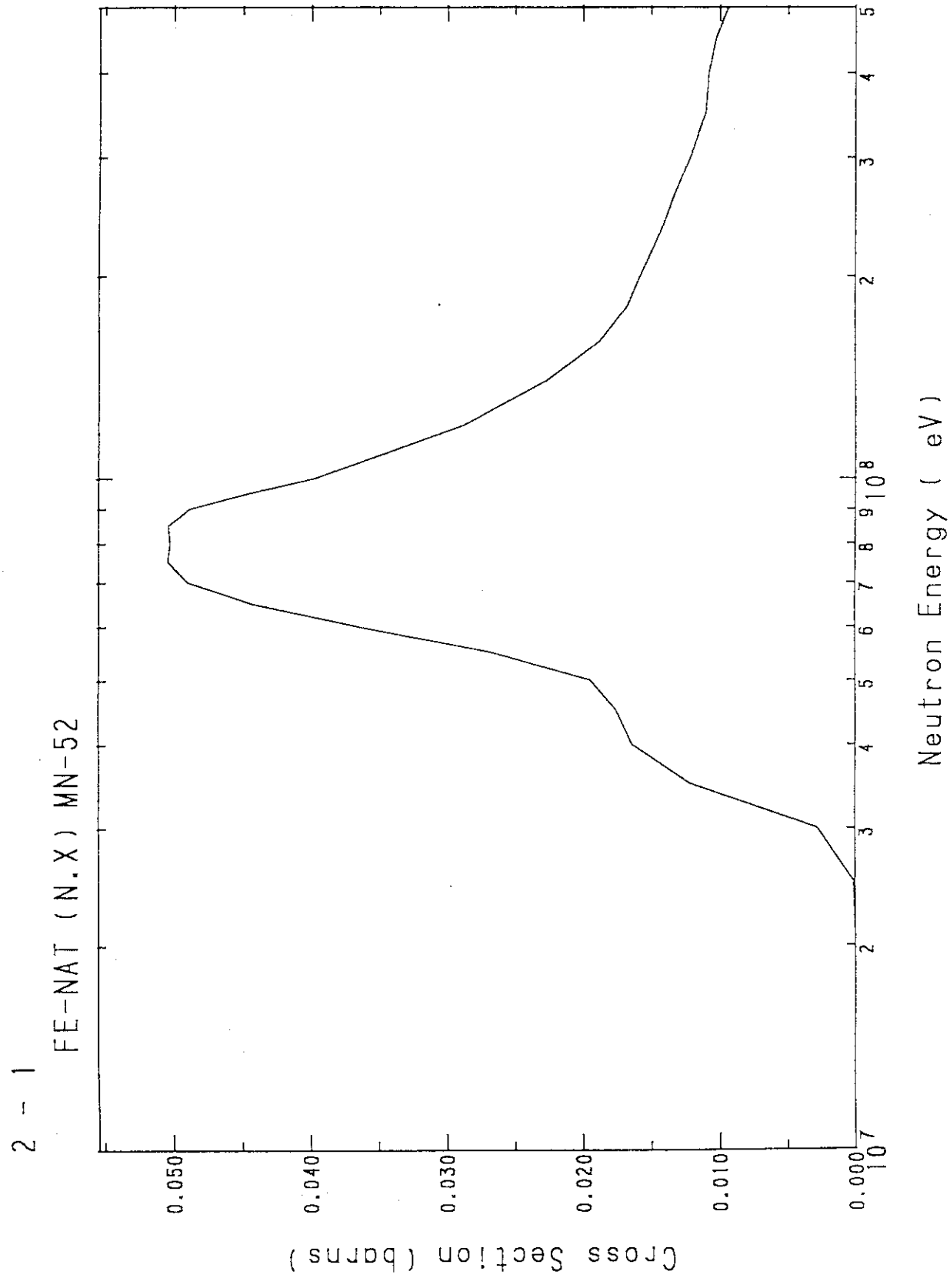

Fig. A.6 Fe(n,x)^{52}Mn cross section.

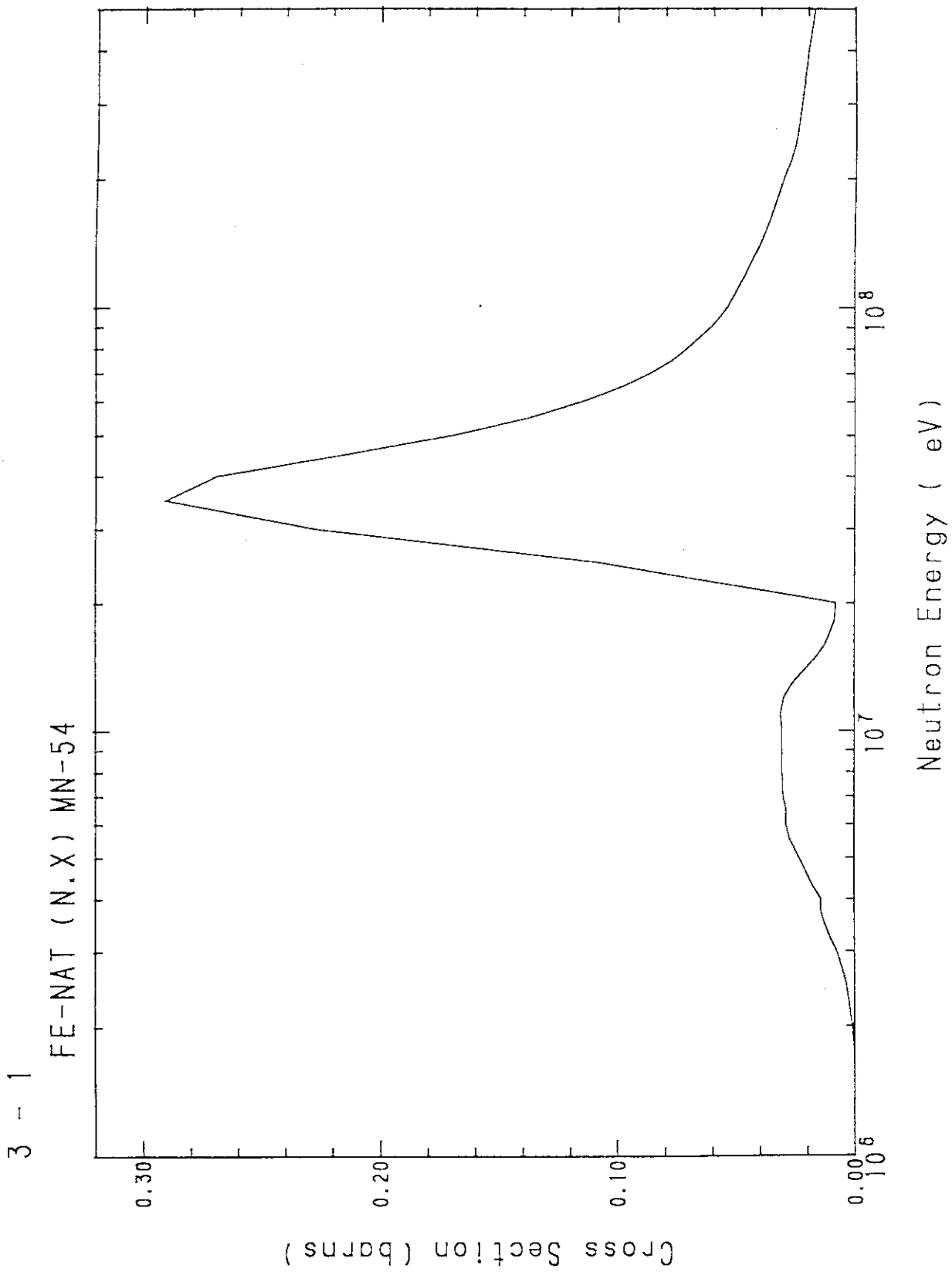

Fig. A.7 Fe(n,x)^{54}Mn cross section.

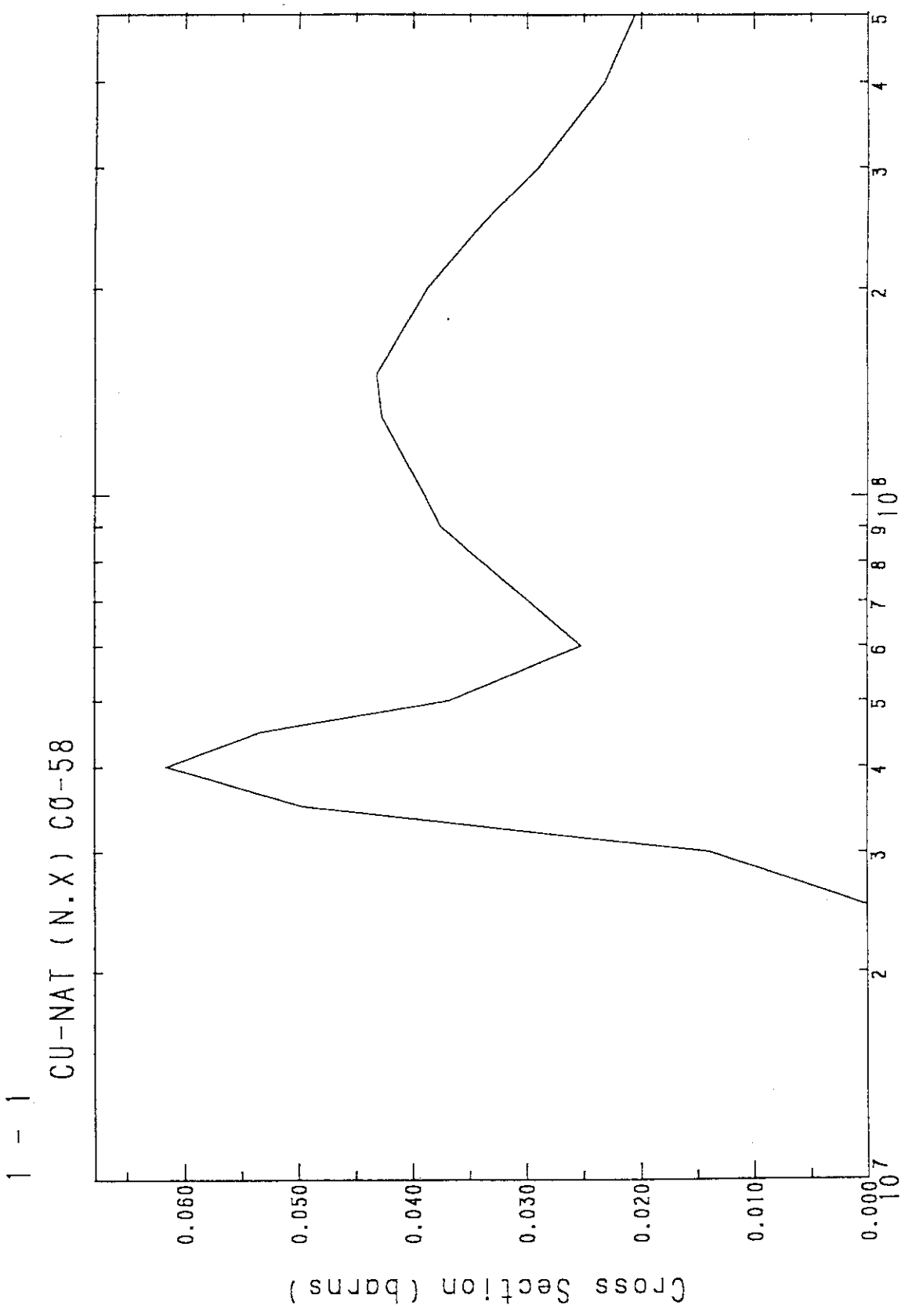

Fig. A.8 Cu(n,x)^{58}Co cross section.

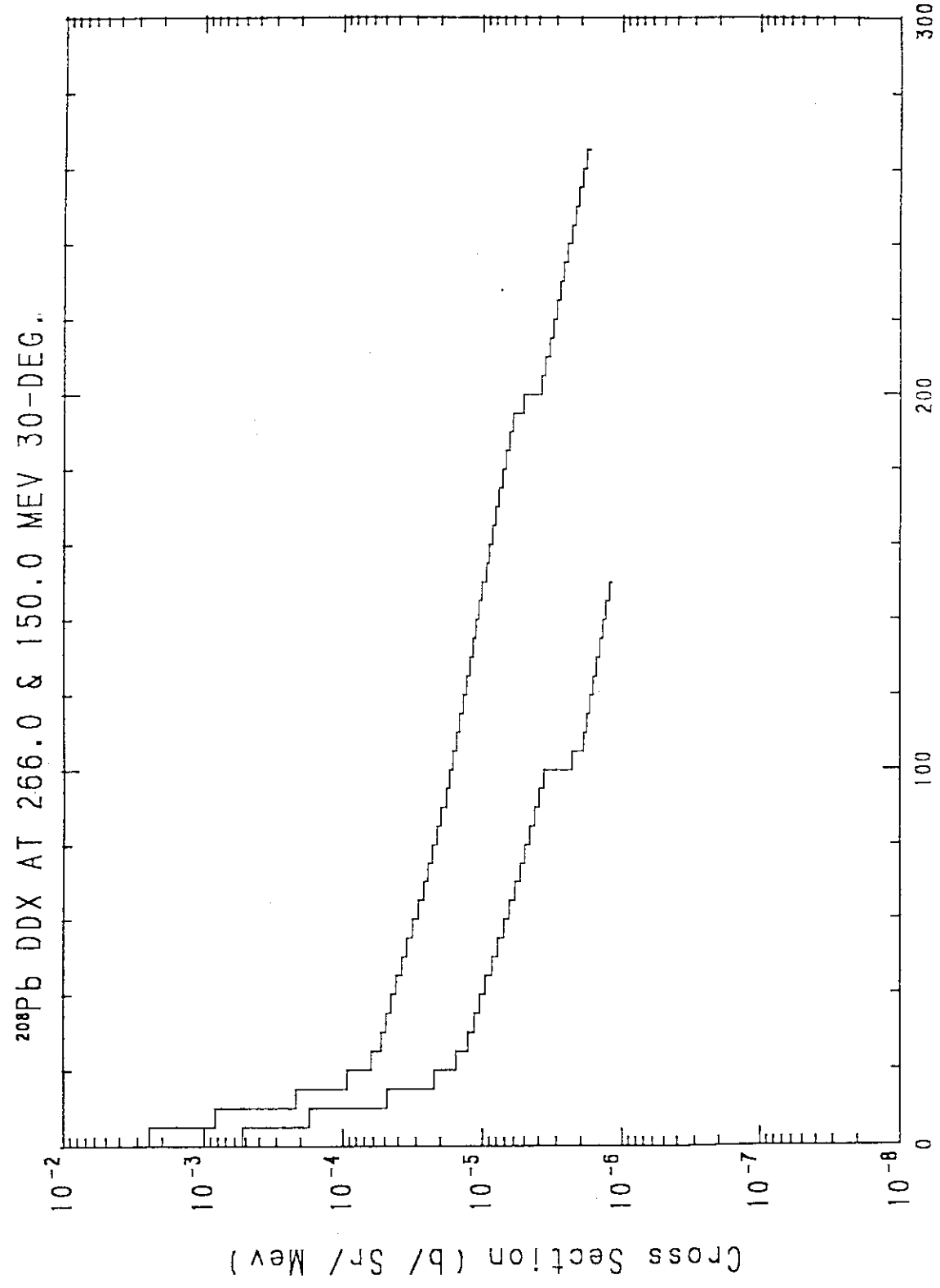

Fig. A.9 Double-differential neutron production cross sections of ^{208}Pb toward 30.0 degree at the photon incident energy of 150 and 266 MeV.

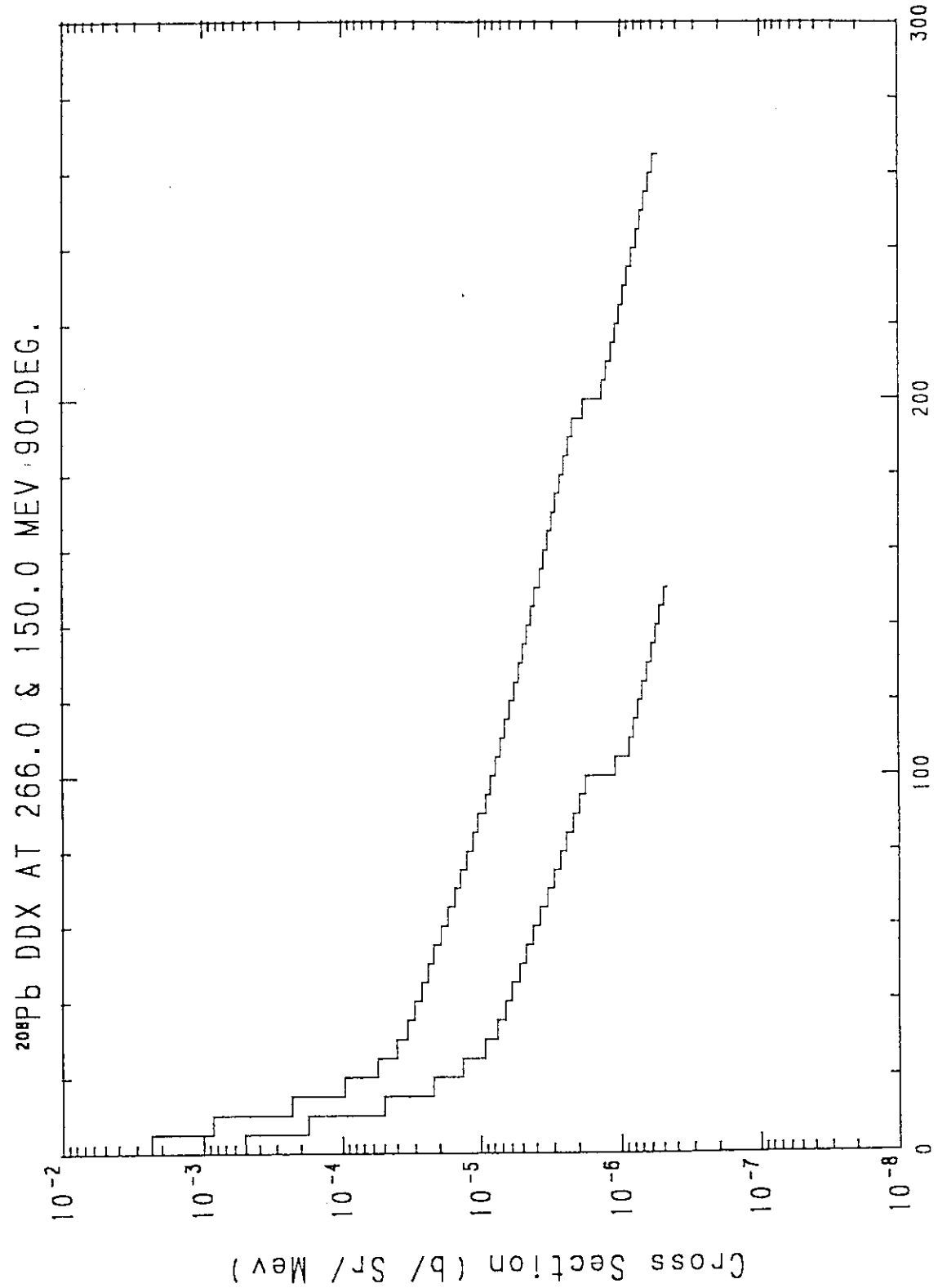

Fig. A.10 Double-differential neutron production cross sections of ^{208}Pb toward 90.0 degree at the photon incident energy of 150 and 266 MeV.

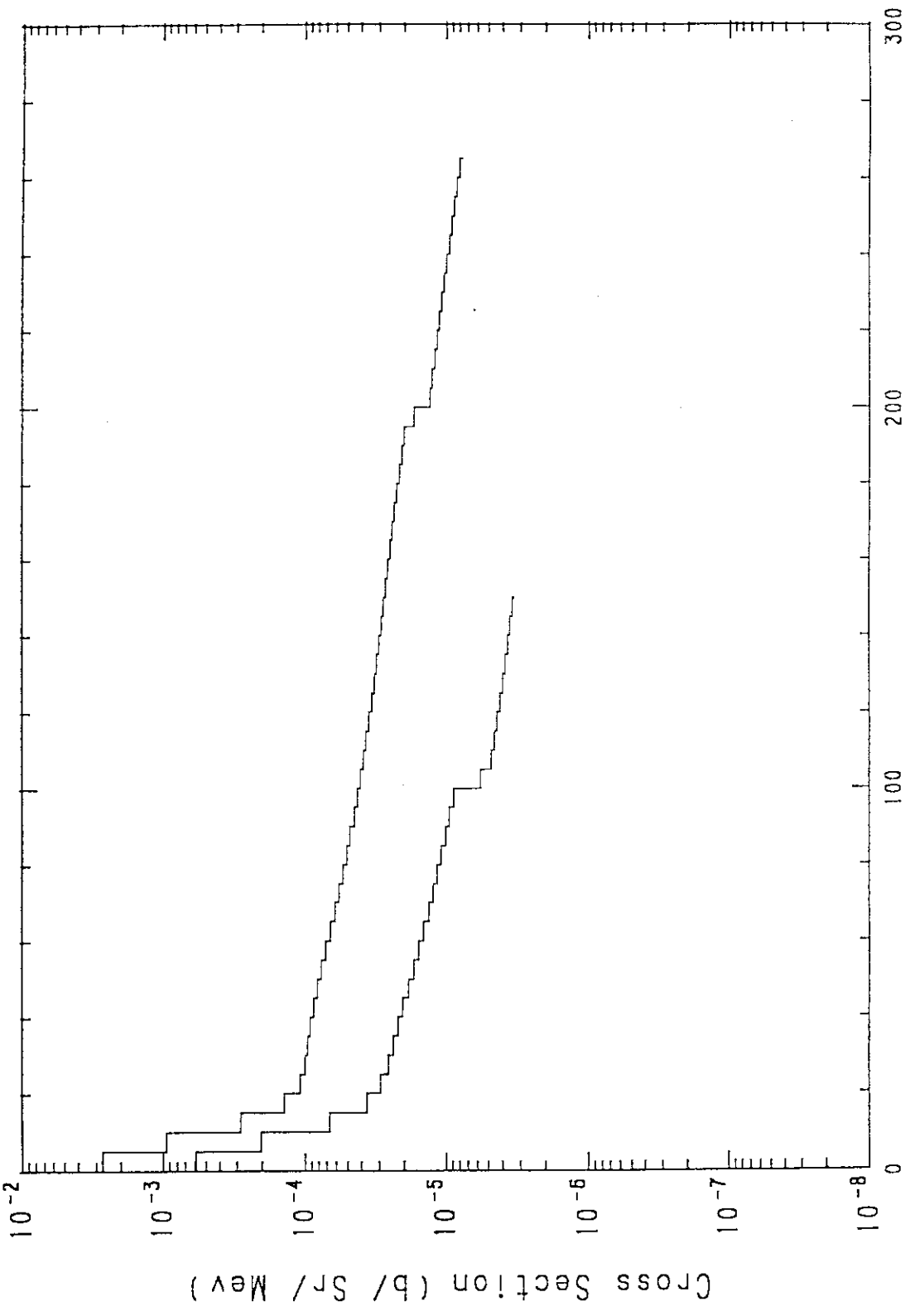

Fig. A.11 Double-differential neutron production cross sections of ^{208}Pb toward 150.0 degree at the photon incident energy of 150 and 266 MeV.